AD_____

GRANT NUMBER DAMD17-94-J-4194

TITLE: Post-Chemotherapeutic Hematopoietic Reconstitution: A Transgenic Mouse Model

PRINCIPAL INVESTIGATOR: David M. Lee, M.D., Ph.D.
Barton F. Haynes, M.D.

CONTRACTING ORGANIZATION: Duke University Medical Center
Durham, North Carolina 27710

REPORT DATE: August 1996

TYPE OF REPORT: Final

PREPARED FOR: Commander
U.S. Army Medical Research and Materiel Command
Fort Detrick, Frederick, Maryland 21702-5012

REPORT DOCUMENTATION PAGE

Form Approved
OMB No. 0704-0188

1. AGENCY USE ONLY *(Leave blank)*	2. REPORT DATE	3. REPORT TYPE AND DATES COVERED
	August 1996	Final (1 Aug 94 - 31 Jul 96)

4. TITLE AND SUBTITLE Post-Chemotherapeutic Hematopoietic Reconstitution: A Transgenic Mouse Model

5. FUNDING NUMBERS
DAMD17-94-J-4194

6. AUTHOR(S)
David M. Lee, M.D., Ph.D.
Barton F. Haynes, M.D.

7. PERFORMING ORGANIZATION NAME(S) AND ADDRESS(ES)
Duke University Medical Center
Durham, North Carolina 27710

8. PERFORMING ORGANIZATION REPORT NUMBER

9. SPONSORING/MONITORING AGENCY NAME(S) AND ADDRESS(ES)
U.S. Army Medical Research and Materiel Command
Fort Detrick
Frederick, Maryland 21702-5012

10. SPONSORING/MONITORING AGENCY REPORT NUMBER

11. SUPPLEMENTARY NOTES

12a. DISTRIBUTION / AVAILABILITY STATEMENT
Approved for public release; distribution unlimited

12b. DISTRIBUTION CODE

13. ABSTRACT *(Maximum 200*

To improve the treatment of breast cancer, it is imperative to address specific shortcomings in autologous bone marrow reconstitution, in particular the frequent failure to reconstitute specific hematopoietic lineages and the length of time required to restore immunocompetence after transplant. Previous studies have shown that the CD7 protein in human identifies multipotent progenitor cells of T-, B- and myeloid. We have developed both CD7 transgenic mouse and CD7 knockout mice as *in vivo* models for studying hematopoietic progenitor cell differentiation and the cytokines which regulate proliferation and differentiation of these progenitors. Work has also been initiated for development of mouse CD7 antibodies. These antibodieswill allow selection of mouse multipotent hematopoietic progenitor cell populations that express the CD7 gene and which in humans are not stem cells, yet are multipotent. Characterization of these cell populations and their growth and differentiation factors will allow both the transplant of more mature progenitor populations to speed engraftment. In addition, we have cloned and sequenced the recently described mouse CD7 gene, and have identified numerous conserved functional sequence elements. These models should provide clinically relevant information about control of hematopoiesis, difficult to obtain directly in humans, allowing development of novel methods for current breast cancer treatment.

14. SUBJECT TERMS	15. NUMBER OF PAGES
High-dose Chemotherapy, Brease Cancer, Bone Marrow Transplant, Transgenic Mice, Hematopoiesis, CD7	101
	16. PRICE CODE

17. SECURITY CLASSIFICATION OF REPORT	18. SECURITY CLASSIFICATION OF THIS PAGE	19. SECURITY CLASSIFICATION OF ABSTRACT	20. LIMITATION OF ABSTRACT
Unclassified	Unclassified	Unclassified	unlimited

DISCLAIMER NOTICE

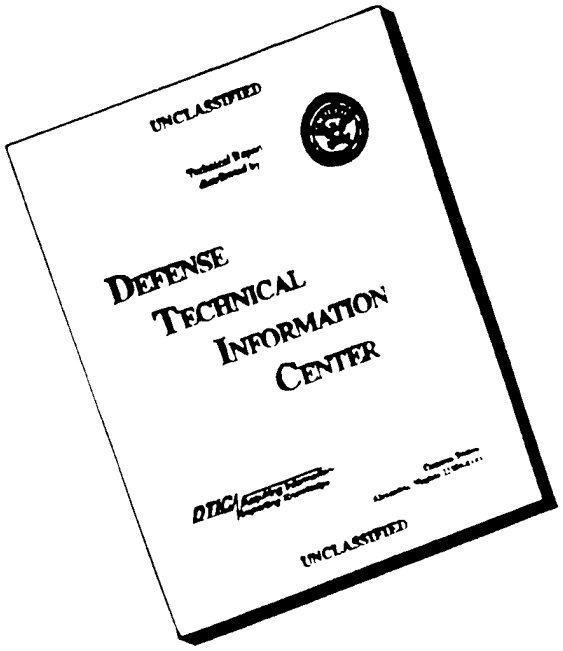

THIS DOCUMENT IS BEST QUALITY AVAILABLE. THE COPY FURNISHED TO DTIC CONTAINED A SIGNIFICANT NUMBER OF PAGES WHICH DO NOT REPRODUCE LEGIBLY.

FOREWORD

Opinions, interpretations, conclusions and recommendations are those of the author and are not necessarily endorsed by the US Army.

__X__ Where copyrighted material is quoted, permission has been obtained to use such material.

__X__ Where material from documents designated for limited distribution is quoted, permission has been obtained to use the material.

__X__ Citations of commercial organizations and trade names in this report do not constitute an official Department of Army endorsement or approval of the products or services of these organizations.

__X__ In conducting research using animals, the investigator(s) adhered to the "Guide for the Care and Use of Laboratory Animals," prepared by the Committee on Care and Use of Laboratory Animals of the Institute of Laboratory Resources, National Research Council (NIH Publication No. 86-23, Revised 1985).

____ For the protection of human subjects, the investigator(s) adhered to policies of applicable Federal Law 45 CFR 46.

__X__ In conducting research utilizing recombinant DNA technology, the investigator(s) adhered to current guidelines promulgated by the National Institutes of Health.

__X__ In the conduct of research utilizing recombinant DNA, the investigator(s) adhered to the NIH Guidelines for Research Involving Recombinant DNA Molecules.

__X__ In the conduct of research involving hazardous organisms, the investigator(s) adhered to the CDC-NIH Guide for Biosafety in Microbiological and Biomedical Laboratories.

8/28/84

PI Signature Date

Table of Contents

Post Chemotherapeutic Hematopoietic Reconstitution: A Transgenic Mouse Model

Breast cancer is currently the most common life threatening neoplasm for women in the US; one woman in nine will be afflicted at some point in her life (Muir et. al. 1987). Although enormous strides have been made in early detection and treatment of non-metastatic lesions, treatment modalities for advanced disease have not significantly improved life expectancy, thus 3.5% of all women die from breast cancer (Government Printing Office 1990). Given such appalling statistics, it is imperative both to further our knowledge of the cellular mechanisms which contribute to breast neoplasia as well as to increase the efficacy of our current pharmacological methods for treatment of this disease. The development of autologous bone marrow transplantation has permitted a new breakthrough in breast cancer chemotherapy wherein high dose consolidation is combined with standard dose adjuvant chemotherapy; disease free interval and overall survival results from initial clinical trials of this regimen are impressive (Peters et. al. 1992). **To improve this treatment, it is imperative to address specific shortcomings in autologous bone marrow reconstitution, in particular the frequent failure to reconstitute specific hematopoietic lineages and the length of time required to restore immunocompetence after transplant.** Previous studies have shown that the CD7 protein in human identifies multipotent progenitor cells of T-, B- and myeloid lineages (Chabannon et. al. 1992 and Grumayer et. al. 1991). Using mice as an animal model system, we are investigating the *in vivo* regulation of CD7 expression, and the signal transduction events which transpire after CD7 ligation. In particular, we have developed a novel CD7 transgenic mouse as an *in vivo* model for studying both hematopoietic progenitor cell differentiation and the cytokines which regulate proliferation and differentiation of these progenitors. This mouse model is unique in that it allows selection of mouse multipotent hematopoietic progenitor cell populations that express the CD7 gene and which are not stem cells, yet are able to differentiate into B-, T- and myeloid lineages in humans. No single equivalent marker has been previously described in mice. Characterization of these cell populations and their growth and differentiation factors will allow both the transplant of more mature progenitor populations (to speed engraftment) and the ability to enhance lineage-specific differentiation, thus decreasing the period of chemotherapy-related immunodeficiency. In addition, we have characterized the recently described mouse cDNA for CD7, cloning and sequencing the CD7 gene, and identifying numerous conserved functional sequence motifs between mouse and human CD7. These models should provide clinically relevant *in vivo* information about control of human hematopoiesis, difficult to obtain directly in humans, and **it may allow development of novel methods to overcome deficiencies in current breast cancer treatment protocols.**

Incidence and Mortality

Most current studies evaluate the lifetime risk of developing invasive breast cancer at 11.1%-12.57% with an overall 3.5% risk of death from this disease (Muir et. al. 1987, Government Printing Office 1990 and Feuer et. al. 1993)e. While the mortality rate from breast cancer has remained stable during the last 40 years, the incidence rates in the USA have climbed dramatically. Between 1940 and 1982, the age-standardized incidence increased approximately 1.2% per year in the state of Connecticut (the site of the oldest cancer registry in the USA) (Miller et. al. 1991). The presence of stable mortality despite a large increase in incidence of breast cancer is encouraging in that the improved survival is most likely attributable to earlier diagnosis and more effective treatments. Nonetheless, the steady increase in the incidence rate for breast cancer in this country, above that which can be attributed to more sensitive screening methods, underscores the importance of developing more effective treatments for those afflicted with this disease.

Risk Factors

While numerous hypotheses exist to explain the steady rise of incidence rates for breast cancer in western countries, no firm causal link has yet been established to account for the increase. It has been clearly established that genetic predisposition is important for a minor subset of breast malignancies (Roberts, 1993), however, population studies argue for a strong environmental influence. Women in populations migrating from regions with a low incidence of breast cancer to nations with a high incidence show a large increase in breast cancer rate, up to the level of the area to which they immigrate (Buell 1973). Several statistically significant relative risk factors have been demonstrated using population statistics, mainly in the USA. These include family history, age at menarche, age at first childbirth, age at menopause, benign breast disease, radiation exposure, obesity, height, oral contraceptive use, alcohol use, and postmenopausal estrogen replacement therapy (Henderson and Canellos 1980). While identification of these relative risk factors can help direct clinicians and patients to heightened awareness and increased surveillance, they are at best weak predictors of disease with a significant subset of breast cancer patients displaying no risk factors. Additionally, many of the risk factors identified (such as height) are not practically modifiable. Thus, while this approach to further understanding of breast cancer holds promise for future direction, it is currently limited by both technical means for investigation and by interventional inability, again highlighting the importance of effective treatment methods.

Treatment Modalities

Current therapy for breast carcinoma involves both local surgical excision and systemic chemotherapy. While the specific surgical and chemotherapeutic regimens are beyond the scope of this discussion, several recent pharmacologic advances are of critical importance. Of particular note is the demonstration that high dose adjuvant chemotherapy administered concurrently with primary local intervention *both prolongs the time of disease free existence and* ***improves overall mortality rate*** (Anonymous 1992). Recently, a further advance in this treatment approach was outlined wherein high dose consolidation was combined with standard dose adjuvant chemotherapy. Although the follow up time for this approach is short, it shows significant improvement both in disease free interval and in overall survival over previously used regimens (Peters et. al. 1993).

Although this treatment regimen is one of the most promising currently in use, there have been two major drawbacks which prevent widespread use: high cost and significant morbidity (Peters et. al. 1993). Both of these drawbacks result in large part from bone marrow ablation in these patients--a direct result of the high dose chemotherapy. While immunodeficient, patients are susceptible to a wide range of opportunistic infections, consequently, patients must be hospitalized under intense care during treatment. Even under the best care available, significant morbidity is a continuing obstacle which requires further refinement in this treatment. In fact, the critical determinant which defines the limits of chemotherapeutic dosages currently tolerable in the non-ablative treatment of breast cancer is the toxic effect on bone marrow hematopoietic cells (O'Shaughnessy and Cowan 1993). Preliminary evidence suggests that delivered chemotherapeutic dose intensity can be increased in metastatic breast cancer if hematopoietic growth factors are administered (O'Shaughnessy and Cowan 1993). In theory, if higher doses were tolerable, they would be more effective at destruction of the metastatic malignant cells. Finally, these specialized intensive treatment protocols are currently extremely expensive, further burdening an already taxed health care system (Peters et al. 1993). **To improve upon these problems of cost, morbidity and efficacy, it is critical to further our ability to intervene in hematopoiesis, defining both the cellular and molecular constituents in bone marrow which will contribute to more rapid and effective lymphoid reconstitution.**

General Hematopoiesis

All hematopoietic lineages derive from pleuripotent cells present in the bone marrow. While the exact population of cells capable of both self renewal and differentiation into all hematopoietic lineages has not been purified and characterized, numerous advances have been made in characterizing lineage specific progenitor cells both in mouse and in humans. Additionally, numerous soluble molecular growth factors responsible for both proliferation and differentiation of various hematopoietic lineages have been characterized, some with potent clinical benefit. In combination, these discoveries have increased the efficacy of both autologous and allogeneic bone marrow transplants in several ways. First, characterization of progenitor cells allows the removal of mature effector cells in bone marrow responsible for graft vs. host responses without removing those progenitor cells needed for reconstitution. Secondly, characterization of growth and differentiation factors has allowed more rapid hematopoietic reconstitution, significantly reducing morbidity associated with the immunodeficient state. Additionally, these characterizations have allowed more efficient *in vitro* manipulation of harvested pre-transplant bone marrow, making the procedure less costly. In light of the results of these advances, it is crucial to continue characterization of early multipotent hematopoietic progenitor populations in bone marrow and to further define those molecular factors responsible for specific differentiation and proliferation possibly increasing the ability to expand progenitor populations with *in vitro* culture prior to transplant. Further advances will both increase the rapidity of restoration of immunocompetance after marrow transplantation and decrease the costs associated with this procedure.

T cell lymphopoiesis and the cell surface molecule CD7

CD7, first described in 1979, is a 40 kilodalton transmembrane glycoprotein expressed on the majority of peripheral blood T-lymphocytes (Haynes et. al. 1980, Haynes et. al. 1979 and Eisenbarth et. al. 1980). It was first described as the best clinical diagnostic marker of T-cell acute lymphocytic leukemia (Haynes 1981), suggesting it is an early marker of T cell lineage development. CD7 expression in peripheral blood T cells and on thymocytes has been well characterized, and significant progress has been made describing CD7+bone marrow populations.

T cell development

T-lymphocytes are a subset of peripheral blood lymphocytes with both immune effector and regulatory function. The T cell developmental pathway is currently characterized by the sequential expression of combinations of surface antigens which are correlated with lineage commitment and specific functional consequences.

Bone marrow

T-cells arise from stem cells present in bone marrow in adult humans; the sequence and nature of the molecular messages required for differentiation are currently unknown. At present we are only beginning to describe a population of progenitor cells present in bone marrow which express lineage commitment markers (ie. CD7), yet are multipotent and capable of T lineage differentiation. This progenitor population has been characterized as CD34+, CD7+ , CD3-, CD4-, CD8- phenotype in adult bone marrow (Haynes et al. 1981 and Tjonnfjord et. al. 1993). These cells can also differentiate into the CD14+ myeloid lineage (Haynes et. al. 1981), consistent with a multipotent progenitor population. In a different experimental system, CD7+, CD34+, CD19+ bone marrow progenitor cells coexpressing B- and T-cell lineage markers are demonstrated, suggesting capability of both B- and T- lineage differentaition *in vitro* (Grumayer et. al. 1991). Finally, in agreement with this model, undifferentiated CD7+ leukemic cell lines with demonstrated multipotent differentiation capability have been described (Mossalay et. al. 1990). Further understanding of the hematopoietic development of this critical

regulatory and effector cell population is essential for developing more effective strategies for lymphoid population reconstitution in bone marrow transplants. In particular, further definition and characterization of T-lymphoid progenitors will allow more effective depletion of harmful mature T lymphocytes in allogeneic bone marrow transplant. Likewise, clinical selection of the more mature progenitor populations will allow more rapid reconstitution of immune function after chemotherapeutic ablation.

Thymocytes

Thymocytes are an immature T cell population, a portion of which are capable of differentiating into multiple lineages. The most immature thymocyte population is found in the subcapsular cortex and is characterized by the CD7+, CD3-, CD4-, CD8- phenotype. This population contains progenitors capable of differentiating into both TcR T-cell and CD16+ NK colonies *in vitro* (Haynes et. al. 1988, Kamps et. al. 1989 and Campana et. al. 1989). As thymocytes mature, they acquire cell surface expression of CD2, CD3, CD4, CD5, CD6, CD8, and TcR, among others, in a regulated fashion. While a complete discussion of thymocyte differentiation is beyond the scope of this paper, results of many experiments show that it is possible to define populations of thymocytes at differing stages of development by simultaneously assaying expression of these antigens which presumably correlate with as yet uncharacterized regulated molecular events.

Peripheral blood lymphocytes

Mature T cells are currently defined as lymphoid cells expressing the T-cell receptor(TcR) complex (includes either the a/b or d/g TcR heterodimer plus the CD3 antigen group). Most mature T cells express CD7 and either CD4 or CD8 which generally correlates with helper or cytotoxic/suppressor functions respectively. Generally, peripheral blood T-cell are terminally differentiated effector cells.

Lymphopoiesis during development

Developmentally, CD7 is first detected in the human fetus at 7-8.5 weeks of gestation (Lobach et. al. 1985). By gestational week 10, CD7(+) cells are seen in fetal liver (Lobach et. al. 1985, Sanchez et. al. 1993 and Trinchieri 1989) as well as thoracic mesenchyme Lobach et. al. 1985 and Hanna and Fidler 1980)--prior to lymphoid colonization of the thymic rudiment; no other T-lymphoid specific marker is present on fetal hematopoietic cells at this time. Culturing this fetal liver CD7(+) (CD3, CD4, and CD8 negative) but not the CD7(-) cell population in PHA conditioned media + rIL2 causes cellular proliferation and formation of T-cell colonies (CFU-T) which express markers of mature T-cells (Lobach et. al. 1985). Interestingly, when this same population is cultured under different conditions (in IL-4 conditioned media), CD7(-) myeloid lineage colonies were observed while CD7(+) CFU-T were absent (Welsh 1986), demonstrating both the multipotentiality of this progenitor population and the correlation of increased CD7 expression and T cell commitment. Taken together, the above data point to definable CD7(+) multipotent hematopoietic progenitor populations, the study of which will facilitate further understanding of hematopoietic differentiation.

Natural Killer Cells

Natural killer (NK) cells are a lymphocyte effector cell population able to kill target cells in an apparently non-MHC restricted manner. They are currently defined as CD16(+) and/or CD56(+), CD3(-), TcR(-) large lymphocytes (reviewed in Perussia et. al. 1983). They play a demonstrated role in tumor surveillance (Ikuta et. al. 1992) and eradication of virally infected cells (Smeland et. al. 1992), although the mechanism of recognition of target cells is currently unknown. They are also implicated in antibody dependent cellular cytoxicity (Denning et. al. 1989). Although a specific role for NK cells in breast cancer response has not been demonstrated, this is a largely under-investigated process whose importance is undefined.

NK cell differentiation pathways are also currently unknown. Thymocytes have clearly been demonstrated to differentiate into NK lineage (Haynes et. al. 1988), however, whether this is the main route of maturation or just a minor default pathway has not been demonstrated. The presence of normal NK populations in athymic nude mice argues against a major common intrathymic differentiation pathway for T cells and NK cells. T cells and NK cells are both CD7+, which is interesting becauses CD7 expression in peripheral blood is otherwise limited to T lymphocytes. Further definition of NK cell maturation will allow more effective stratategies for lymphoid reconstitution after chemotherapeutic depletion and aid in understanding the process by which NK cells determine self from non-self (or altered self). This may be of importance for immunological eradication of neoplasm, in particular breast carcinoma. An effective means of approaching this issue is to study CD7+ BM progenitors and define those signals which promote NK cell differentiation.

While numerous advances outlined above have been immensely important in defining human multipotent hematopoietic progenitor populations, further advance is currently limited by *in vitro* technical considerations and difficulty in obtaining fresh tissue appropriate for study. Development of an animal model is imperative for *in vivo* characterization of these compelling cellular subsets. Currently, no animal equivalent for CD7 has been characterized and no mouse multipotent hematopoietic progenitor population capable of T-, B-, and myeloid differentiation has been described. An animal model of this progenitor population will be invaluable for studying the *in vivo* differentiation capability of these bone marrow cellular subsets as well as examining the *in vivo* relevance of those regulatory molecular messages identified *in vitro*. We propose to further define CD7 expressing multipotent progenitor populations in CD7 transgenic mouse bone marrow. After identification of these hematopoietic subsets, we will define the *in vivo* roles of soluble cytokines (whose list is ever increasing) in regulating proliferation and differentiation of these progenitor populations both in sub-lethally irradiated and in chemotherapy ablated recipient mice. Knowledge gained with this *in vivo* mouse model system will have direct impact on efficacious treatment for breast carcinoma in that **it may allow more rapid and specific bone marrow reconstitiution after high dose chemotherapeutic ablation.**

C. Mouse CD7

A powerful means of examining the function and regulation of human genes is to study their biology in a different species; mice have proven to be an ideal animal model system due to short generation intervals, economics of housing, the availability of inbred strains with defined genetics and the vast amount of reagents and information available from prior characterization. Until recently, CD7 had been described only in humans, however, during the course of this work, a mouse cDNA with a high degree of homology to human CD7, designated mouse CD7, was described (Yoshikawa et. al. 1993). This molecule had extensive regions of up to 63% homology to human CD7, with only one notable gap when compared to CD7-- the membrane proximal "stalk region" appeared to be absent. When tissue expression of mRNA for mouse CD7 was analyzed, it was noted to have a lymphoid restricted expression, in congruence with human CD7 (Yoshikawa et. al. 1993) Of note, nude mice had similar levels of CD7 mRNA expression when compared to normal mice, whereas SCID mice were deficient in CD7 mRNA. No further analysis of CD7 had been accomplished when this work was intitiated. In particular, no evidence other than sequence homology and possible tissue specific expression confirmed that this was mouse CD7. This work confirmed the CD7 designation of this cDNA by localizing its chromosomal map position to the region homologous to human CD7. This work extends the characterization of mouse CD7 by cloning and sequencing the mouse CD7 gene. We demonstrate that the structure of the mouse CD7 gene is highly similar to that of human CD7 and define functionally relevant regions of homology in the promoter

regions of these genes.

Hypothesis/Purpose

We hypothesize that a population or populations of CD7 expressing cells in human bone marrow is able to differentiate *in vivo* into multiple hematopoietic lineages under control of specific soluble or cell surface molecular messages. This population of differentiated progenitors, while not stem cells, contributes significantly to early myelo- and lymphopoiesis during the time period required for stem cell progeny to differentiate. Enrichment of these progenitors, possibly via expansion in *in vitro* culture, would significantly decrease the period of immunodeficiency after chemotherapy. We will define both the populations of progenitor cells and those events which control their proliferation and differentiation both in our CD7 transgenic mouse model as well as using the endogenous mouse CD7 gene. We will characterize the recently described mouse CD7 gene, defining the development of endogenous CD7 expressing cells in mice as a model system for studying differetiative capability of human $CD7^+$ progenitors.

Technical Objectives

To address the differentiative capability of CD7+ bone marrow progenitors and to define the role of known cytokines on the proliferation and differentiation of these populations in an *in vivo* chemotherapy model we have pursued the following specific aims:

1: Using our CD7 transgenic mice to model the biology of the human system, we have defined CD7+ bone marrow hematopoietic progenitor cell populations using direct immunofluorescence flow cytometry using monoclonal antibodies known to define multipotent hematopoietic progenitor subsets.

2: We have cloned and sequenced the mouse CD7 gene. Using the obtained sequence data, we have performed comparative analysis of mouse and human CD7, identifying conserved sequence motifs which will indicate possible functionally important nuclear regulatory motifs. After identification of these conserved motifs, we will determine possible functional roles for these motifs.

3: Using the cloned mouse CD7 gene, we have constructed CD7 deficient mice, examining the effect of lack of CD7 expression on mouse hematopoiesis.

4: Using the cloned mouse CD7 gene, we have expressed recombinant mouse CD7 in bacteria and have used this protein to generate polyclonal sera and monoclonal antibodies.

The above work has laid a foundation for future important work outlined below.

1: We will test the ability of characterized hematopoietic growth factors and cytokines to affect *in vivo* proliferation and differentiation of CD7+ multipotent hematopoietic progenitor populations from donor mice transferred into recipient mice which have undergone sublethal irradiation.

2: Since it is likely that chemotherapeutic agents used for treatment of breast cancer have a toxic effect on bone marrow stroma and thus could have an indirect effect on autologous bone marrow reconstitution, we will test the *in vivo* differentiation capability of bone marrow CD7+ multipotent progenitor cell subsets in recipient mice which have undergone chemotherapeutic bone marrow ablation. These results will be compared with reconstitution in sub-lethally irradiated recipient mice. In addition, we will compare the ability of characterized hematopoietic growth factors and cytokines to

affect proliferation and differentiation in recipient mice which have undergone chemotherapeutic bone marrow ablation.

Body

A Characterization of Human CD7 Transgenic Mice

Production of transgenic mice

A 12 kb Sal I fragment from the previously characterized 17 kb lambda clone LSCD7-1 (Schanberg et. al. 1991) was isolated on low melting temperature agarose. This genomic DNA fragment contained the 3 kb coding region of the CD7 gene as well as approximately seven kb of 5' flanking region and two kb 3' of the gene. Both of the previously reported upstream DNase I hypersensitive sites were included in this DNA fragment (Schanberg et. al. 1991) (Figure 1A). Purified DNA was microinjected into the male pronuclei of eggs from C57BLxSJL mice and implanted into pseudopregnant recipient mice (Brinster and Palmiter 1985). These transgenic mice were produced by the Shared Transgenic Mouse Resource of the Duke Comprehensive Cancer Center. Transgenic animals were identified by Southern analysis and slot blot of tail biopsy DNA (see below) using a CD7 cDNA probe. Four independent stable CD7 transgenic lines were generated, and two lines, designated 555 and 216, expressed the human CD7 transgene. The integrity of the transgene was confirmed using Southern analysis (Southern 1975) under conditions described in Sambrook et. al. (1987) (see below) and CD7 transgene copy number was estimated by slot blot analysis (see below) and quantitated using both densitometer (Electrophoresis Data Center, Helena Laboratories, Beaumont, Texas) and PhoshorImager (Molecular Diagnostics, Sunnyvale, CA).

DNA extraction

DNA was extracted by incubating tail tissue in buffer containing 50 mM Tris pH 8.0, 100mM EDTA, 0.5% SDS, and 1 mg/ml proteinase K at 55°C overnight. The samples were phenol/chloroform extracted, ethanol precipitated with 3M sodium acetate pH 6.0 and resuspended in TE (10mM Tris pH 8.0, 1 mM EDTA). The proteinase K digestion was repeated overnight at 55°C. DNA was again phenol/chloroform extracted, ethanol precipitated and resuspended in TE and quantitatied by fluorimetry (Model TKO 100, Hoeffer Scientific. San Francisco, CA).

Southern Blot

Purified genomic DNA (10 μg) was digested with the restriction endonuclease Bgl II and electrophoresed in 0.8% agarose gels in TAE buffer containing ethidium bromide. DNA was transferred to nitrocellulose membrane (Schleicher and Schuell, Keene, NH) using capillary action as described by Southern (1975) and fixed by baking the membrane at 80° C for 2 hours under vacuum. The CD7 transgene was identified by pre-hybridization of the membranes for 1 hour at 65° C in a solution containing 3X SSC, 10X Denhardt's solution, 0.1% SDS, 1 mM EDTA and 10 mg/ml salmon sperm DNA and hybridization overnight at 60° C in hybridization solution: pre-hybridization solution containing 7% Dextran Sulfate and at least $1X10^6$ cpm/ml ^{32}P labeled probe. Human CD7 cDNA (Aruffo and Seed 1987) random primer labeled using an OligoLabelling kit (Pharmacia, Uppsalla, Sweden) was used as a probe to identify the CD7 trangene.

Slot Blot

5 μg of purified genomic DNA was applied to nylon membrane (Duralon UV, Stratagene, LaJolla, CA) using a BioBlot apparatus (BioRad, Richmond, CA) and fixed by baking the membrane at 80° C for 2 hours under vacuum. Presence of the transgene was identified

by pre-hybridization of the membranes for 1 hour at 65° C in a solution containing 3X SSC, 10X Denhardt's solution, 0.1% SDS, 1mM EDTA and 10 mg/ml salmon sperm DNA and hybridization overnight at 60° C in hybridization solution: pre-hybridization solution containing 7% Dextran Sulfate and at least $1X10^6$ cpm/ml ^{32}P labeled probe. Human CD7 cDNA (Aruffo and Seed 1987) random primer labeled using an OligoLabelling kit (Pharmacia, Uppsalla, Sweden) was used as a probe to identify the CD7 trangene.

RNA preparation and analysis

Immediately after harvesting, mouse tissues were snap frozen in liquid nitrogen, weighed, and diced with a sterile blade. Tissue was ground with a pestle in a sterile microfuge tube (Kontes Scientific Glassware, Vineland, New Jersey) containing 300 ml of 4M guanidinium isothiocyanate, 5 mM sodium citrate pH 7.0, 0.5% sarkosyl, and 0.1mM dithiothreotol. The sample was added to 3 mls of buffer, overlayed upon 1.5 mls of 5.7M CsCl and centrifuged overnight at 35,000 x gravity (Glissen et. al. 1974 and Manniatis et. al. 1987). The RNA pellet was washed with 70% ethanol, resuspended in 200 µl diethylpyrocarbonate (DEP)-treated H_2O and ethanol precipitated. The RNA was resuspended in 100 ml DEP-H_2O and quantitated by spectrophotometry. For each sample, 15 µg of total RNA was electrophoresed through a 1.2% agarose gel containing 2.2 M formaldehyde in MOPS buffer as described (Lehrach et. al. 1977). RNA was transferred to a nitrocellulose membrane (Scleicher and Schuell, Keene, NH) using capillary action(Southern 1975) and then hybridized as described by Sambrook (1987). The ^{32}P random-labeled (Pharmacia, Uppsala, Sweden) human CD7 cDNA was used as a probe. Membranes were washed under final conditions of 0.5 X SSC, 0.1% SDS at 58° C for 10 minutes to remove non-specific hybridization and exposed to radiographic film (Kodak, Rochester, NY).

Mitogenic Stimulation of Splenocytes and Thymocytes

Cells were mechanically dissociated from fresh mouse spleen and thymus into 4° C RPMI 1640 (Gibco, Grand Island, NY) and mononuclear cells were obtained by centrifugation over a Ficoll-Hypaque cushion as described (Mishell and Shiigi, 1980). Purified mononuclear cells were subsequently cultured in RPMI (Gibco, Grand Island, NY) containing 1 µg/ml PHA, (Burroughs Wellcome, Research Triangle Park, NC), 10% fetal calf serum (FCS) and 10 units/ml recombinant IL-2 (Cetus, Emeryville, CA). After 72 hours in culture in 5% CO_2 in air, the cells were assayed for CD7 induction by fluorescent activated flow cytometry (Haynes et. al. 1981b) or underwent RNA extraction for subsequent Northern blot analysis, described above.

Antibodies and reagents

Monoclonal antibodies Thy1.2 (Anti-Thy-1, Becton Dickinson, Mountain View, CA), Ly5 (anti-B220, Pharmingen, San Diego, CA), Lyt2 (anti-CD8, Becton Dickinson, Mountain View, CA), L3T4 (anti-CD4, Becton Dickinson, Mountain View, CA), CD7 (Caltag, South San Francisco, CA), OX-12 (anti-rat IgG, Sera-Labs, Crawley Down, Sussex, England), and streptavidin-phycoerythrin (Pharmingen, San Diego, CA) were used at saturating titers for immunohistology and flow cytometry. Monoclonal antibodies 3A1a (anti-CD7)(ATCC # HB 2) and PK136 (anti-NK1.1)(ATCC # HB 191) were produced from hybridomas cultured in serum free media (SFM Gibco, Grand Island, NY) and purified using affinity chromatography over a Staph protein A/G column (Pierce, Rockford, NY). These purified antibodies were subsequently fluorescein conjugated (Goding 1976) and saturating titers determined. Affinity purified monoclonal antibody 3A1a was pepsin digested (Lamoyi et. al. 1983) and F'(ab) fragments were obtained after

removal of the Fc portion by affinity chromatography over a protein A/G column (Pierce, Rockford, NY). The F'(ab) fragments were biotinylated as described (Hnatowich et. al. 1987) and titer determined with streptavidin-phycoerythrin (Pharmingen, San Diego, CA). Monoclonal antibodies E13 (anti-Sca-1) (gift of I. Weissman, Stanford, CA) and F4/80 (ATCC # HB 198) (anti-macrophage subset) were cultured in DMEM media (Gibco, Grand Island, NY) supplemented with FCS. Spent culture supernatants were used in indirect IF assays and flow cytometry.

Indirect immunofluorescence assays and flow cytometry

Analysis of cell surface phenotype was performed in both direct- and indirect-immunofluorescence assays as described (Haynes et. al. 1981b). Briefly, 50 µl cells suspended at 2 X 10^7 cells/ml in PBS wash (phosphate buffered saline containing 2% bovine serum albumin and 0.1% sodium azide) were mixed with 50 µl antibody solution at saturating titer for 30 minutes at 4° C. These cells were then washed twice with 1 ml of PBS wash and resuspended in 50 µl fluorochrome conjugated secondary reagent at saturating titer diluted in PBS wash for 30 minutes at 4° C. Cells were subsequently washed twice with 1ml of PBS wash and resuspended in 1ml PBS wash containing 4% paraformaldehyde for fixation and stored at 4° C in foil wrap until flow cytometric analysis was performed. Directly conjugated primary reagents were performed as above, except fixation occurred after the first wash series. Cell suspensions were analyzed using a FACStar plus flow cytometer (Becton-Dickinson, Moutain View, CA).

Preparation of cell suspensions

For all flow cytometry experiments, freshly obtained suspensions of cells were used. Peripheral blood was obtained via retro-orbital bleed into a heparinized pasteur pipette. Erythrocytes were eliminated using the immunolyse reagent (Becton-Dickinson, Mountain View, CA) per manufacturer protocol and the remaining mononuclear cell population was analyzed via immunofluorescence flow cytometry. Peritoneal lavage cells were obtained by two sequential 7.5 ml injections of RPMI 1640 into the peritoneum of a sacrificed mouse with subsequent drainage of this media via 16 ga. needle. These cells were washed once with RPMI 1640 media and subsequently analyzed via immunofluorescence flow cytometry. To obtain bone marrow cells, femurs were dissected and flushed with 2ml ice cold RPMI 1640. The femoral material was mechanically dissociated through a 29 ga. needle, washed once with RPMI 1640 and subsequently analyzed via immunofluorescence flow cytometry. To obtain splenocytes and thymocytes, dissected spleen and thymus were mechanically dissociated and mononuclear cells were isolated by density centrifugation (Mishell and Shiigi, 1980). Fluorescence activated cell sorted populations of bone marrow cells were prepared on a microscope slide using a cytoprep apparatus and subsequently stained with Wright-Giemsa reagents (Sigma, St. Louis, MO).

Indirect IF histology

Dissected tissue was snap frozen and stored in liquid nitrogen. Frozen tissue mounts were made using OCT compound (Miles Laboratories, Elkhart IN) and 4 µm frozen sections were prepared and subsequently fixed in 4° C acetone for 5 minutes and air dried for 20 minutes. Indirect IF assays on tissue sections were performed as described (Haynes et. al. 1989). Briefly, tissue slides were scored with a diamond tip pen to define the sample area. Antibody at saturating dilution in 50 µl PBS wash (phosphate buffered saline containing 2% bovine serum albumin and 0.1% sodium azide) was applied and allowed to incubate in a humid chamber for 30 minutes at room temperature. Slides were

then washed gently with PBS, placed in a slide rack and washed three times for 5 minutes at 4° C in a PBS bath. Excess PBS was carefully removed and secondary fluorochrome-conjugated reagent was applied at saturating titer in 50 µl PBS wash for 30 minutes at room temperature in a humid chamber. Slides were then washed as before, excess PBS was removed and coverslipped under a PBS/30% glycerol solution. Slides were stored at 4° C wrapped in foil until analyzed via fluorescence microscopy (Nikon Optiphot, Nippon Kogaku, JAPAN).

B. Chromosomal Mapping of Mouse Cd7

Probe sequence

A mouse CD7 cDNA probe was generated using the polymerase chain reaction (PCR)(Innis et. al. 1990) with mouse CD7 specific primers from the published cDNA sequence (Yoshikawa et. al. 1993). In brief, PCR reaction were performed at 60° C annealing temperature for 30 seconds, 72°C extension temperature for 60 seconds and 94° dissociation temperature for 30 seconds for 30 cycles. These reactions were performed with DeepVent polymerase (New England Biolabs, Beverly, MA) using manufacturer buffers. The resulting 568 bp product spanned coordinates 115-683 of the published cDNA sequence. The PCR was performed with a mouse thymocyte cDNA library (C67BL/6 adult female from Stratagene, LaJolla, CA) as a template and a single product of predicted sequence was observed when analyzed via electrophoresis through ethidium bromide stained 1.2% agarose (Sigma, St. Louis, MO) in TAE buffer. This PCR product was purified using a Wizard PCR prep spin column (Promega, Madison, WI) and eluted in 20 µl water. The identity of this fragment was confirmed via sequencing.

DNA sequence analysis

The PCR generated mouse CD7 cDNA fragment (above) was sequenced according to protocols of the manufacturer using an Applied Biosystems 373A automated sequencer and fluoresceinated dye terminator cycle sequencing methods. Template for sequencing was the PCR products generated directly from the lambda cDNA library described above.

RFLV identification

Restriction fragment length variants (RFLV) were identified by Southern blot hybridization of mouse CD7 cDNA to genomic DNA from C3H/HeJ-*gld* and (C3H/HeJ-*gld* x *Mus spretus*) F1 parental mice digested with various restriction endonucleases as previously described (Seldin et al. 1988). DNA purification, restriction endonuclease digestion, agarose gel electrophoresis, transfer to nylon membrane and hybridization conditions were performed as described (Watson and Seldin 1994).

Chromosomal Localization

The chromosomal location of mouse CD7 (designation *Cd7*) was determined by using a series of genomic DNA samples obtained from an interspecific cross of C3H/HeJ-*gld* and (C3H/HeJ-*gld* x *Mus spretus*) F1 digested with the restriction endonuclease Taq-1 as previously desribed (Seldin et al. 1988). The RFLV haplotypes of 114 interspecific cross offspring were analyzed via Southern blot analysis and results were compared with over 500 previously characterized loci as described (Seldin et. al. 1988). Map position was determined using a Wingz spread sheet (Informatix software, Lenexa KS) on a Sun UNIX platform (Sun Microsystems, Mountain View, CA) which used the Bishop formula (Bishop 1988) to determine correct gene order. The confidence interval of the map position was determined using the standard error formula $[r(1-r)/n]^{1/2}$ where r is the recombination frequency and n is the population number (Green 1981).

C. Cloning and Characterization of Mouse CD7

Probe sequences

A mouse CD7 cDNA probe to be used for subsequent cloning experiments was generated by the polymerase chain reaction (PCR)(Innis et. al. 1990) with mouse CD7 specific primers from the published cDNA sequence (Yoshikawa et. al. 1993). In brief, PCR reaction were performed at 60° C annealing temperature for 30 seconds, 72°C extension temperature for 60 seconds and 94° dissociation temperature for 30 seconds for 35 cycles. These reactions were performed with Taq polymerase (Gibco/BRL Grand Island, NY) using manufacturer buffers. The resulting 347 bp product spanned coordinates 126-472 of the published cDNA sequence. The PCR was performed with a mouse thymocyte cDNA library (C67BL/6 adult female from Stratagene, LaJolla, CA) as a template and a single product of predicted sequence was observed when analyzed via electrophoresis through ethidium bromide stained 1.2% agarose in TAE buffer. The identity of this fragment was confirmed via sequencing.

Isolation of mCD7 genomic clones

Two separate 129 strain mouse liver genomic libraries were plated and transferred to nylon membranes (Magna Lift, MSI, Westboro, MA) as previously described (Arber et. al. 1983 and Sambrook et. al. 1987). These libraries were a Sau3A partial digest cloned in lambda FIX (Stratagene, LaJolla, CA) and a Mbo-1 partial digest cloned in lambda Charon 35 (Loenen and Blattner, 1983) (kind gift of Dr. Hyung-Suk Kim, University of North Carolina, Chapel Hill, NC). Libraries were screened with a ^{32}P random-labeled cDNA probe (Pharmacia, Uppsala, Sweden) using standard techniques (Benton and Davis 1977 and Manniatis et. al. 1987). Filters were probed in a sealed bag containing 4 filters prehybridized for 1 hour at 65° C in a solution containing 3X SSC, 10X Denhardt's solution, 0.1% SDS, 1mM EDTA and 10 mg/ml salmon sperm DNA and hybridized overnight at 60° C in hybridization solution: pre-hybridization solution containing 7% Dextran Sulfate and at least $1X10^6$ cpm/ml ^{32}P labeled probe. These filters were washed at a final stringency of 0.5X SSC, 0.1%SDS at 55° C for 15 minutes and exposed to film (Kodak, Rochester, NY). Two positive lambda clones were subsequently characterized by Southern blot restriction endonuclease analysis (Southern, 1975 and Sambrook et. al. 1987) and subcloned into pBluescript SK+ (Stratagene, LaJolla, CA). The clones 13-2 and 21-1 were obtained from the Charon 35 and the FIX library respectively.

DNA sequence analysis

Subcloned lambda fragments were sequenced according to protocols of the manufacturer using an Applied Biosystems 373A automated sequencer and fluoresceinated dye terminator cycle sequencing methods. Primers used for PCR reactions and sequencing were generated both from sequences obtained while sequencing was in progress and from published cDNA sequences (Table 1)(Table 2). Templates for sequencing were PCR products generated directly from plasmid subclones containing mouse CD7 DNA obtained from lambda clones. All sequence analyses were performed two or more times.

Sequence comparisons

Database searches were performed using both the Wisconsin Package database search and analysis algorithm (Program Manual, Wisconsin Package, 1994) and the Signal Scan analysis program (Prestridge 1991). Open reading frames were identified using Fickett's method of analysis available on the Wisconsin Package (Program Manual, Wisconsin Package, 1994). Exon donor and acceptor splice sites were visually identified by the presence of canonical sequences (Prestridge 1991).

Electrophoretic Mobility-Shift Assay (EMSAs)

Nuclear extracts were prepared from the mouse lymphoma cell line EL4 (ATCC # TIB 39) and human cell lines K562 (ATCC# CCL 243), a chronic myelogenous leukemia and Jurkat, (ATCC # TIB 152), an acute T cell leukemia, by the method of Dignam (Dignam et. al. 1983). Electrophoretic mobility shift assays were performed as previously described (Sykes and Kaufman 1990). The nucleotide sequences used as double stranded probe in the EMSAs were as follows:
hCD7-5',GATCATTGGGTCCCAGCAGAAAGTACCCCAGAGGACCAGGCAGG;
mCD7-5', AACACATCCCAGCAGAAAATGACACAAAAGACCAGAGGAC;
hCD7-3', AGAGCTCAGAGAGGGCTTCCTGGAGGCGGTGCCTCA;
mCD7-3', TCCACCTTCATCTTCAGGAAGCCCTCCCTCGGAGCT.
Nuclear extract (10ng) and end-labeled probe (1-3ng; 50,000 cpm) were combined with nonspecific DNA (1.25 mg poly dI-dC and 0.3 mg herring sperm DNA) for the binding reaction. Competition experiments included 160 fold molar excess of self, related, and non-specific oligonucleotides in the binding reactions. Complexes were fractionated on 5% nondenaturing polyacrylamide gels, dried and visualized by autoradiography.

Table 1 Primers used in sequencing the mouse CD7 gene. Shown is a list of the names and sequences of the primers used for sequencing the mouse CD7 gene. 5' primers sequence orientation is 5'-3' relative to the orientation of the coding strand of the gene, while 3' primers have sequence oriented 3'-5' relative to the coding DNA strand.

MCD7 3' PRIMERS

1. MCD7 3'-1 "CGGGATCCCTGGTACTGGTTGGGGATGCATGG"
2. MCD7 3'-2 "CCTGGCCAGGCGGCTCCAAGGCAG"
3. MCD7 3'-3 "GTACCTCCCCACCCCCAAGCTTTG"
4. MCD7 3'-4 "TGGGATCTGTATGCTTCTTGG"
5. MCD7 3'-5 "TCCTGTCTACTGTGGGCTCC"
6. MCD7 3'-6 "AGATCCCTTCCAGGTGCC"
7. MCD7 3'-7 "AGCACTGCCTGCTGAGTCA"
8. MCD7 3'-9 "AGAGGCCGGGAGGGAGTTGA"
9. MCD7 3'-10 "GACTACTCCCCACCCTGGCT"
10. MCD7 3'-13 "TGCTCCCCCTGTAGGTGGGTT"
11. MCD7 3'-14 "TCACAAGCACCAAGGGTAGA"
12. MCD7 3'-15 "TCCTATCCCAGAAGTTCCGA"
13. MCD7 3'-18 "TGAGAGTCTGGAGTAGATGC"
14. MCD7 3'-19 "TTCACCACAACCGTGGTGAA"
15. MCD7-EC-3'-2 "TTCGGGATCCCGTGGGAAGGAAAATGATGTCTGCAG"
16. MCD7-EC-3'-1 "CGGGATCCTGGGAAGGAAAATGATGTCTGCAG"

Vector Primers

1. T7 "GTAATACGACTCACTATATAGGGC"
2. T3 "AATTAACCCTCACTAAAGGG"

MCD7 5' PRIMERS

1. MCD7 5'-1 "CATGCCATGGGACGTACACCAGTCCCCCCGACT"
2. MCD7 5'-2 "CATGCCATGGATGCCCAAGACGTACACCAGT"
3. MCD7 5'-3 "CCGCGGGTACCCGACGTACACCAGTCCCCC"
4. MCD7 5'-4 "CATGCTCGAGATGACTCAGCAGGCAGTGCT"
5. MCD7 5'-5 "TGTACTCGAGATCACCTGGATTTGGGCGTCATG"
6. MCD7 5'-6 "ACAGGGCTCTGCAATCTGTCACCA"
7. MCD7 5'-7 "CACACCCCGCCCAACTCCCCAGCA"
8. MCD7 5'-8 "TTTGAAGACCGGCAGGAG"
9. MCD7 5'-9 "GCCAGAGTGGCTGATTTGGCT"
10. MCD7 5'-10 "TGTTGTAGCCAGAGTGGCTG"
11. MCD7 5'-11 "TGCAGCATGCTGAGGAAG"
12. MCD7 5'-13 "TCAACTCCCTCCCGGCCTCT"
13. MCD7 5'-14 "CAGGCACAATTCTTGTGCA"
14. MCD7 5'-15 "ACCCATTCTAGATGGCCAT"
15. MCD7 5'-16 "CTGGCTCTGGTACCAGCAAT"
16. MCD7 5'-17 "TGTGATGGAGGAGGCATCTC"
17. MCD7 5'-18 "AGGAATCTCCGTGCGTAGTG"
18. MCD7 5'-19 "CAGCAGAAACAACGTTACCC"
19. MCD7 5'-20 "TCGACTGTTTGCCCTGGGCC"
20. MCD7 5'-21 "CTAAGGAAGGATCACCCAGG"
21. MCD7 5'-22 "CATGCTTCTAAGGAAGGATC"
22. MCD7 5'-23 "CAAGGCTACTGGGTATGCTGTGTC"
23. MCD7-MID "GAAGAACCTGACCATCATCA"

Table.2 Relative Position of Oligonucleotide Primers Used in Sequencing Mouse CD7. Oligonucleotide primers listed in Table 1 were used in cycle sequencing reactions incorporating dye-terminators for analysis on an ABI automated sequencer. The relative position and orientation of these oligo primers on mouse CD7 is demonstrated in this figure. Multiple reactions were run with each oligo primer, only a representative reaction is shown in this figure.

Table 2

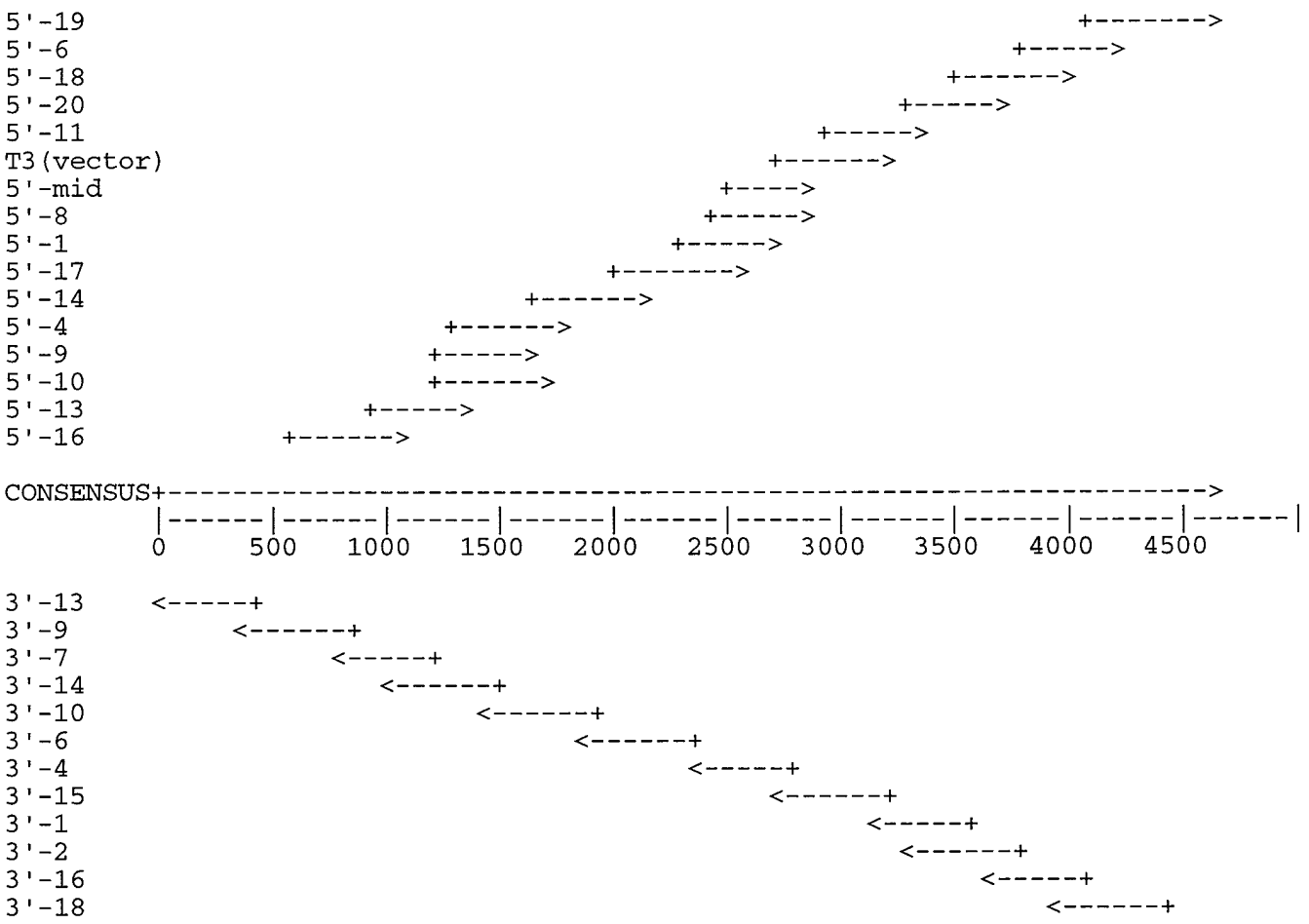
Primer Name
Orientation of Primer
5'-19
5'-6
5'-18
5'-20
5'-11
T3(vector)
5'-mid
5'-8
5'-1
5'-17
5'-14
5'-4
5'-9
5'-10
5'-13
5'-16
CONSENSUS
0
500
1000
1500
2000
2500
3000
3500
4000
4500
3'-13
3'-9
3'-7
3'-14
3'-10
3'-6
3'-4
3'-15
3'-1
3'-2
3'-16
3'-18

D. Generation of CD7 Deficient Mice

Construction of CD7 deficient mice: Disruption of the mouse CD7 gene was accomplished in 129 strain embryonic stem (ES) cells using standard methods. [koller ref]. A homologous recombination cassette was constructed using the pPNT vector (kind gift of R.C. Mulligan) (see Figure 21) by inserting 1.5kb of the mouse CD7 gene ending midway through exon 3 (corresponding to the predicted membrane proximal extracellular domain), with the addition of an in-frame stop codon 5' of the neomycin resistance gene. A 3' fragment of the mouse CD7 gene, beginning midway through intron 3 and extending 3kb 3' of exon 4 was inserted 3' of the neo gene and 5' to the herpes thymidine kinase gene. ES cell clones with homologous recombination of the disrupted allele of CD7 were identified via Southern Blot analysis of Eco R1 digested genomic DNA due to a 2 kb restriction fragment length polymorphism resulting from the insertion of the neo gene. All offspring with disrupted CD7 were identified by Southern blot analysis of DNA purified from tail tissue and digested with EcoR1 endonuclease (see Figure 22).

Tail DNA was extracted by incubating tail tissue in buffer containing 50 mM Tris pH 8.0, 100 mM EDTA, 0.5% SDS, and 1 mg/ml proteinase K at 55^{o}C overnight. The samples were phenol/chloroform extracted, ethanol precipitated with 3M sodium acetate pH 6.0 and resuspended in TE (10mM Tris pH 8.0, 1 mM EDTA).

Antibodies and reagents. Monoclonal antibodies Thy1.2 (Anti-Thy-1, Becton Dickinson, Mountain View, CA), Ly5 (anti-B220, Pharmingen, San Diego, CA), Lyt2 (anti-CD8, Becton Dickinson, Mountain View, CA), L3T4 (anti-CD4, Becton Dickinson, Mountain View, CA), CD7 (Caltag, South San Francisco, CA), OX-12 (anti-rat, Sera-Labs, Crawley Down, Sussex, England), and streptavidin-phycoerythrin (Pharmingen, San Diego, CA) were used at saturating titers for immunohistology and flow cytometry. Monoclonal antibody PK136 (anti-NK1.1) was produced from hybridoma cultured in serum free media (SFM Gibco, Grand Island, NY) and purified using affinity chromatography over a Staph protein A/G column (Pierce, Rockford, NY). This purified antibody was subsequently fluorescein conjugated and saturating titers determined. Monoclonal antibodies E13 (anti-Sca-1) (gift of I. Weissman, Stanford, CA) and F4/80 (ATCC, Rockville, MD) (anti-macrophage subset) were cultured in DMEM supplemented with FCS. Supernatants were used in indirect IF assays and flow cytometry.

Indirect immunofluorescence assays and flow cytometry. Analysis of cell surface phenotype was performed in both direct- and indirect-IF assays. Cell suspensions were analyzed using a FACStar plus flow cytometer (Becton-Dickinson, Moutain View, CA).

Preparation of cell suspensions. For all flow cytometry experiments, freshly obtained suspensions of peripheral blood and peritoneal wash cells were used. Femurs were dissected and flushed with 2ml ice cold RPMI 1640 to obtain bone marrow. Splenocytes and thymocytes were isolated by density centrifugation.

Immunization. Mice were immunized with 50 μg tetanus toxoid in complete Freund's adjuvant (CFA) on day 0 and boosted with 50 μg tetanus toxoid in incomplete Freund's adjuvant (IFA) on day 28 or 35 after the primary immunization. Mice were anesthetized with ketamine/xylazine for all immunizations.

Sample collection. Blood was collected from the retroorbital plexus using a heparinized Natelson capillary tube (Baxter Healthcare Corporation, McGaw Park, IL) while mice were under isoflurane anesthesia. Fresh fecal samples were collected and extracted using

PBS with 0.1% sodium azide. One milliliter of PBS-azide was added for every 100 mg of feces, the samples were then vortexed for 20 - 30 minutes and centrifuged in a microcentrifuge for 10 minutes. All samples were stored at -20 °C until assayed for anti-tetanus toxoid antibodies.

ELISA. Enzyme-linked immunosorbent assay (ELISA) was used to determine the presence of anti-tetanus toxoid antibodies in serum samples. TT was suspended in CBC buffer (15 mM Na_2CO_3, 35 mM $NaHCO_3$, pH 9.6) at a concentration of 3 µg/ml and plated to 96 well microtiter plates (Costar #3590, Cambridge, MA) at 50 ml/well. After overnight incubation at 4 °C, the contents of the wells was discarded and blocking buffer (CBC with 3% non-fat dry milk) was added at 200 µl/well. After incubating at room temperature for two hours, plates were stored at -20 °C until used. ELISA plates were washed four times with ELISA wash buffer (PBS, 0.05% Tween-20, 0.1% sodium azide) before the addition of samples. All samples were diluted in serum diluent (PBS, 2.5% bovine serum albumin, 2.5% non-fat dry milk, 5% normal goat serum, 0.1% sodium azide, 0.05% Tween-20) and added to ELISA plates at 100 µl/well (serum and fecal) or 50 ml/well (vaginal and salivary). After overnight incubation at 4 °C, plates were washed four times with ELISA wash buffer before the detection antibody was added. Alkaline phosphatase conjugated, goat anti-mouse IgG, -IgA, or -IgM [Southern Biotechnology Associates (SBA), Birmingham, AL] was diluted 1:1,000 (PBS, 0.05% Tween-20, 0.5% bovine serum albumin) and used as the detection antibody (100 µl/well). After incubation at room temperature for three hours, plates were washed 4 times with ELISA wash buffer and reacted with the alkaline phosphatase substrate p-nitrophenyl phosphate. After a 10 minute incubation, plates were read at 405 nm on a Titertek Multiscan Plus plate reader.

Cell isolation. Lymphocytes were removed from the spleen (SP) for in vitro assays. The SP was removed from the animal using sterile technique and placed in 15 ml complete media in a 15 x 100 mm sterile petri dish. Each spleen was cut into 5 - 6 sections using sterile scissors. Cells were expressed from each section of the spleen by pressing each section of the spleen against the bottom of the petri dish using the end of plunger from a sterile, plastic 5 cc syringe (Becton Dickinson, #9603). Leaving the spleen capsule in the petri dish, spleen cells were transferred to a 15 cc conical centrifuge tube and placed on ice for 5 minutes to allow large sections of tissue to settle. The top 13 ml of cells was then transferred to another 15 cc conical centrifuge tube and centrifuged for 8 minutes at 1,500 rpm (Sorvall RT6000B refrigerated centrifuge). To the cell pellet, buffered ammonium chloride was added (1 ml/spleen) and incubated on ice for 5 minutes to lyse red blood cells. Cells were washed 3 times in complete media and used for proliferation assays.

E. Production of Recombinant Mouse CD7 and Antibodies

Recombinant mouse CD7: A vector for bacterial production of mouse CD7 was constructed using the commercial expression cassete pQE60 (Qiagen Corp., Chatsworth, CA) which features a 5' 6-Histidine tag for easy purification. The cDNA encoding for the extracellular domain of mouse CD7 was obtained using RT-PCR with mRNA obtained from C57BL/6 thymus. The primers used in this reaction contained restriction endonuclease sequences, allowing easy cloning into the pQE60 vector. E. coli were transformed according to manufacturer protocols and induced to express mouse CD7 (mCD7) with IPTG (per manufacturer protocols). A protein corresponding to the correct apparent molecular weight was identified using SDS-PAGE. This protein was purified to homogeneity using a nickel agarose column per manufacturer protocols. The sequence of this protein was verified using Edman degradation microsequencing.

Generation of reactive antisera: mCD7 protein (250 ug) was injected in complete Freund's adjuvant followed by incomplete Freunds adjuvant into 6 week old LOU rats. Serum was obtained via retroorbital bleed and reactivity was assessed via Western blot on recombinant mCD7, thymic and splenic NP-40 extracts. Reactivity was also assessed via ELISA assay on recombinant mCD7. Finally, reactivity to C57BL/6 thymocytes was assessed as detailed above.

Generation of monoclonal antibodies to recombinant mCD7: Splenocytes were isolated from a rat with serum reactive to recombinant mCD7 and fused with mouse myeloma P3X63 cells using PEG fusion. Reactivity in resultant hybridomas was assessed via ELISA assay with plates coated with recombinant mCD7. Reactivity was confirmed via Western blot assay on recombinant mCD7, thymic and splenic NP-40 extracts (see Figure 23).

Results

A. Generation and Characterization of Human CD7 Transgenic Mice

When these studies were initiated, prior to the cloning of mouse CD7, little was known about the tissue specific and developmentally specific mechanisms regulating CD7 expression. In addition, it was hypothesized that mouse Thy-1 may be a functional homologue of human CD7 in mice. Since transgenic mice had proven to be a powerful tool for the *in vivo* study of regulation and function of numerous genes, including mouse Thy-1 (Kollias et. al. 1987), human CD4 and human CD2, human CD7 transgenic mice were constructed. The transgenic construct used in these mice included 7 kb of 5' flanking sequence and 2 kb of 3' flanking sequence in addition to the 3 kb CD7 gene. This construct was used to allow study of the *in vivo* tissue and developmentally specific transcriptional regulation of human CD7 as assayed by mRNA and protein expression in the transgenic mice. In addition, because this construct was designed to potentially give tissue specific and developmentally appropriate expression of human CD7, possible functional consequences of human CD7 expression in mouse immune cell populations were assessed.

Generation of CD7 transgenic mice

The 12 kb CD7 genomic fragment (Figure 1A) was microinjected into mouse zygotes and produced four stable CD7 transgenic lines. Two mouse lines (lines 215 and 558) showed no measurable levels of expression of the CD7 transgene in any tissue and had transgene copy numbers of one and ten, respectively. The experiments described here were performed with mouse lines 216 and 555 that carried three and five copies of the CD7 transgene, respectively, and expressed the human CD7 transgene.

Tissue-specific expression of the human CD7 transgene

Heterozygous transgene positive animals from lines 216 and 555 were studied for the presence of CD7 mRNA in multiple tissues (cecum, brain, heart, kidney, liver, spleen and thymus) using northern blot analysis. Northern blot analysis of RNA from three mice of transgenic line 216 and 555 showed the expected CD7 1.3 kb band in only spleen and thymus (Figure 1B).

CD7 transgene expression in spleen and thymus by IF assay

Next, we assayed for human CD7 protein expression in spleen and thymus using direct IF assay. In immunohistologic analysis of frozen tissue sections from line 216, CD7 transgene expression was present in both thymus and spleen with an expression pattern similar to that of CD7 in humans. Transgenic line 216 thymus expressed CD7 primarily in medullary thymocytes (Figure 2A). In 216 transgenic mouse spleen, CD7 transgene expression was similar to human CD7 expression in humans; most cells around splenic follicles were $CD7^+$ (Figure 3B). Mouse Thy-1 was expressed in a homogeneous pattern on both 216 thymocytes and splenic T cells (Figures 2B, 3A); a pattern unchanged from control mice. In line 555, there were only scattered brightly staining $CD7^+$ cells in both the spleen and thymus (Figures 2C and 3D).

Thymocyte subset expression of the CD7 transgene

Human CD7 expression levels vary on different thymocytes subpopulations. Using three color flow cytometry, we studied CD7 transgene expression on subsets of 216 mice

thymocytes and compared CD7 transgene expression with endogenous CD7 expression in human thymus. All 216 line mouse thymocytes were $CD7^+$ with most thymocytes $CD7^{lo+}$. Both $CD8^+CD4^-$ (single positive, SP) and the $CD4^-CD8^-$(double negative, DN) populations had greater CD7 transgene expression than $CD4^+CD8^+$ (double positive, DP) and $CD4^+CD8^-$ SP thymocytes (Figure 4). An identical pattern of CD7 expression was seen in SP, DN and DP human thymocytes (Figure 5).

Comparison of CD7 transgene expression with mouse Thy-1 expression

Mouse Thy-1 is expressed on brain tissues as well as T-lymphocytes. To compare expression patterns of mouse Thy-1 and the CD7 transgene, we analyzed adult mouse brain, thymus and spleen tissues in IF assays (Figures 2, 3, and 6). In transgenic mouse lines 216 and 555, the expression of mouse Thy-1 in thymus, brain, and spleen was identical to that of non-transgenic litter mates. In line 216 (Figure 6) and 555 brain (not shown), brain cortex was $Thy\text{-}1^+$ and human CD7 negative, an expression pattern like that in humans. Note the expression of the CD7 transgene in a meningeal leukocyte (identified by an arrow in Figure 6) in the 216 line brain tissue.

Hematopoietic subset expression of the CD7 transgene

In humans, mature T and NK cells as well as the earliest progenitors of myeloid, NK, B, and T cells express CD7 (Chabannon et. al. 1992, Grumayer et. al. 1991, Haynes et. al. 1989, Haynes et. al. 1979, Barcena et. al. 1993, Rabinowich et. al. 1994a and Cicuttini et. al. 1993). Therefore, splenocytes, peripheral blood leukocytes, peritoneal lavage macrophages and bone marrow cells of transgenic mouse lines 216 and 555 were analyzed for expression of the CD7 transgene. We found the CD7 transgene expressed in $Thy\text{-}1^+$ T cells, $Ly\text{-}5^+$ B cells, $PK136^+$ NK cells and $F4/80^+$ macrophages in 216 line CD7 transgenic mice, while expression of the CD7 transgene was seen only on T and B cells in the 555 transgenic line (Figure 7). The CD7 transgene expression levels were slightly higher on T-cells and NK cells than on B cells in the 216 line transgenic mice.

To assess the effect of CD7 transgene expression on mouse leukocyte populations, we quantified T, B, NK and monocyte/macrophage cell subpopulations in spleen and thymus of transgenic lines 216 and 555 compared to non-transgenic control animals (Tables 3 and 4). No perturbation of numbers of thymocyte, splenocyte, PB or peritoneal lavage leukocyte populations were observed in CD7 transgenic mice compared to control mice.

Bone marrow cell expression of the human CD7 transgene.

Human CD7 is expressed on several subsets of bone marrow progenitor cells capable of giving rise to myeloid and lymphoid lineages (Chabannon et. al. 1992, Tjonnfjord et. al. 1993 and Pohla et. al. 1993). Using flow cytometric analysis, we assayed for CD7 transgene expression in adult bone marrow from the 216 transgenic line. $CD7^{hi+}$, $CD7^{lo+}$, and $CD7^-$ populations were seen in 216 bone marrow cells (Figure 8). Analysis of CD7 expression on $Sca\text{-}1^+$ early progenitor populations in bone marrow was performed. All bone marrow Sca-1 positive cells were also $CD7^{hi+}$, indicating that CD7 was expressed on immature hematopoietic progenitors.

Finally, we used flow cytometric sorting to isolate the three CD7 subpopulations of cells in bone marrow (CD7-, $CD7^{lo+}$ and $CD7^{hi+}$) (Figure 9). Morphologic examination by light microscopy revealed that $CD7^-$ bone marrow cells were predominantly red blood cells, $CD7^{lo+}$ cells were predominantly mature granulocytes (PMNs) and $CD7^{hi+}$ cells were immature mononuclear cells (Figure 9), confirming that $CD7^{hi+}$ cells contained

immature hematopoietic populations.

CD7 transgene is an antigen of mouse T cell activation

In humans, CD7 is an antigen of T cell activation with upregulation of CD7 expression by ionomycin as well as PHA and IL-2. To assess the inducibility of the CD7 transgene in transgenic mice, we cultured splenocytes and thymocytes in the presence of IL-2 (10 U/ml) and PHA (1mg/ml) for 24 hours; the resulting levels of CD7 surface expression were assayed via flow cytometry and CD7 mRNA determined by Northern blot analysis. We found induction of the CD7 transgene cell surface expression in both 216 thymocytes and splenocytes (Figure 10 A,B). Activated splenocytes and thymocytes from line 216 showed a greater than 5 fold increase in the level of steady state CD7 mRNA as well (Figure 10C). These data indicate that the transgene used in constructing these mice includes regulatory sequences necessary to confer inducibility by PHA and IL-2.

Developmental expression of CD7 transgene

To assess the developmental expression of the CD7 transgene in transgenic mice, direct IF assays were performed on tissue obtained from mouse fetal yolk sac and liver. Numerous $CD7^+$ cells with high level CD7 expression were seen at gestational day 13 in both yolk sac and liver (Figure 11). While numerous $CD7^+$ cells were present in fetal liver, few $Thy\text{-}1^+$ cells were present, demonstrating a difference between CD7 transgene and mouse Thy-1 expression.

We analyzed gestational day 15 fetal thymus from transgenic line 216 for both CD7 and Thy-1 expression using direct immunofluorescence histology. As seen in Figure 11H, there were numerous $CD7^+$ bright cells present in the thymic medulla. Gestational day 15 fetal bone marrow from line 216 was also studied using direct IF histology. This represented a stage in development shortly after colonization of the fetal bone marrow with stem cells (Rugh 1990). Figures 11B and C show that cells in gestational day 15 bone marrow of the 216 transgene line expressed both mouse Thy-1 and the CD7 transgene. Taken together, these fetal data indicate that the transgene used to construct these mice contains the control elements necessary to confer developmentally appropriate expression of CD7.

Thus, initial characterization of human CD7 transgenic mice shows that the transgenic construct used in these mice confers expression of human CD7 in a manner similar to that in humans. The demonstration that the CD7+ bone marrow in these mice contains very early hematopoietic progenitor populations shows these mice will provide an excellent model in which to study hematopoietic reconstitution after chemotherapeutic ablation.

B. Chromosomal Mapping, Cloning and Analysis of the Mouse CD7 Gene

During the characterization of our CD7 transgenic mouse model, Yoshikawa et al. published a mouse cDNA sequence which was similar both in sequence and in mRNA expression pattern to human CD7, which they tentatively designated as mouse CD7 (Yoshikawa et. al. 1993). This finding was congruent with those observed in the human CD7 transgenic model wherein significant expression differences were noted between the human CD7 transgene and the hypothesized mouse functional homologue Thy-1. To confirm the identity of this putative mouse homologue of CD7, and to further characterize the biology of CD7 in an animal model, the mouse chromosomal map position of CD7 was determined. Subsequently, the gene for mouse CD7 was cloned, sequenced and analyzed, comparing mouse CD7 to both human CD7 and other immunoglobulin gene superfamily members. Finally, initial studies to identify possible functionally relevant transcriptional control elements in the 5' region of both mouse and human CD7 were performed.

RFLV identification

The chromosomal location of *Cd7* (mouse chromosomal locus designation of CD7) was determined using a series of genomic DNA samples obtained from an interspecific cross previously characterized for over 500 genomic loci (Seldin et. al. 1988). A probe to detect mouse CD7 was obtained using reported sequences (Yoshikawa et al. 1993) to design primers for use in the polymerase chain reaction (PCR). This probe, spanning base pairs 115-683 of the published cDNA sequence, was obtained using a mouse thymocyte cDNA library as a template from which a single product of predicted sequence was observed. Restriction fragment length variants (RFLV) were determined by Southern blot hybridization of this probe to genomic DNA from C3H/HeJ-*gld* and (C3H/HeJ-*gld* x *Mus spretus*)F1 parental mice digested with various restriction endonucleases as previously described (Seldin et al. 1988). An informative RFLV was identified using TaqI restricted DNA: C3H/HeJ-*gld*, 3.6 kb; *Mus spretus*, 2.4 kb (Figure 12).

Chromosomal map determination

To determine the map position of mouse *Cd7*, genomic DNA from 114 offspring resulting from crossing C3H/HeJ-*gld* and (C3H/HeJ-*gld* x *Mus spretus*)F1 parental mice were analyzed for the above mouse CD7 RFLV using Taq-1 restriction endonuclease. The resulting RFLV pattern correlated most closely with the genes *Pkca* and *Timp*-2, which had previously been localized to mouse chromosome 11 and were thus used as reference loci. Haplotypes of the backcross mice are shown in Figure 13. Gene order, determined by minimization of chromosome crossover events, was: *Pkca* -4.3cM +/- 1.9cM--*Timp*-2- 1.8cM+/-1.2cM--*Cd7*. Thus mouse Cd7 maps just distal to *Timp-2* on Chromosome 11. Interestingly, the *nude* mutation, which also maps to chromosome 11, maps proximal to *Pkca*, thus ruling out a mutation in CD7 as the cause of the *nude* phenotype.

Cloning of the mCD7 gene

Two lambda mouse genomic DNA libraries were screened using a random-labeled mCD7 cDNA probe. The first library, a Sau3a partial digest of 129 strain mouse genomic DNA in lambda FIX, yielded an 14kb clone designated lmCD7 21-1 (Figure 14A). Screening of a second library, a Mbo-1 partial digest of 129 strain mouse genomic DNA cloned into Charon 35, revealed a 18 kilobase clone, designated lmCD7 13-2, that contained the entire mCD7 gene (Figure 14 A).

Structure and sequence of mCD7

The mCD7 gene and promoter region was sequenced in its entirety, revealing a gene spanning 2672 bp composed of four exons separated by three short introns (Figure 14 B). In all, 4453 bp were sequenced including 1230 bp of 5' flanking sequence region, the coding region of the gene, and 552 bp of 3' flanking sequence (Figure 15). The intron-exon borders were deduced by comparison with the published cDNA sequence. All intron-exon borders contained appropriate donor and acceptor splice sites (Padgett et. al. 1986). All exonic sequences matched the previously reported mouse CD7 cDNA sequence (Yoshikawa et al. 1993).

Analysis of 5' flanking sequence

Approximately 1.2 kb of genomic DNA 5' of the initiation of transcription as defined by the first nucleotide in the mCD7 cDNA (Yoshikawa et al. 1993) were sequenced and analyzed. This region had 52.8% GC content. Using the Signal Scan analysis program (Prestridge, 1991), we analyzed the promoter region of mCD7 for the presence of previously described transcription factor binding motifs. No TATA or CCAAT motifs were identified; however, numerous nuclear transcription factor binding motifs were identified (Figure 18 A) including motifs for transcription factors known to be important in hematopoietic cells including TCF-1, CACC boxes, PEA-3, and GATA.

Comparison of mCD7 with hCD7 and mouse Thy-1

Initially, the mouse CD7 gene was compared to the human CD7 gene using the sequence analysis program COMPARE algorithm on the Wisconsin Package (Program Manual, Wisconsin Package, 1994). Figure 17 demonstrates the similarity observed between the two genes includes only the exonic sequence, with very little similarity observed elsewhere. This was significant, because in genes such as Thy-1, transcriptional regulatory elements have been described in introns 1 and 3. Overall structural organization of mCD7, mouse Thy-1 and hCD7 genes was compared and found to be similar in that all three genes were small and contained four exons (Figure 19). Intron sizes varied, but mCD7 and hCD7 had similar intron-exon boundaries. Using the sequence analysis program BESTFIT and COMPARE algorithms on the Wisconsin Package (Program Manual, Wisconsin Package, 1994), the promoter region of the mCD7 gene was compared to the 5' flanking regions of hCD7 and mouse Thy-1 (Figures 16,17). One distinct area of sequence similarity was present in all three genes (Figure 18B); another region was shared between mCD7 and hCD7 (Figure 18C).

A novel feature of the mouse Thy-1 gene is that it has two first exons, alternatively spliced at the RNA level (Ingraham and Evans 1986). We analyzed the promoter region of mCD7 using Ficket's method of open reading frame (ORF) detection (Program Manual, Wisconsin Package, 1994). An ORF of 105 bp (35 amino acids) was identified near exon one from bp 741-840 with an in-frame donor splice sequence (Padgett et. al. 1986) from bp 839-846 in mCD7. This ORF is similar in both relative size and position to exon 1a in mouse Thy-1 (Ingraham and Evans 1986). However, no transcript containing this sequence could be identified by either Northern blot or RT-PCR analysis in either splenic or thymic tissue from mature C57BL/6 female mice (data not shown). In addition, no homologous region was observed in the human CD7 5' region. While this was not an exhaustive method of analysis for the transcript, the level of transcription would have had to be exceedingly low to miss detection, or the transcript is only present either at a different developmental stage or in different tissues.

Similarity Regions Interact With Ubiquitous and Tissue-Restricted Proteins

To determine whether the identified promoter sequence similarity regions (Figures 18 B,C) were involved in DNA-protein interactions, electrophoretic mobility shift assays (EMSA) were performed using both the human and mouse sequences as probe. The most

3' similarity region probe, which includes a putative *ets* binding site (GGAA), gave the same pattern on EMSA using both the mouse and human sequence as probe (Fig 20 A and B). With the hCD7 3' probe, three discrete complexes were present as indicated by the arrows. Complex 1 was present in the three cell lines tested. Complex 2 was present as a doublet only in the mouse T cell line EL4, while complex 3 was unique to the human T cell line Jurkat. The differences in complexes 2 and 3 may represent species variation between similar factors. Both the human and mouse CD7 sequences cross-competed for the formation of complexes 2 and 3. EMSA performed with a probe in which the GGAA was mutated gave similar results; protein binding was not prevented by altering the GGAA, and the mutated oligonucleotide effectively competed the wild type oligonucleotide (data not shown), suggesting that it may not be an *ets* factor that binds to this region.

EMSA performed using oligonucleotide probes of the more 5' region of similarity showed DNA-protein interactions only in the human cell lines tested (Fig 20 C and D). The human and mouse probes for this region identified three complexes (complexes 4,5 and 6). Complexes 4 and 6 are specifically competed by self, while complex 5 shows minimal self competition. As in the earlier gel shifts, one complex (complex 4) is formed with Jurkat extract only (Fig 20 C), suggesting binding of a tissue restricted factor.

Thus we have confirmed the identity of the mouse CD7 homolog. Further examination of this gene and gene product will shed light on both the molecular mechanisms of developmentally appropriate, hematopoietic specific expression of CD7 as well as possible functional roles for CD7 during hematopoiesis. This characterization, when combined with the analysis of the biology of human CD7 in the human CD7 transgenic mouse model, will clearly establish a model system for further examination of CD7 and its relevance for human biology. This in turn will contribute to our understanding of molecular events which transpire during hematopoiesis, an understanding which will allow therapeutic intervention in the post-chemotherapeutic phase of breast cancer treatment.

C. Generation of CD7 deficient mice

To insert a null allele of mouse CD7, embryonic stem (ES) cells were transfected with linearized pCK7KO (figure 21). This vector contains a deletion of the distal half of exon 3 (encoding for the transmembrane region of mouse CD7) with an insertion of the neo^r gene at the site of the exonic deletion. In addition, an in frame stop codon was introduced at the truncated end of exon 3. It was hypothesized that the deletion and stop codon mutations would prevent the production of surface bound mouse CD7. In addition, it was postulated that removal of the mRNA concensus splice site at the distal end of exon 3 and the addition of the neo^r gene would interfere with mRNA processing, thus minimizing the production of secreted soluble CD7.

ES cell clones which contained a homologous recombination at the CD7 gene as well as offspring of chimeric mice which carried the null CD7 mutation were identified by southern hybridization (figure 22). In all offspring screened, the southern pattern was consistent with that expected from the pCD7KO map.

Since no monoclonal antibody reagents are available for mouse CD7, demonstration that homozygous CD7KO mice were deficient in CD7 production, RT-PCR of RNA from spleen and thymus were performed to identify CD7 transcripts. No full length message was identified (data not shown).

General Health

CD7 deficient mice were fertile and developed no opportunistic infections in standard housing through at least 1 year of age. The null allele of CD7 was transmitted in a mendelian fashion, and no sex bias for reproduction was noted in the population.

Lymphocyte Populations in CD7 deficient mice

To assess an influence of CD7 deficiency on lymphoid maturation, the cellular composition of spleen, thymus, peripheral blood and bone marrow was analyzed via flow cytometry. We found no pertubations in spleen, peripheral blood or bone marrow in either organ size, lymphoid subpopulation percentages or absolute counts (figure 24). A consistent difference was noted in the thymi of CD7 deficient mice, where approximately twice as many thymocytes were present (figure 24). Upon analysis of CD4/CD8 thymic subpopulations, these thymocytes were members of the CD4+CD8+ (DP) subpopulation exclusively (figure 25). We also analyzed the effect of age on this increase in thymocyte numbers and found that this difference, while not present in the first 3 weeks of life (when the thymii of both CD7 deficient and control mice are at maximal size), the difference was present by 3 months of age and persisted with increasing difference through 6 months of age.

CD7 deficient mice are competent to mount humoral responses

Antibody responses in CD7 deficient mice were assessed by analysis of both general immunoglobulin levels and of immunoglobulin responses to specific antigen. To assess general Ig production, quantitative immunoglobulin levels were measured by ELISA assay. As seen in figure26, no differences were noted either in absolute Ig levels, or in specific isotype amounts. To assess humoral response to the T cell dependent antigen tetanus toxoid, 4 month old mice were immunized with tetanus toxoid in complete freund's adjuvant. As seen in figures 27-29, no differences were noted in isotype specific responses to tetanus toxoid antigen.

D. Generation of mouse CD7 Antibodies

Generation of mCD7 reactive antisera

Wistar rats were immunized with bacterially expressed recombinant mouse CD7. Serum reactivity was assessed via ELISA assay (data not shown) and via Western blot assay against the immunogen (mCD7) and thymic and splenic extracts.

Generation of CD7 reactive antibodies.

Having obtained reactive sera in LOU rats, splenocytes from one of these rats were fused with the mouse myeloma line P3X63 and reactive hybridomas were identified via ELISA assay against recombinant mCD7. The reactivity of these hybridomas was also assessed via Western blot assay against the immunogen (mCD7) and thymic and splenic extracts. Shown is the reactivity pattern of supernatant from these hybridomas against this immunogen as well as against C57BL/6 thymocyte and splenocyte extracts (figure 23).

Reactivity pattern of CD7 monoclonal antibodies

After assessing reacivity on recombinant mCD7 and on splenic and thymic extracts, reactivity of the CD7 monoclonal antibodies was assessed on whole thymocytes via flow

cytometry . Unfortunately, these monoclonal antibodies are not reactive to whole protein on thymocyte cell surface (data not shown).

Conclusions

A. Molecular Characterization of CD7

Analysis of in vivo regulation of CD7 in transgenic mice

In this work we have characterized human CD7 transgenic mice and demonstrated that expression of the human CD7 transgene was regulated in a tissue-specific pattern that resembled the pattern of CD7 expression in humans. Further, there were differences between the expression of CD7 and Thy-1 in CD7 transgenic mice throughout development. Finally, the presence of the human CD7 molecule on mouse hematopoietic cells did not alter T cell lymphopoiesis.

Human CD7 is found on T lymphocytes throughout T cell development, and is expressed on 1% of cells in fetal liver, on most thymocytes and on 85% of PB T cells (Haynes et. al. 1989 and Haynes et. al. 1979). In humans, CD7 is also found on NK cells (Rabinowich et. al. 1994a), $CD19^+$ B-lineage fetal bone marrow cells (Grumayer et. al. 1991) and TdT^+, $My9^+$ early myeloid lineage cells (Chabannon et. al. 1992). In $CD7^+$ transgenic mice we have shown expression of CD7 throughout hematopoiesis, from early precursor cells in mouse gestational day 13 yolk sac, day 15 fetal liver and day 15 fetal thymus, as well as in the mature hematopoietic cells of several lineages, including B and T lymphocytes, macrophages and NK cells.

Although no functional consequence of human CD7 expression in transgenic mouse fetal yolk was noted, CD7 presence in placental yolk sac is consistent with expression of CD7 in human yolk sac at gestational week 7 (Haynes et. al. 1988). Since CD7 expression is tissue and developmentally restricted, and since gene expression often implies functional necessity, CD7 presence in these embryonic lymphoid precursors suggests a role for CD7 in the earliest stages of lymphopoiesis.

Consistent with CD7 playing a role in the earliest stages of lymphopoiesis was the presence of the CD7 transgene on the earliest progenitor bone marrow populations (see Figure 8) in the 216 transgenic line. Analysis of the co-expression of Sca-1, present on stem cells in bone marrow, revealed that all $Sca\text{-}1^+$ cells were also $CD7^+$. While Sca-1 expression is not limited to stem cells, it is present on stem cells, and since 100% of Sca-1+ cells were $CD7^+$, it is likely that CD7 is also expressed on stem cells in bone marrow. Sorting of $CD7^{bright, dim}$ and negative bone marrow populations (Figure 9) demonstrated that the $CD7^{bright}$ population consists largely of immature hematopoietic cells, again consistent with CD7 transgene expression on very early hematopoietic populations.

While CD7 expression in transgenic mice was comparable to the expression of CD7 in humans during lymphopoiesis, and CD7 was present on the surface of early hematopoietic progenitors in both systems, CD7 in the transgenic mice continued to be expressed on mature cells of the myeloid and B cell lineages. During normal human development, subsets of myeloid and B cell progenitors bearing the CD7 molecule have been described (Chabannon et. al. 1992 and Grumayer et. al. 1991), but as these cells terminally differentiate, CD7 expression is lost. Our results predict that either the transgene lacks negative regulatory elements for turning off CD7 transcription in non-T and non-NK cells or the mouse environment is missing one or more factors that is necessary to down-regulate CD7 in mature B and myeloid cells. As we have previously

demonstrated, human CD7 gene expression is regulated at both the transcriptional and post-transcriptional level (Ware and Haynes 1993); either mechanism may occur in this transgenic setting.

In both the fetal and adult thymus of $CD7^+$ transgenic mice, expression of the CD7 molecule resembled the pattern of human CD7 expression in several ways. Adult and fetal thymus in the transgenic mice displayed the same characteristic staining pattern on IF histology as is seen in human thymus; medullary thymocytes stained brightly, while most cortical thymocytes stained dimly, with only scattered bright $CD7^+$ cells. In addition, the differing levels of CD7 expression seen in double negative, double positive and single positive thymocytes in human thymus were comparable to the differing levels of CD7 expression seen on the thymocytes of $CD7^+$ transgenic mice (see Figure 5). These data suggest that the transgene includes regulatory elements needed for the appropriate expression of the CD7 gene throughout intrathymic T cell development and that the necessary transcription factors are conserved in the mouse and human systems.

The fact that CD7 expression is enhanced on the $CD8^+$ population of thymocytes in both human and in the transgenic mice provides insight into a functional role in this population. Genetic evidence from CD28 deficient mice, which demonstrate an intact CTL response (Shahinian et. al. 1993), suggests that molecules other than CD28 are providing co-stimulatory function in this population. Consistent with those findings, it has recently been shown that CD28 ligation in mouse $CD4^+$ or $CD8^+$ peripheral blood T-cell subsets leads to disparate results, with more marked effects on the $CD4^+$ population (Abe et. al. 1995). Furthermore, in humans, CD7 expression is down regulated and shut off in mature $CD4^+$ $CD45RO^+$ T cells, but remains high in both $CD8^+$ CTL and in NK cells. Taken together, these data suggest that CD7 may function preferentially in lymphocyte populations responsible for cell mediated responses. While the evidence for this remains circumstantial, these questions could be addressed in this model, comparing CTL responses in CD7 transgenic mice with non-transgenic littermates. In addition, examination of the endogenous mouse CD7 expression pattern will allow confirmation of preferential CD7 expression on $CD8^+$ T-cells and NK cells. Finally, future examination of CD7 deficient mice may demonstrate aberrant cell mediated responses to specific immunologic challenges.

The mouse Thy-1 gene is known to have distinct regulatory elements 3' of the promoter region that act independently to control expression in various tissues, but the elements responsible for the developmentally appropriate expression on peripheral T lymphocytes have not been identified (Vidal et. al. 1990 and Spanapoulou et. al. 1991). Expression of a mouse Thy-1 gene in transgenic mice demonstrated normal expression in bone marrow and T cell precursors but no expression in mature T cells, a pattern that resembled Thy-1 expression in human hematopoietic cells, rather than the normal mouse Thy-1 gene (Kollias et. al. 1987).

The promoters of the CD7 gene and the mouse Thy-1 gene have several similarities, including enhanced GC content, the presence of duplicated CACCC motifs, and the absence of TATA or CCAAT boxes (Schanberg et. al. 1991). There are also two areas of extensive nucleotide sequence homology one of which includes a potential ets transcription factor binding motif (Macleod et. al. 1992). Ets transcription factors are important in the regulation of many hematopoietic cell specific genes, including the immunoglobulin genes (Leiden 1993), the T cell receptor genes (Leiden 1993), and the lck gene (Seth et. al. 1992 and Wasylyk et. al. 1993). Ets binding sites have also been shown to be functional in the HTLV-1 long terminal repeats (Gitlin et. al. 1991). We

have recently cloned the mouse CD7 gene (Lee et. al. 1995) Comparison of the promoter regions of human CD7, mouse CD7 and mouse Thy-1 genes reveals conservation of the potential ets binding site motif (GGAA). Further studies are needed to identify whether these elements are important in the regulation of CD7 and mouse Thy-1 expression in T lymphocytes.

The CD7 molecule in humans is an antigen of T cell activation (Ware et. al. 1994, Morishima et. al. 1982, Haynes et. al. 1981 and Carrera et. al. 1988). CD7 expression in splenocytes from $CD7^+$ transgenic mice was inducible by rIL2 and PHA as shown by both Northern analysis and flow cytometry. These data suggested that the regulatory elements that convey inducibility following T cell activation are contained within the 12 kb CD7 transgene. Since ets factors are frequently involved in growth factor signaling pathways that regulate gene expression (Shimizu et. al. 1992), the ets binding site is a strong candidate for the induction response element.

Thus, the expression of human CD7 in transgenic mice closely follows the pattern of CD7 expression in humans, both in tissue distribution and hematopoietic development. In murine lines that expressed the CD7 transgene, regulation was appropriate, but only half the transgene stable lines expressed the CD7 transgene. Therefore, transgene expression was integration site dependent and the 12 kb fragment must not contain all of the genetic information needed to insure expression. The transgene may need a domain organizer and may be expressed only if inserted into DNA that is in a open configuration and permissive of transcription. Future experiments will identify the regulatory elements responsible for mitogenic inducibility, tissue specificity and developmental expression of human CD7 in transgenic mice. In addition, this work has shown that this transgenic model closely follows the pattern of CD7 expression in humans and thus will be a useful animal model in which to study post-chemotherapeutic hematopoietic reconstitution.

B. Identification, cloning and characterization of mouse CD7

When this work was initiated, no mouse homologue of CD7 had been described. The data from our transgenic mouse model strongly suggested that Thy-1 was not the hypothesized functional homologue of CD7. Concurrently, a mouse cDNA with similarity to human CD7 was published (Yoshikawa et al 1993). To establish the identity of this potential homologue, and to further explore the biology of CD7 in a mouse model, we initially mapped the chromosomal location of mouse CD7 and subsequently cloned and analyzed the mouse CD7 gene.

Chromosomal Mapping of mouse CD7

A powerful tool for establishing the homology of a gene between species has been to demonstrate that the gene candidates map to homologous loci in those species (Danvis and Goldby 1963 and Oakley et. al. 1992). To confirm the identity of the putative mouse CD7 cDNA, we examined the map position of mouse CD7 in a backcross system characterized for over 500 loci (Seldin et. al. 1988). Mouse CD7 was mapped adjacent to the reference loci genes *Pkca* and *Timp*-2 which had been previously localized to mouse Chromosome 11. Gene order, determined by minimization of chromosome crossover events, was: *Pkca* -4.3cM +/- 1.9cM--*Timp*-2- 1.8cM+/-1.2cM--*CD7*. These data correlated with the previously characterized map position of human CD7, which maps on the long arm of human Chromosome 17 at band q25 confirming the identity of this gene as mouse CD7. We found that the chromosomal location of mouse CD7 did not map to any immunologically related or otherwise characterized mouse mutation.

Cloning and analysis of the mouse CD7 gene

Having confirmed the identity of the mouse homologue of CD7, cloning of the mouse CD7 gene was pursued. The goals of cloning and sequencing mouse CD7 were twofold.

First, the gene was cloned and sequenced so that comparative sequence analysis between mouse and human CD7 could be performed, searching for conserved sequence elements which would imply functionally important sequence motifs. Secondly, once the gene was obtained, it would provide a powerful tool for molecular genetic techniques such as deletion analysis to examine promoter function, or as part of a gene-targeting vector for use in making CD7 deficient mice.

In this work, we have described the cloning and characterization of the mouse CD7 gene and have identified two regions of similarity in the 5' flanking regions of the mouse and human CD7 genes that may represent cis-acting regulatory elements. Computer analysis revealed the mouse CD7 gene was similar to human CD7 both in structure and size (see figure 19). Like human CD7, the mouse gene for CD7 consisted of four exons residing on approximately 3 kb of DNA. The promoter of both mouse CD7 and human CD7 were deficient in TATA and CCAAT motifs. The promoter for mouse CD7 was not as GC rich as its human counterpart with human CD7 having 66.6 % GC content over 506 b.p. (Schanberg et. al. 1991) and mCD7 having 52.8% GC content over 1250 b.p.

Extending previous comparisons of the 5' flanking sequence of the mouse Thy-1 and human CD7 genes (Schanberg et. al. 1991) to include the mouse CD7 gene revealed multiple similarities. All three promoters contain neither a TATA nor a CCAAT box. Additionally, duplicated CACCC motifs are present in each of these promoters, as well as consensus sequence motifs for the ubiquitous transcription factors Sp1 and AP-2. Of note, one of the similarity regions reported earlier in mouse Thy-1 and human CD7 is also conserved in the 5' flanking region of the mouse CD7 gene: at bp 1111-1160 of the mouse gene (see Figure 17 and Figure 18). We have also identified a second region of similarity present in the mouse and human CD7 genes at bp 864-892 (see Figure 18C). Both of these regions are sites of DNA-protein interaction *in vitro* as shown by EMSA, and may be functionally important in the developmental and tissue-specific regulation of these T cell genes.

The most proximal of the homology regions spans a 34 bp region that encompasses a CACC motif and a putative *ets* binding site (GGAA). The conservation of this region in three T cell-specific genes across species (mouse Thy-1, mCD7 and hCD7) suggests this region may contain elements important in conveying tissue specific gene expression. CACCC elements are important in the regulation of other hematopoietic genes, including globin genes (Lin et. al. 1992 and Baysal et. al. 1994), T cell receptor genes (Wang et. al. 1993), and immunoglobulin genes (Xu and Stavnezer 1992). The cooperative association of a CACCC element with a *ets -1* binding site was recently described in the parathyroid hormone-related protein promoter (Dittmer et. al. 1994). These two binding sites may work cooperatively to regulate activity of the mouse and hCD7 promoters. The putative *ets* binding site in this region matches identically an octamer (CAGGAAGC) recently identified as an *ets* binding site in the IL6 response element in the junB promoter (Nakajimi et. al. 1993). A similar octamer (CAGGAAGT) in the lck type I promoter has also been shown to bind *ets* related transcription factors (McCracken et. al. 1994). In the junB promoter, mutating the ets binding site disrupted binding of *ets* factors, but did not prevent IL6 induction. Further studies suggested that IL6 responsiveness in the junB promoter is conveyed by the complexing of multiple STAT family transcription factors with the *ets* binding site (Fujitani et. al. 1994). IL6, like interferons (Darnell et. al. 1994) and IL4 (Hou et. al. 1994), activates the tyrosine phosphorylated STAT factors resulting in the translocation of the proteins from the cytoplasm to the nucleus where IL6 responsive genes are activated (Darnell et. al. 1994). IL6 is known to be involved with T cell activation, growth and differentiation (Van Snick 1990) and could exert some of these affects through the regulation of CD7. While it is not known whether CD7 is an IL6 responsive gene, it may be that STAT factors, activated by IL6 or another cytokine,

are important in the regulation of the CD7 gene. However, the possibility that a single region could bind both *ets* and STAT transcription factors permits a convergence of several distinct signal transduction pathways to control a single gene. Further studies to delineate the factors that bind to this similarity region in the CD7 mouse and human genes are ongoing.

The further upstream similarity region, shared between mouse and human CD7, complexed with extract from the two human cell lines tested, but not the mouse cell line. This may suggest that binding of mouse factors requires additional sequence not included within the region of the probe or that there are different factors with different DNA recognition sites in the human and mouse environment. This region falls at -347 in human CD7 which corresponds to an area that appears to contain a repressor by transient transfection studies performed in Jurkat cells (Schanberg, LE unpublished observation). Additional studies are needed to characterize the factors that bind to this region.

Consistent with CD7 being a lymphoid specific gene, numerous lymphohematopoeitic transcription factor consensus sites were identified in the 5' region of mouse CD7 (Figure 5A). Of note, there were a large number of TCF-1 recognition motifs. TCF-1, a member of the High Mobility Group (HMG) protein family, is a T cell specific transcription factor known to be important in the tissue-specific activation of the T cell receptor a gene (Waterman et. al. 1991 and Oosterwagel et. al. 1991), lck gene (Waterman et. al. 1991), and the CD3e gene (Oosterwagel et. al. 1991, Waterman and Jones 1990 and van der Wetering et. al. 1991). Interestingly, the activity of the TCF-1 binding site in the T cell receptor a chain has been shown to be dependent on neighboring elements (Waterman and Jones 1990), one of which binds *ets-1* (Ho et. al. 1990). Several potential binding sites for *ets* family proteins were identified in the promoter of mCD7, one in close proximity to a TCF-1 consensus site. *Ets* factors are expressed in T- and B- cell lineages and have been implicated as a component of the signal transduction network in these cells (Seth et. al. 1992 and Wasylyk et. al. 1993).

Thus, the mCD7 promoter, like the hCD7 promoter, contains the motifs for both ubiquitous and tissue-specific transcription factors. These transcription factors likely work in concert to control both tissue-specific and developmental regulation of this gene. While identification of consensus sequence motifs for DNA binding factors has been demonstrated a powerful technique for targeting sequence regions for further investigation, it must be remembered that this method of analysis by itself is only suggestive of functional sequence motifs. Further analysis of the promoters of hCD7 and mCD7, using functional assays such as EMSA and deletional expression analysis will be important for understanding lymphoid tissue specificity in these genes and may lead to insights in the molecular mechanisms of T cell lineage determination and T cell maturation.

In addition, this work has provided the tools for construction of CD7 deficient mice, whose analysis will provide further insight into the role of CD7 in T-cell lineage determination and maturation. Herein, we describe construction and initial characterization of CD7 deficient mice. In short, these mice are healthy and viable, without obvious immunodeficiency, with healthy CD7 deficient offspring surviving to over a year of age. Lymphoid development was not substantially altered in these mice, which exhibit no perturbations in lymphoid subsets in bone marrow, spleen or peripheral blood. Normal serum immunoglobulin levels as well as typical immunoglobulin responses to specific antigen demonstrate no obvious defect in T-cell dependent humoral responses.

CD7 deficient mice did demonstrate some intriguing differences compared with control mice. In particular, the presence of an expanded CD4+CD8+ thymocyte population in CD7 deficient mice suggests a role for CD7 in thymopoiesis. This is particularily interesting since in humans, CD7 is one of the earliest differentiation markers expressed on the most immature thymocyte populations. Whether this increase in thymocyte numbers is due to a partial defect in thymocyte apoptosis, or a hyperproliferative state of selecting thymocytes or to a subtle defect in the process of thymocyte selection (either positive or negative) is not clear at present. Regardless of the exact nature of the thymic defect, the overall process of selection remains intact evidenced by the lack of lymphoid subset perturbation in the periphery (spleen, peripheral blood) of CD7 deficient mice. The exact nature of the thymic defect is currently being tested in a series of T-cell receptor transgenic crosses with CD7 deficient mice.

Finally, using the mCD7 sequence to generate recombinant mCD7, this work will continue the development of antibodies reactive to mCD7 which will allow further characterization of CD7+ cells in mice. This reagent will also allow purification of CD7+ bone marrow progenitors for hematopoietic reconstitution studies.

Future Directions

While the human CD7 transgenic mice have provided valuable insight into the biology of CD7 on hematopoietic precursors in an animal model, the confirmation of the identity of the mouse CD7 homolog provides a compelling new course of action for further investigation of both the role of CD7 in hematopoiesis, and characterization of the hematopoietic progenitors which express CD7 in mice. Toward this end, we initiated two new approaches for further study of CD7 in mice (see revised SOW). The first is to develop antibody reagents to study the expression pattern of CD7 in mice. In particular, we will continue to focus on T-lineage cells in the periphery and on hematopoietic progenitors in the bone marrow. This is a particularily attractive direction because of the large number of antibody reagents currently available which will allow precise delineation of bone marrow progenitors expressing CD7. Given the vast amount of work previously done in mice as an animal model for human hematopoiesis, the data gathered in this project will be readily interpretable for human applications.

The second approach we have undertaken to define the role of CD7 in mouse hematopoiesis has been to construct a CD7 deficient mouse line using targeted homologous recombination. These mice have been made using the mouse CD7 gene (whose cloning and characterization is descibed above) subcloned into a targeted homologous recombination vector (pPNT, kind gift of R.C. Mulligan). Examination of CD7 deficient mice will afford further insight into the role of CD7 during hematopoiesis. These mice will also clarify the importance of the CD7+ population of progenitors present in bone marrow during hematopoietic reconstitution. By defining the differentiative potential of possible hematopoietic progenitors lacking CD7, the importance of including this marker in bone marrow reconstituting populations will be defined.

Bibliography

1. Abe, R.; Vandenberghe, P.; Craighead, N.; Smoot, D. S.; Lee, K. P.; June, C. H. Distinct signal transduction in mouse CD4+ and CD8+ splenic T cells after CD28 receptor ligation. J Immunol. 1995; 154(3): 985-97.

2. Anonymous. Systemic treatment of early breast cancer by hormonal, cytotoxic, or immune therapy. 133 randomised trials involving 31,000 recurrences and 24,000 deaths among 75,000 women. Early Breast Cancer Trialists' Collaborative Group [see comments]. Lancet. 1992 Jan 11; 339(8785): 71-85.

3. Arber, W. Enquist , L., Hohn, B., Murray, N. and Murray, K. Lambda II: Experimental Methods For Use With Lambda. Cold Spring Harbor, NY: Cold Spring Harbor Laboratory Press; 1983.

4. Aruffo, A.; Seed, B. Molecular cloning of two CD7 (T-cell leukemia antigen) cDNAs by a COS cell expression system. EMBO J. 1987; 6(11): 3313-6.

5. Barcena, A.; Muench, M. O.; Galy, A. H.; Cupp, J.; Roncarolo, M. G.; Phillips, J. H.; Spits, H. Phenotypic and functional analysis of T-cell precursors in the human fetal liver and thymus: CD7 expression in the early stages of T- and myeloid-cell development. Blood. 1993; 82(11): 3401-14.

6. Baysal, E.; Ribeiro, M. L.; Huisman, T. H. Binding of nuclear factors to the proximal and distal CACCC motifs of the beta-globin gene promoter: implications for the -101 (C-->T) 'silent' beta-thalassemia mutation. Acta Haematol. 1994; 91(1): 16-20.

7. Benton, W. D.; Davis, R. W. Screening lambdagt recombinant clones by hybridization to single plaques in situ. Science. 1977; 196(4286): 180-2.

8. Bishop, D. T. The information content of phase-known matings for ordering genetic loci [published erratum appears in Genet Epidemiol 1987;4(2):159]. Genet Epidemiol. 1985; 2(4): 349-61.

9. Brinster R.L.; Palmiter, R. D. Genetic Manipulation of the Mammalian Ovum and Early Embryo. New York: Cold Spring Harbor Laboratory Press; 1985.

10. Buell, P. Chkanging incidence of breast cancer in Japanese-American women. Journal of the National Cancer Institute. 1973; 51: 1479-1483.

11. Campana, D.; Janossy, g.; Coustane-Smith, E.; Amlot, P. L.; Tian, W. T.; Ip, S.; Wong, L. The expression of T cell receptor-associated proteins during T cell ontogeny in man. Journal of Immunology. 1989; 142: 57-66.

12. Cancer incidence in five continents. Lyon, France; 1987; 5. (Muir, C.; Waterhouse, J.; Mack, T.; Powell J.; Whelan, S.International Agency for Research on Cancer).

13. Carrera, A. C.; Rincon, M.; Sanchez-Madrid, F.; Lopez-Botet, M.; de, Landazuri MO. Triggering of co-mitogenic signals in T cell proliferation by anti-LFA-1 (CD18, CD11a), LFA-3, and CD7 monoclonal antibodies. J Immunol. 1988; 141(6): 1919-24.

14. Chabannon, C.; Wood, P.; Torok-Storb, B. Expression of CD7 on normal human myeloid progenitors. J Immunol. 1992; 149(6): 2110-2113.

15. Cicuttini, F. M.; Martin, M.; Petrie, H. T.; Boyd, A. W. A novel population of natural killer progenitor cells isolated from human umbilical cord blood. J Immunol. 1993; 151(1): 29-37.

16. Danvis, D. E. and Goldby, F.B. Principles in Mammalogy. New York, NY: Van Nostrand-Reinhold; 1963.

17. Darnell, JE Jr; Kerr, I. M.; Stark, G. R. Jak-STAT pathways and transcriptional activation in response to IFNs and other extracellular signaling proteins. [Review]. Science. 1994; 264(5164): 1415-21.

18. Denning, S. M.; Kurtzberg, J.; Leslie, D. S.; Haynes, B. F. Human postnatal CD4-CD8- CD3- thymic T cell precursors differentiate in vitro into T cell receptor delta-bearing cells. Journal of Immunology. 1989 May 1; 142(9): 2988-97.

19. Dignam, J. D.; Lebovitz, R. M.; Roeder, R. G. Accurate transcription initiation by RNA polymerase II in a soluble extract from isolated mammalian nuclei. Nucleic Acids Res. 1983; 11(5): 1475-89.

20. Dittmer, J.; Gegonne, A.; Gitlin, S. D.; Ghysdael, J.; Brady, J. N. Regulation of parathyroid hormone-related protein (PTHrP) gene expression. Sp1 binds through an inverted CACCC motif and regulates promoter activity in cooperation with Ets1. J Biol Chem. 1994; 269(34): 21428-34.

21. Eisenbarth, G. S.; Haynes, B. F.; Schroer, J. A.; Fauci, A. S. Production of monoclonal antibodies reacting with peripheral blood mononuclear cell surface differentiation antigens. Journal of Immunology. 1980 Mar; 124(3): 1237-44.

22. Feuer, E. J.; Wun, L. M.; Boring, C. C.; Flanders, W. D.; Timmel, M. J.; Tong, T. The lifetime risk of developing breast cancer [see comments]. Journal of the National Cancer Institute. 1993 Jun 2; 85(11): 892-7.

23. Fujitani, Y.; Nakajima, K.; Kojima, H.; Nakae, K.; Takeda, T.; Hirano, T. Transcriptional activation of the IL-6 response element in the junB promoter is mediated by multiple Stat family proteins. Biochem Biophys Res Commun. 1994; 202(2): 1181-7.

24. Genetics Computer Group. Program Manual for the Wisconsin Package, Version 8. Madison, Wisconsin.; 1994.

25. Gitlin, S. D.; Bosselut, R.; Gegonne, A.; Ghysdael, J.; Brady, J. N. Sequence-specific interaction of the Ets1 protein with the long terminal repeat of the human T-lymphotropic virus type I. J Virol. 1991; 65(10): 5513-23.

26. Glisin, V.; Crkvenjakov, R.; Byus, C. Ribonucleic acid isolated by cesium chloride centrifugation. Biochemistry. 1974; 13(12): 2633-7.

27. Green, E. L. Genetics and Probability in Animal Breeding Experiments. New York, NY: Oxford University Press; 1981.

28. Grumayer, E. R.; Griesinger, F.; Hummell, D. S.; Brunning, R. D.; Kersey, J. H. Identification of novel B-lineage cells in human fetal bone marrow that coexpress CD7. Blood. 1991; 77(1): 64-8.

29. Hanna, N.; Fidler, I. J. Role of natural killer cells in the destruction of circulating tumor emboli. Journal of the National Cancer Institute. 1980 Oct; 65(4): 801-9.

30. Haynes, B. F. Human T lymphocyte antigens as defined by monoclonal antibodies. [Review]. Immunol Rev. 1981; 57: 127-161.

31. Haynes, B. F.; Denning, S. M.; Singer, K. H.; Kurtzberg, J. Ontogeny of T-cell precursors: a model for the initial stages of human T-cell development. Immunol Today. 1989; 10(3): 87-91.

32. Haynes, B. F.; Eisenbarth, G. S.; Fauci, A. S. Human lymphocyte antigens: production of a monoclonal antibody that defines functional thymus-derived lymphocyte subsets. Proc Natl Acad Sci U S A. 1979; 76(11): 5829-33.

33. Haynes, B. F.; Mann, D. L.; Hemler, M. E.; Schroer, J. A.; Shelhamer, J. H.; Eisenbarth, G. S.; Strominger, J. L.; Thomas, C. A.; Mostowski, H. S.; Fauci, A. S. Characterization of a monoclonal antibody that defines an immunoregulatory T cell subset for immunoglobulin synthesis in humans. Proceedings of the National Academy of Sciences of the United States of America. 1980 May; 77(5): 2914-8.

34. Haynes, B. F.; Martin, M. E.; Kay, H. H.; Kurtzberg, J. Early events in human T cell ontogeny. Phenotpyic characterization and immunohistologic localization of T cell precursors in early human fetal tissues. Journal of Experimental Medicine. 1988; 168: 1061-1080.

35. Haynes, B. F.; Metzgar, R. S.; Minna, J. D.; Bunn, P. A. Phenotypic characterization of cutaneous T-cell lymphoma. Use of monoclonal antibodies to compare with other malignant T cells. N Engl J Med. 1981; 304(22): 1319-23.

36. Henderson, I. C.; CAnellos, G. P. Cancer of the breast: the past decade. New England Journal of Medicine. 1980; 302: 17-30, 79-80.

37. Hnatowich, D. J.; Virzi, F.; Rusckowski, M. Investigations of avidin and biotin for imaging applications. J Nucl Med. 1987; 28(8): 1294-302.

38. Ho, I. C.; Bhat, N. K.; Gottschalk, L. R.; Lindsten, T.; Thompson, C. B.; Papas, T. S.; Leiden, J. M. Sequence-specific binding of human Ets-1 to the T cell receptor alpha gene enhancer. Science. 1990; 250(4982): 814-8.

39. Hou, J.; Schindler, U.; Henzel, W. J.; Ho, T. C.; Brasseur, M.; McKnight, S. L. An interleukin-4-induced transcription factor: IL-4 Stat. Science. 1994; 265(5179): 1701-6.

40. Ikuta, K.; Uchida, N.; Friedman, J.; Weissman, I. L. Lymphocyte development from stem cells. Annual Review of Immunology 1992;10:759-83.

41. Ingraham, H. A.; Evans, G. A. Characterization of two atypical promoters and alternate mRNA processing in the mouse Thy-1.2 glycoprotein gene. Mol Cell Biol. 1986; 6(8): 2923-31.

42. Innis, M. A.; Gelford, D. H.; Sninsky, J. J.; White T.J. PCR Protocols: A Guide to Methods and Applications. San Diego, CA: Academic Press; 1990.

43. Kamps, W. A.; Timens, W.; De, Boer GJ; Spanjer, H. H.; Poppema, S. In situ study of haemopoiesis in human fetal liver. Scandinavian Journal of Immunology. 1989 Oct; 30(4): 399-408.

44. Kollias, G.; Spanopoulou, E.; Grosveld, F.; Ritter, M.; Beech, J.; Morris, R. Differential regulation of a Thy-1 gene in transgenic mice. Proc Natl Acad Sci U S A. 1987; 84(6): 1492-6.

45. Lamoyi, E.; Nisonoff, A. Preparation of F(ab')2 fragments from mouse IgG of various subclasses. J Immunol Methods. 1983; 56(2): 235-43.

46. Lee, D. M.; Watson, M. L.; Seldin, M. F. Mouse Cd7 maps to chromosome 11. Immunogenetics. 1994; 39(4): 289-90.

47. Leiden, J. M. Transcriptional regulation of T cell receptor genes. [Review]. Annu Rev Immunol. 1993; 11: 539-570.

48. Lin, H. J.; Han, C. Y.; Nienhuis, A. W. Functional profile of the human fetal gamma-globin gene upstream promoter region. Am J Hum Genet. 1992; 51(2): 363-70.

49. Lobach, D. F.; Hensley, L. L.; Ho, W.; Haynes, B. F. Human T cell antigen expression during the early stages of fetal thymic maturation. Journal of Immunology. 1985; 135: 1752-1759.

50. Loenen, W. A.; Blattner, F. R. Lambda Charon vectors (Ch32, 33, 34 and 35) adapted for DNA cloning in recombination-deficient hosts. Gene. 1983; 26(2-3): 171-9.

51. Macleod, K.; Leprince, D.; Stehelin, D. The ets gene family. [Review]. Trends Biochem Sci. 1992; 17(7): 251-6.

52. McCracken, S.; Leung, S.; Bosselut, R.; Ghysdael, J.; Miyamoto, N. G. Myb and Ets related transcription factors are required for activity of the human lck type I promoter. Oncogene. 1994; 9(12): 3609-15.

53. Miller, B. A.; Feuer, E. J.; Hankey, B. F. The incresing incidence of breast cancer since 1982: relevance of early detection. Cancer Causes Control. 1991; 2: 67-74.

54. Mishell, B. B.; Shiigi, S. M. Selected Methods in Cellular Immunology. New York, NY: W.H. Freeman and Co.; 1980.

55. Morishima, Y.; Kobayashi, M.; Yang, S. Y.; Collins, N. H.; Hoffmann, M. K.; Dupont, B. Functionally different T lymphocyte subpopulations determined by their sensitivity to complement-dependent cell lysis with the monoclonal antibody 4A. J Immunol. 1982; 129(3): 1091-8.

56. Mossalayi, M. D.; Dalloul, A. H.; Bertho, J. M.; Lecron, J. C.; Goube, de Laforest PG; Debre, P. In vitro differentiation and proliferation of purified human thymic

and bone marrow CD7+CD2- T-cell precursors. Experimental Hematology. 1990 May; 18(4): 326-31.

57. Nakajima, K.; Kusafuka, T.; Takeda, T.; Fujitani, Y.; Nakae, K.; Hirano, T. Identification of a novel interleukin-6 response element containing an Ets-binding site and a CRE-like site in the junB promoter. Mol Cell Biol. 1993; 13(5): 3027-41.

58. National Center for Health Statistics. Vital Statistics for the United States, 1987. Mortality. Part A. Washington D.C. Government Printing Office. 1990; 2.

59. Oakey, R. J.; Watson, M. L.; Seldin, M. F. Construction of a physical map on mouse and human chromosome 1: comparison of 13 Mb of mouse and 11 Mb of human DNA. Hum Mol Genet. 1992; 1(8): 613-20.

60. Oosterwegel, M.; van, de Wetering M.; Dooijes, D.; Klomp, L.; Winoto, A.; Georgopoulos, K.; Meijlink, F.; Clevers, H. Cloning of murine TCF-1, a T cell-specific transcription factor interacting with functional motifs in the CD3-epsilon and T cell receptor alpha enhancers. J Exp Med. 1991; 173(5): 1133-42.

61. O'Shaughnessy, J. A.; Cowan, K. H. Dose-intensive therapy for breast cancer. Journal of the American Medical Association. 1993; 270(17): 2089-2092.

62. Padgett, R. A.; Grabowski, P. J.; Konarska, M. M.; Seiler, S.; Sharp, P. A. Splicing of messenger RNA precursors. [Review]. Annu Rev Biochem. 1986; 55: 1119-1150.

63. Perussia, B.; Starr, S.; Abraham, S.; Fanning, V.; Trinchieri, G. Human natural killer cells analyzed by B73.1, a monoclonal antibody blocking Fc receptor functions. I. Characterization of the lymphocyte subset reactive with B73.1. Journal of Immunology. 1983 May; 130(5): 2133-41.

64. Peters, W. P.; Ross, M.; Vredenburgh, J. J.; Meisenberg, B.; Marks, L. B.; Winer, E.; Kurtzberg, J.; Bast, RC Jr; Jones, R.; Shpall, E.; et, a. l. High-dose chemotherapy and autologous bone marrow support as consolidation after standard-dose adjuvant therapy for high-risk primary breast cancer. Journal of Clinical Oncology. 1993 Jun; 11(6): 1132-43.

65. Pohla, H.; Adibzadeh, M.; Buhring, H. J.; Siegels-Hubenthal, P.; Deikeler, T.; Owsianowsky, M.; Schenk, A.; Rehbein, A.; Schlotz, E.; Schaudt, K.; et, a. l. Evolution of a CD3+CD4+ alpha/beta T-cell receptor+ mature T-cell clone from CD3-CD7+ sorted human bone marrow cells. Dev Immunol. 1993; 3(3): 197-210.

66. Prestridge, D. S. SIGNAL SCAN: a computer program that scans DNA sequences for eukaryotic transcriptional elements. Comput Appl Biosci. 1991; 7(2): 203-6.

67. Rabinowich, H.; Lin, W. C.; Herberman, R. B.; Whiteside, T. L. Signaling via CD7 molecules on human NK cells. Induction of tyrosine phosphorylation and beta 1 integrin-mediated adhesion to fibronectin. J Immunol. 1994; 153(8): 3504-13.

68. Rabinowich, H.; Pricop, L.; Herberman, R. B.; Whiteside, T. L. Expression and function of CD7 molecule on human natural killer cells. J Immunol. 1994; 152(2): 517-26.

69. Roberts, L. Zeroing in on a breast cancer susceptibility gene [news]. Science. 1993 Jan 29; 259(5095): 622-5.

70. Rugh, R. The Mouse: Its Reproduction and Development. New York, New York: Oxford University Press; 1990.

71. Sanchez, M. J.; Gutierrez-Ramos, J. C.; Fernandez, E.; Leonardo, E.; Lozano, J.; Martinez, C.; Toribio, M. L. Putative prethymic T cell precursors within the early human embryonic liver: a molecular and functional analysis. Journal of Experimental Medicine. 1993 Jan 1; 177(1): 19-33.

72. Schanberg, L. E.; Fleenor, D. E.; Kurtzberg, J.; Haynes, B. F.; Kaufman, R. E. Isolation and characterization of the genomic human CD7 gene: structural similarity with the murine Thy-1 gene. Proc Natl Acad Sci U S A. 1991; 88(2): 603-7.

73. Seldin, M. F.; Morse, HC 3d; Reeves, J. P.; Scribner, C. L.; LeBoeuf, R. C.; Steinberg, A. D. Genetic analysis of autoimmune gld mice. I. Identification of a restriction fragment length polymorphism closely linked to the gld mutation within a conserved linkage group. J Exp Med. 1988; 167(2): 688-93.

74. Seth, A.; Ascione, R.; Fisher, R. J.; Mavrothalassitis, G. J.; Bhat, N. K.; Papas, T. S. The ets gene family. [Review]. Cell Growth Differ. 1992; 3(5): 327-34.

75. Shahinian, A.; Pfeffer, K.; Lee, K. P.; Kundig, T. M.; Kishihara, K.; Wakeham, A.; Kawai, K.; Ohashi, P. S.; Thompson, C. B.; Mak, T. W. Differential T cell costimulatory requirements in CD28-deficient mice. Science. 1993; 261(5121): 609-12.

76. Shimizu, Y.; van, Seventer GA; Ennis, E.; Newman, W.; Horgan, K. J.; Shaw, S. Crosslinking of the T cell-specific accessory molecules CD7 and CD28 modulates T cell adhesion. J Exp Med. 1992; 175(2): 577-82.

77. Smeland, E. B.; Funderud, S.; Kvalheim, G.; Gaudernack, G.; Rasmussen, A. M.; Rusten, L.; Wang, M. Y.; Tindle, R. W.; Blomhoff, H. K.; Egeland, T. Isolation and characterization of human hematopoietic progenitor cells: an effective method for positive selection of CD34+ cells. Leukemia. 1992 Aug; 6(8): 845-52.

78. Southern, E. M. Detection of specific sequences among DNA fragments separated by gel electrophoresis. J Mol Biol. 1975; 98(3): 503-17.

79. Spanopoulou, E.; Giguere, V.; Grosveld, F. The functional domains of the murine Thy-1 gene promoter. Mol Cell Biol. 1991; 11(4): 2216-28.

80. Sykes, K.; Kaufman, R. A naturally occurring gamma globin gene mutation enhances SP1 binding activity. Mol Cell Biol. 1990; 10(1): 95-102.

81. Tjonnfjord, G. E.; Veiby, O. P.; Steen, R.; Egeland, T. T lymphocyte differentiation in vitro from adult human prethymic CD34+ bone marrow cells. Journal of Experimental Medicine. 1993; 177(6): 1531-9.

82. Trinchieri, G. Biology of natural killer cells. Advances In Immunology 1989;47:187-376.

83. van, de Wetering M.; Oosterwegel, M.; Dooijes, D.; Clevers, H. Identification and cloning of TCF-1, a T lymphocyte-specific transcription factor containing a sequence-specific HMG box. EMBO J. 1991; 10(1): 123-32.

84. Van, Snick J. Interleukin-6: an overview. [Review]. Annu Rev Immunol. 1990; 8: 253-278.

85. Vidal, M.; Morris, R.; Grosveld, F.; Spanopoulou, E. Tissue-specific control elements of the Thy-1 gene. EMBO J. 1990; 9(3): 833-40.

86. Wang, Y.; Kobori, J. A.; Hood, L. The ht beta gene encodes a novel CACCC box-binding protein that regulates T-cell receptor gene expression. Mol Cell Biol. 1993; 13(9): 5691-701.

87. Ware, R. E.; Haynes, B. F. T cell CD7 mRNA expression is regulated by both transcriptional and post-transcriptional mechanisms. Int Immunol. 1993; 5(2): 179-87.

88. Wasylyk, B.; Hahn, S. L.; Giovane, A. The Ets family of transcription factors [published erratum appears in Eur J Biochem 1993 Aug 1;215(3):907]. [Review]. Eur J Biochem. 1993; 211(1-2): 7-18.

89. Waterman, M. L.; Fischer, W. H.; Jones, K. A. A thymus-specific member of the HMG protein family regulates the human T cell receptor C alpha enhancer. Genes Dev. 1991; 5(4): 656-69.

90. Waterman, M. L.; Jones, K. A. Purification of TCF-1 alpha, a T-cell-specific transcription factor that activates the T-cell receptor C alpha gene enhancer in a context-dependent manner. New Biol. 1990; 2(7): 621-36.

91. Watson, M. L. and Seldin, M.F. Application of Mouse Crosses toward Defining Genetics of Disease Phenotypes. Methods in Molecular Genetics. 5 ed. New York, NY: Academic Press; 1994: 369-387.

92. Welsh, R. M. Regulation of virus infections by natural killer cells. A review. Natural Immunity & Cell Growth Regulation. 1986; 5(4): 169-99.

93. Xu, M. Z.; Stavnezer, J. Regulation of transcription of immunoglobulin germ-line gamma 1 RNA: analysis of the promoter/enhancer. EMBO J. 1992; 11(1): 145-55.

94. Yoshikawa, K.; Seto, M.; Ueda, R.; Obata, Y.; Fukatsu, H.; Segawa, A.; Takahashi, T. Isolation and characterization of mouse CD7 cDNA. Immunogenetics. 1993; 37(2): 114-9.

Appendix

Figure 1 CD7 Transgene Map and Tissue Distribution of Transgene Expression. Panel A shows the restriction map of the human genomic DNA fragment used to construct CD7 transgenic mice. Bold arrows represent previously identified DNase I hypersensitivity sites. Darkened boxes correspond to CD7 exons. Panel B shows the tissue distribution of human CD7 mRNA expression in CD7 transgenic mouse line 216 as assessed by Northern Blot analysis. The upper panel is a representative Northern blot radiograph. The lower panel is an acridine orange stain of the agarose gel used in the Northern blot to control for RNA loading. Data are representative of three animals studied. Ribosomal bands and apparent migration size of the RNA species are as labeled. Tissues used in Northern screen: C=cecum, B=brain, H=heart, K=kidney, L=liver, S=spleen, T=thymus and J=human Jurkat T cell line positive control. Restriction enzyme sites labeled in panel A: E=Eco-R1, H=HindIII, B=Bam-H1, X=Xba-1, S=Sal-1.

Map of LSCD7-1 Clone

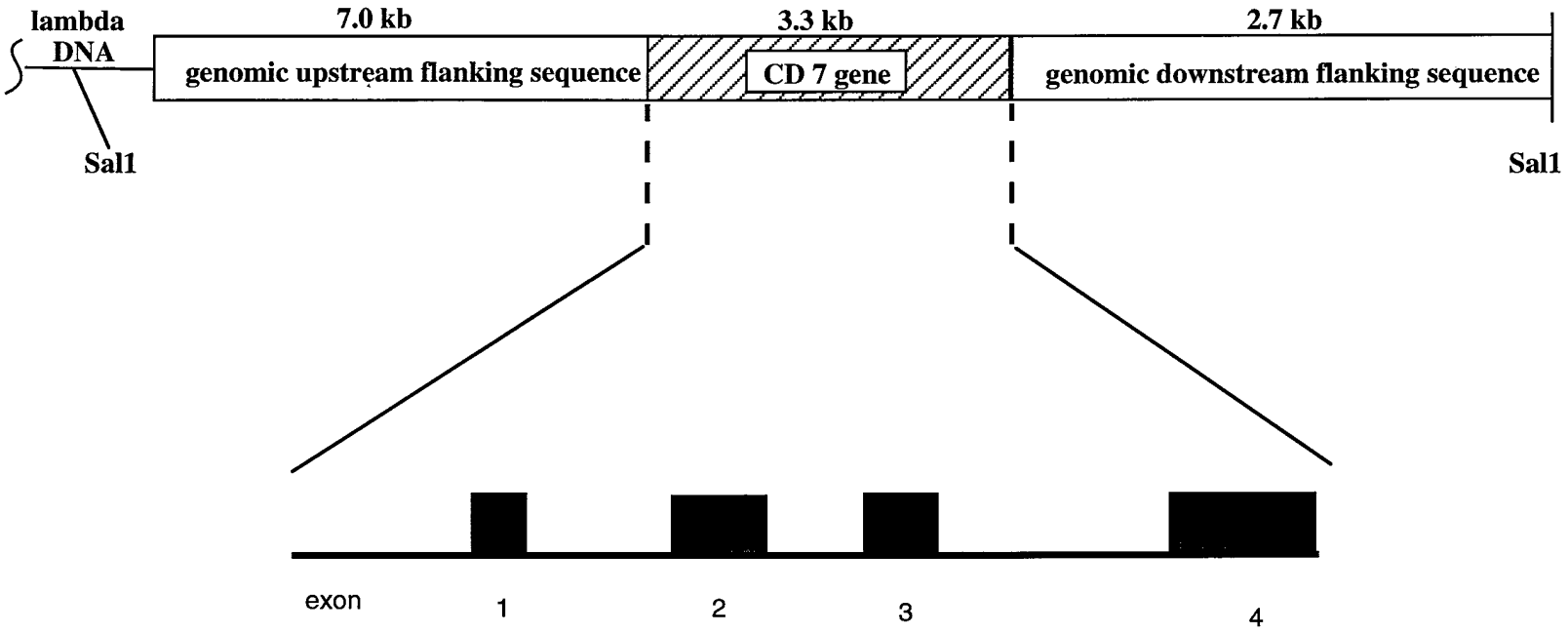

Figure 1

Transgenic Mice

CD7 transgenic mice were generated using a Sal1 fragment of the lambda clone LSCD7-1, shown above in figure 1. Founder animals were identified by Southern analysis of tail DNA.

Figure 1B

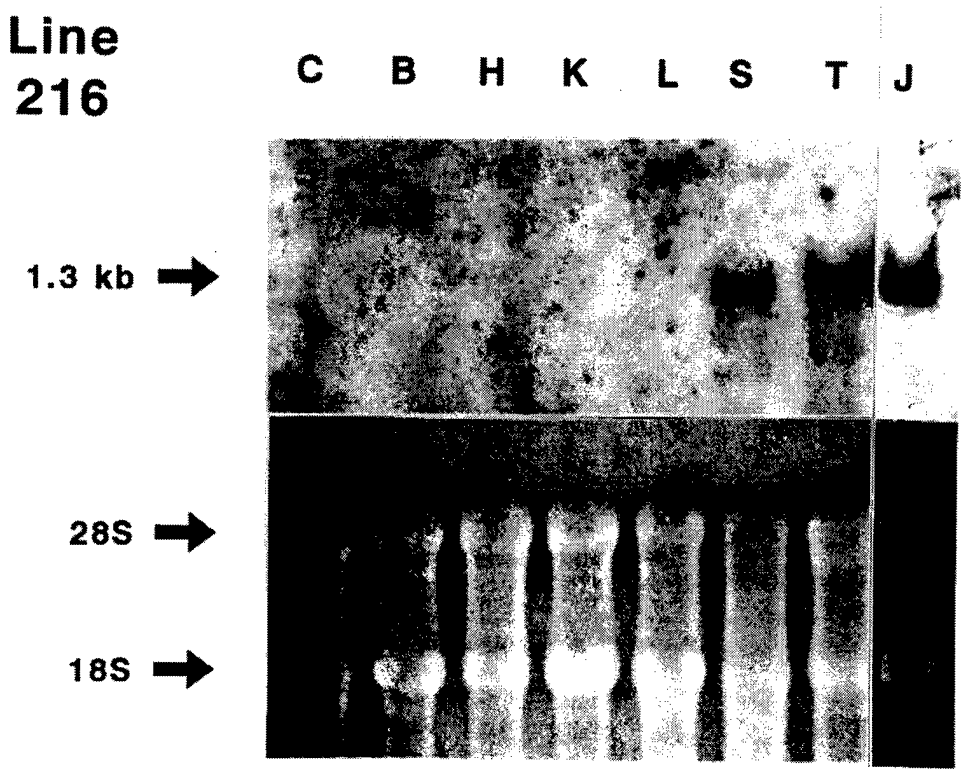

Figure 2 Comparison of CD7 Transgene and Thy-1 Expression in CD7 Transgenic Mouse Postnatal Thymus. CD7 transgene and mouse Thy-1 expression were compared in 216 and 555 line CD7 transgenic mouse thymus in direct IF assays on 4mm frozen, acetone fixed tissue sections. Panels A and C show CD7 transgene expression using CD7 MAb Leu9-FITC at the thymic cortical/medullary junction in transgenic lines 216 and 555 respectively. Panels B and D show Thy-1 transgene expression at the cortical/medullary junction in transgenic lines 216 and 555 respectively. Data are representative of two animals studied.

Figure 2

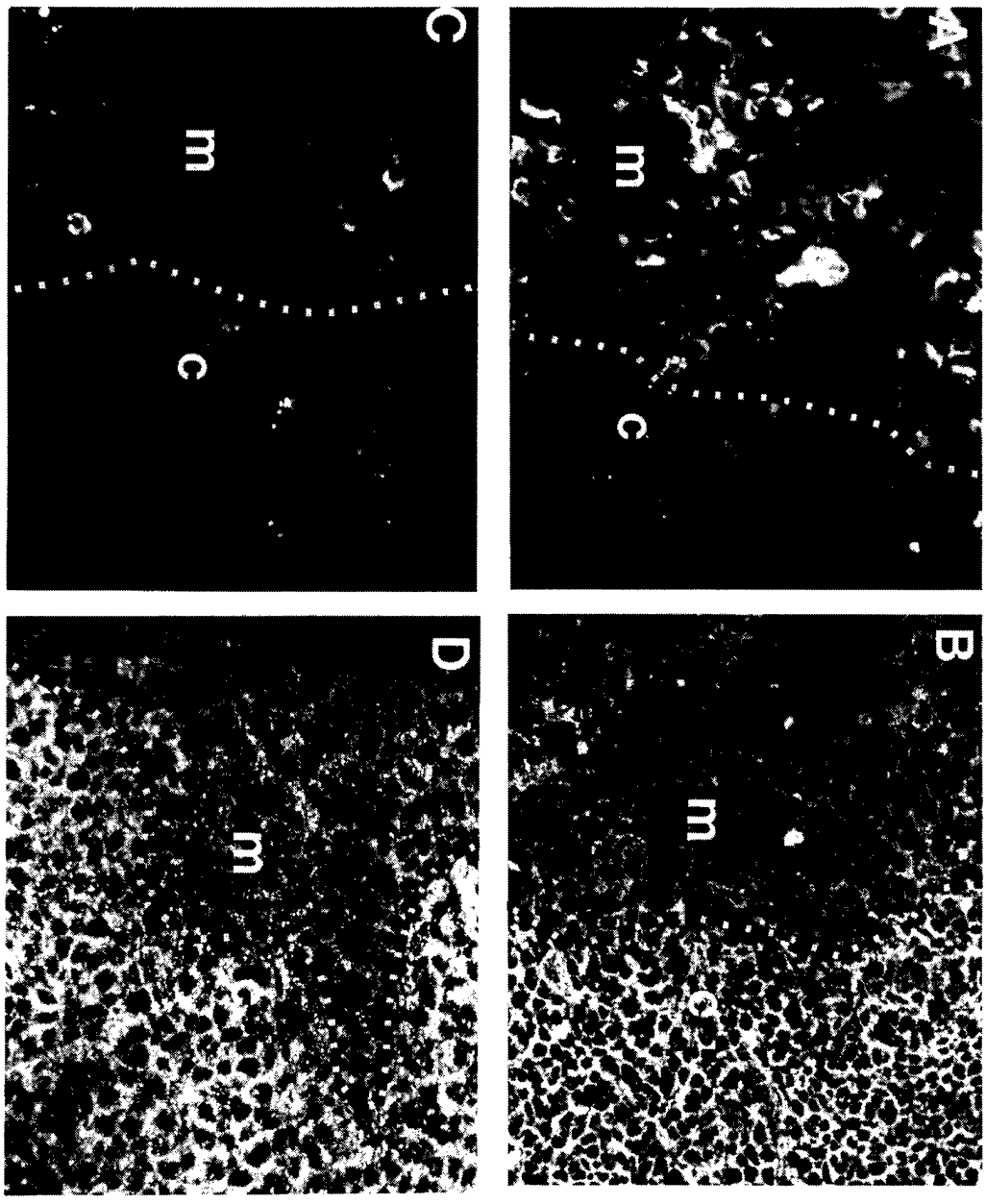

Figure 3 Comparison of CD7 Transgene and Mouse Thy-1 Expression in CD7 Transgenic Mouse Spleen. CD7 transgene and Thy-1 expression were compared on adult spleen in direct IF assay on frozen acetone fixed tissue sections from CD7 transgene lines 216 and 555. Panels A and C show mouse Thy-1 expression in transgenic lines 216 and 555, respectively. Panels B and D show CD7 transgene expression in a peri-arteriolar T-cell splenic region (Thy-1+ region) in transgenic lines 216 and 555 respectively. Data are representative of two animals studied.

Figure 3

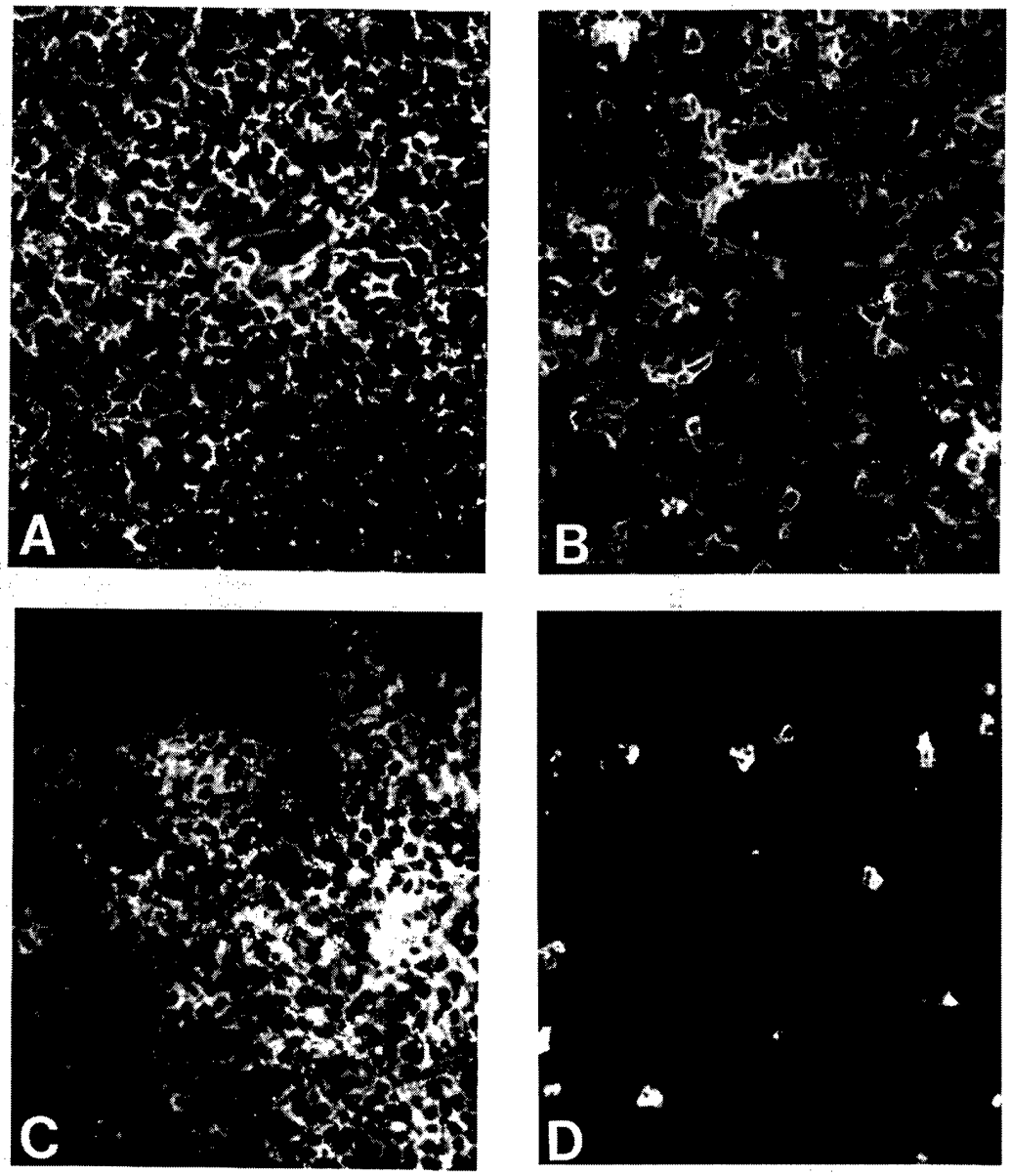

Figure 4 Expression of CD7 Transgene in Transgenic Mouse Thymocyte Subpopulations. Three color flow cytometric analysis of thymocyte co-expression of mouse CD4, CD8 and human CD7 is shown. Panel A shows a representative dot plot of co-expression of CD4 and CD8. Gates of thymocyte subpopulations were selected as shown and used to examine CD7 transgene expression on these populations. Panels B-F show CD7 transgene expression on thymocyte subsets of 216, 555 and non-transgenic mice. Gates chosen for B-F are B) all thymocytes, C) $CD4^+CD8^+$ double positive thymocytes, D) $CD4^-CD8^-$ double negative thymocytes, E) $CD8^+CD4^-$ single positive thymocytes, and F) $CD4^+CD8^-$ single positive thymocytes. Mean fluorescence values for each population are shown in figure 5. Data are representative of six animals studied.

Figure 4

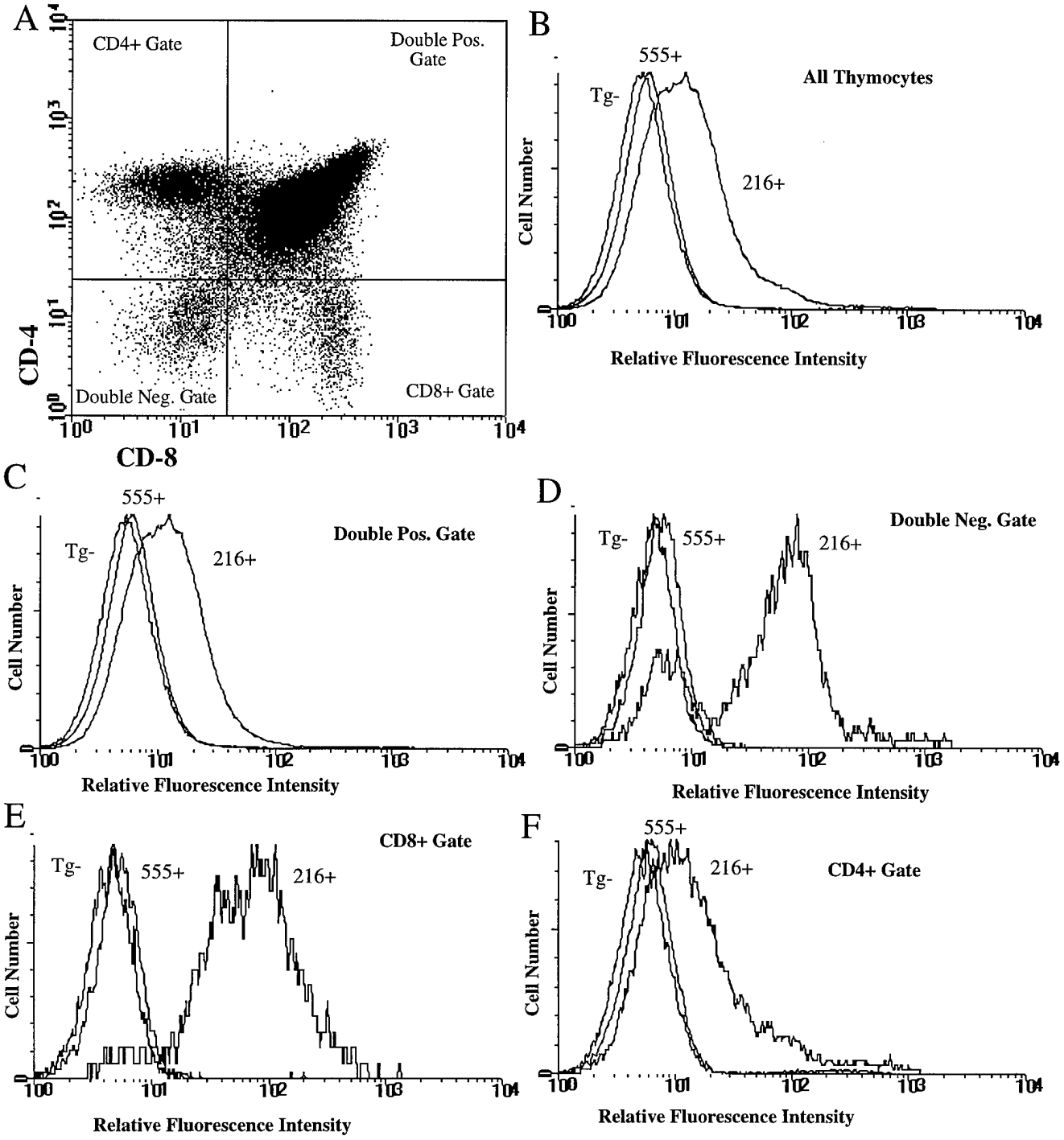
A
CD4+ Gate
Double Pos. Gate
Double Neg. Gate
CD8+ Gate
CD-4
CD-8
B
555+
Tg-
216+
All Thymocytes
Cell Number
Relative Fluorescence Intensity
C
555+
Tg-
216+
Double Pos. Gate
Cell Number
Relative Fluorescence Intensity
D
Tg-
555+
216+
Double Neg. Gate
Cell Number
Relative Fluorescence Intensity
E
Tg-
555+
216+
CD8+ Gate
Cell Number
Relative Fluorescence Intensity
F
555+
Tg-
216+
CD4+ Gate
Cell Number
Relative Fluorescence Intensity

Figure 5 Comparison of CD7 Expression on Thymocyte Subpopulations of Line 216 Transgenic and Control Mice with CD7 Expression on Human Thymocyte Subpopulations. Thymocyte subpopulations were defined by expression of CD4 and CD8 (mouse or human as appropriate) and gates defining these populations were selected using three color flow cytometry. Levels of CD7 expression on these thymocyte subpopulations were assessed in human, transgenic and control mouse thymocytes. Note that flow cytometry analysis on human and mouse thymocytes were performed on separate days and thus direct comparison between human and mouse thymocytes was not possible. Panel A shows results for mouse thymocytes and Panel B shows results for human thymocytes. Data are representative of six animals studied.

Figure 5

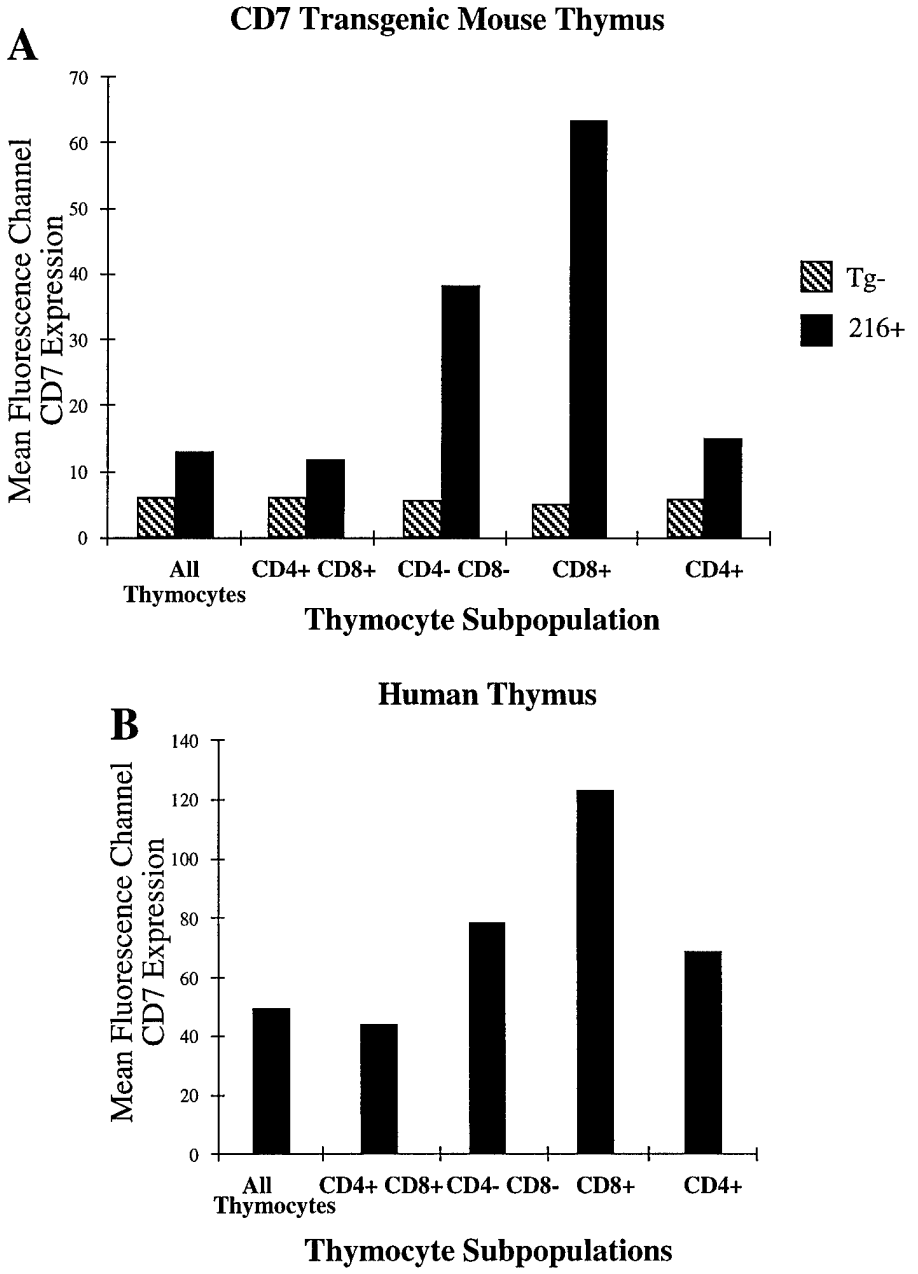
A
CD7 Transgenic Mouse Thymus
Mean Fluorescence Channel
CD7 Expression
70
60
50
40
30
20
10
0
Tg-
216+
All Thymocytes
CD4+ CD8+
CD4- CD8-
CD8+
CD4+
Thymocyte Subpopulation
B
Human Thymus
Mean Fluorescence Channel
CD7 Expression
140
120
100
80
60
40
20
0
All Thymocytes
CD4+ CD8+
CD4- CD8-
CD8+
CD4+
Thymocyte Subpopulations

Figure 6 Comparison of CD7 Transgene and Mouse Thy-1 Expression on CD7 Transgenic Mouse Adult Brain. Adult mouse brain tissue was analyzed in direct immunofluorescence assay for CD7 transgene and mouse Thy-1 expression on sequential tissue sections. Panel A demonstrates bright Thy-1 staining of mouse brain, while Panel B shows absence of CD7 expression on a sequential section of the same tissue. The large arrow points to an extravasating leukocyte present in both serial sections (one animal studied). M= meningeal tissue, C=cortical tissue.

Figure 6

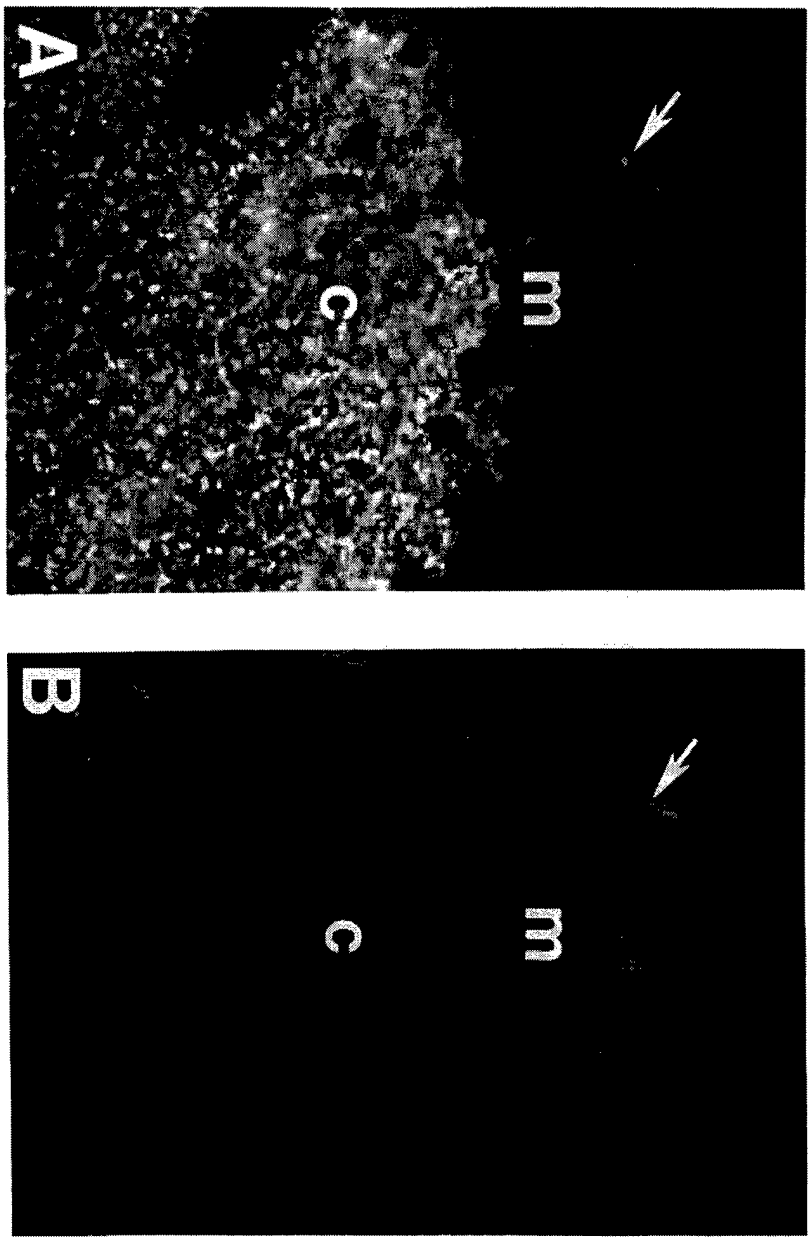

Figure 7 CD7 Transgene Expression on Leukocyte Subsets. Freshly isolated leukocytes were assayed for co-expression of the CD7 transgene and mouse hematopoietic lineage specific markers. Panels A-D show CD7 transgene expression on both 216 and 555 lineage Ly-5$^+$ splenic B cells, Thy-1$^+$ splenic T cells, NK1.1$^+$ splenic NK cells and F4/80$^+$ peritoneal macrophages respectively (two animals studied). Analysis of these populations was performed in the same experiment, allowing direct comparison of CD7 transgene expression levels in these populations.

Figure 7

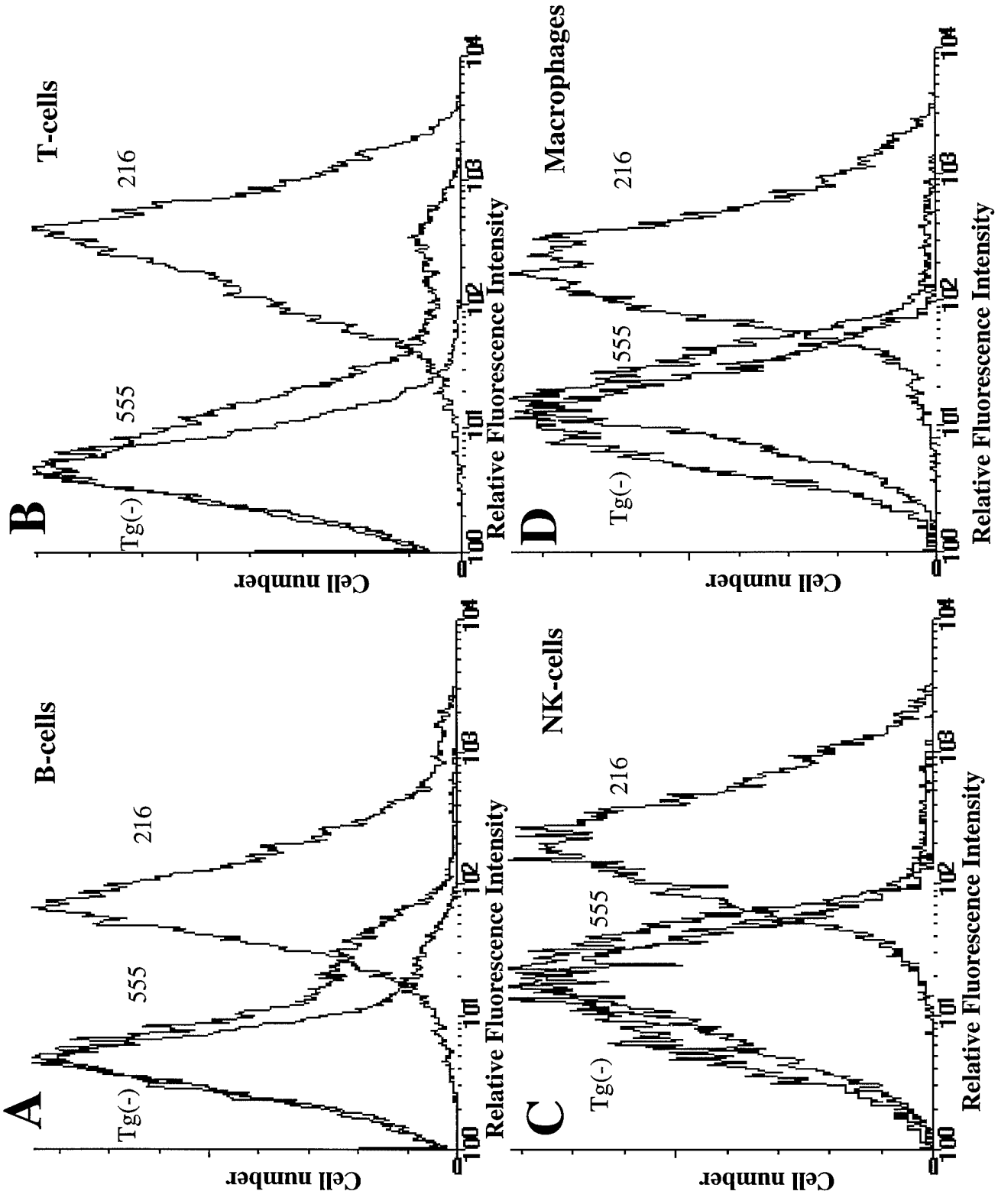
A
B-cells
Tg(-)
555
216
Cell number
Relative Fluorescence Intensity
B
T-cells
C
NK-cells
D
Macrophages

Figure 8 CD7 Transgene Expression on Mouse Bone Marrow Cells. Freshly isolated bone marrow cells were analyzed for CD7 transgene and mouse Sca-1 co-expression using two color flow cytometry. Panels A-C show representative populations found in 216^{+}(A), 555^{+}(B) and non-transgenic mice (C). Panel D shows single color analysis of CD7 transgene expression in bone marrow from 216^{+}, 555^{+} and non-transgenic mice (two animals studied).

Figure 8

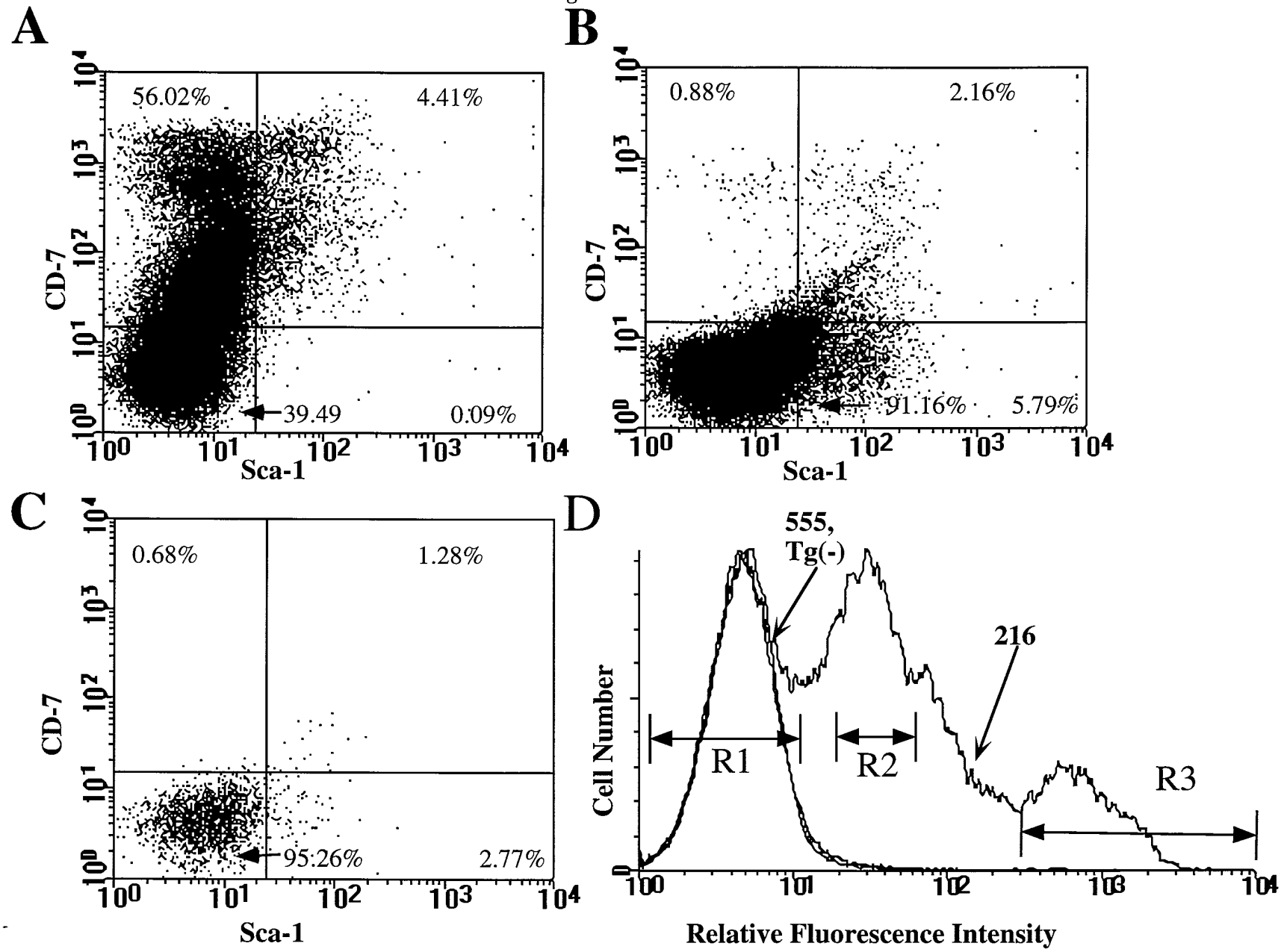
A
56.02%
4.41%
39.49
0.09%
CD-7
Sca-1
B
0.88%
2.16%
91.16%
5.79%
CD-7
Sca-1
C
0.68%
1.28%
95.26%
2.77%
CD-7
Sca-1
D
555,
Tg(-)
216
R1
R2
R3
Cell Number
Relative Fluorescence Intensity

Figure 9 Analysis of CD7 Subsets In Transgenic Bone Marrow. Panels A-C show the results of flow cytometric sorting of transgenic line 216 bone marrow, gating on CD7 bright (Panel A), dim (Panel B) and negative (Panel C) bone marrow populations (R3, R2 and R1 respectively, Figure 8). After sorting, these populations underwent cytoprep preparation followed by Wright-Giemsa staining. $CD7^{hi+}$ cells (R3 group) were 35% lymphoid precursors, 12% metamyelocytes, 42% myelocytes, 3% promyelocytes, 12% myeloblasts, 5% plasma cells, rare megakaryocytes and histiocytes. The $CD7^{lo+}$ cells (R2 group) were 58% myeloid lineage and 39% erythroid precursors. The $CD7^{-}$ cells (R1 group) were 98% erythrocytes, 1% myeloid progenitors, and 1% erythroid progenitors (two animals studied).

Figure 9

Figure 10 Induction of CD7 Transgene in Splenocytes and Thymocytes in CD7 Transgenic Mice. Freshly isolated splenocytes and thymocytes from CD7 transgenic and control mice were cultured for 24 hours in the presence of PHA and IL-2. CD7 transgene cell surface expression was assessed pre- and post- culture by flow cytometry on the same day, allowing direct comparison of expression levels of the CD7 transgene. Panel A shows induction of CD7 expression on splenocytes. Panel B demonstrates induction of expression on thymocytes. Panel C shows induction of CD7 mRNA in activated versus fresh splenocytes and thymocytes from line 216 as assessed by Northern Blot analysis. The upper panel is a representative Northern blot radiograph. The lower panel is an acridine orange stain of the agarose gel used in the Northern blot to control for RNA loading. Ribosomal bands and apparent migration size of the RNA species are as labeled. Tissues used in Northern screen: S=splenocytes, T=thymocytes, IS=induced splenocytes and IT=induced thymocytes. mice, indirect IF assays were performed on tissue obtained from mouse fetal yolk sac and liver. Numerous $CD7^+$ cells with high level CD7 expression were seen at gestational day 13 in both yolk sac and liver (Figure 11). While numerous $CD7^+$ cells were present in fetal liver, few Thy-1^+ cells were present, demonstrating a difference between CD7 transgene and mouse Thy-1 expression.

Figure 10

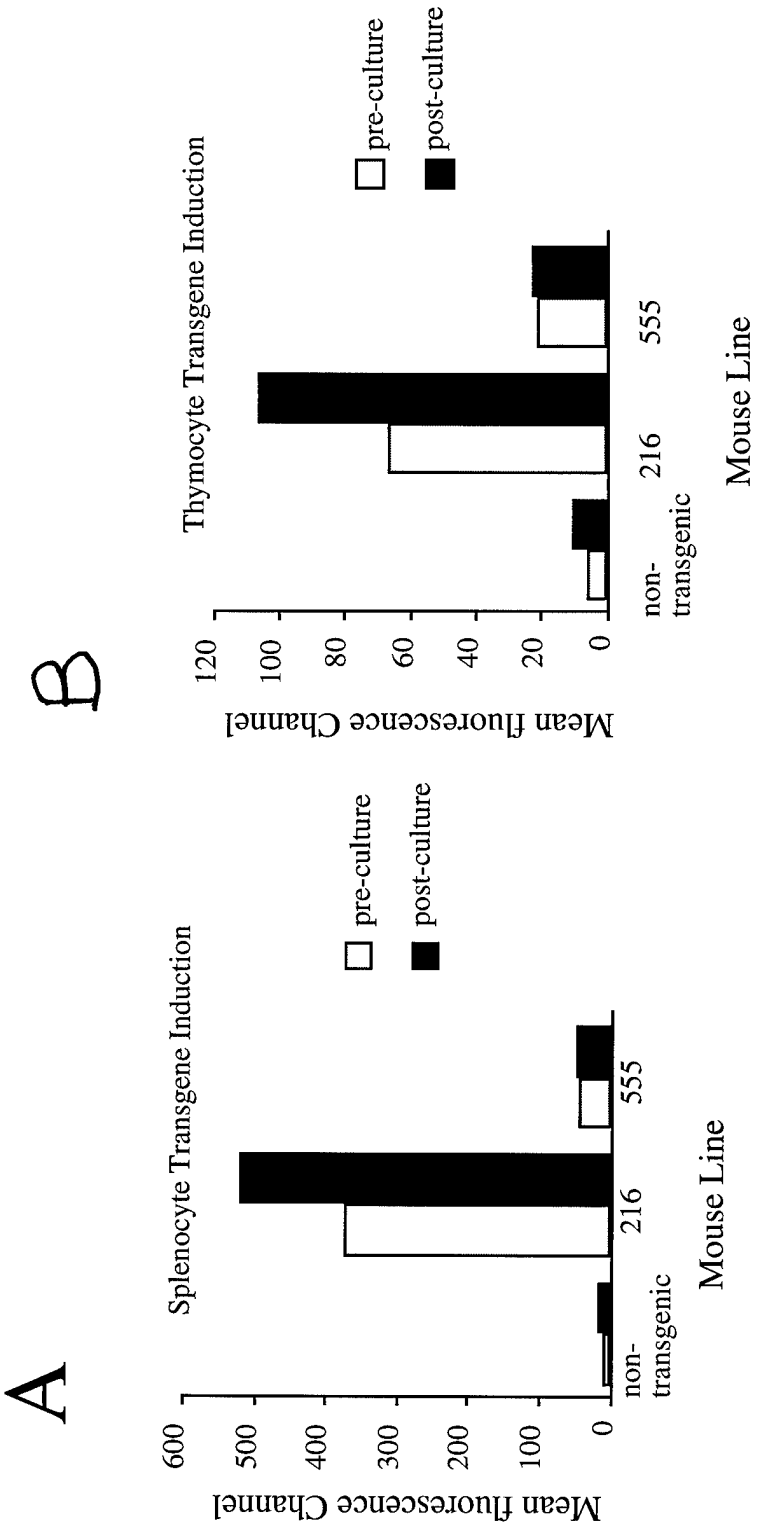
A
Splenocyte Transgene Induction
Mean Fluorescence Channel
600
500
400
300
200
100
0
pre-culture
post-culture
non-transgenic
216
555
Mouse Line
B
Thymocyte Transgene Induction
Mean Fluorescence Channel
120
100
80
60
40
20
0
pre-culture
post-culture
non-transgenic
216
555
Mouse Line

Figure 10 C

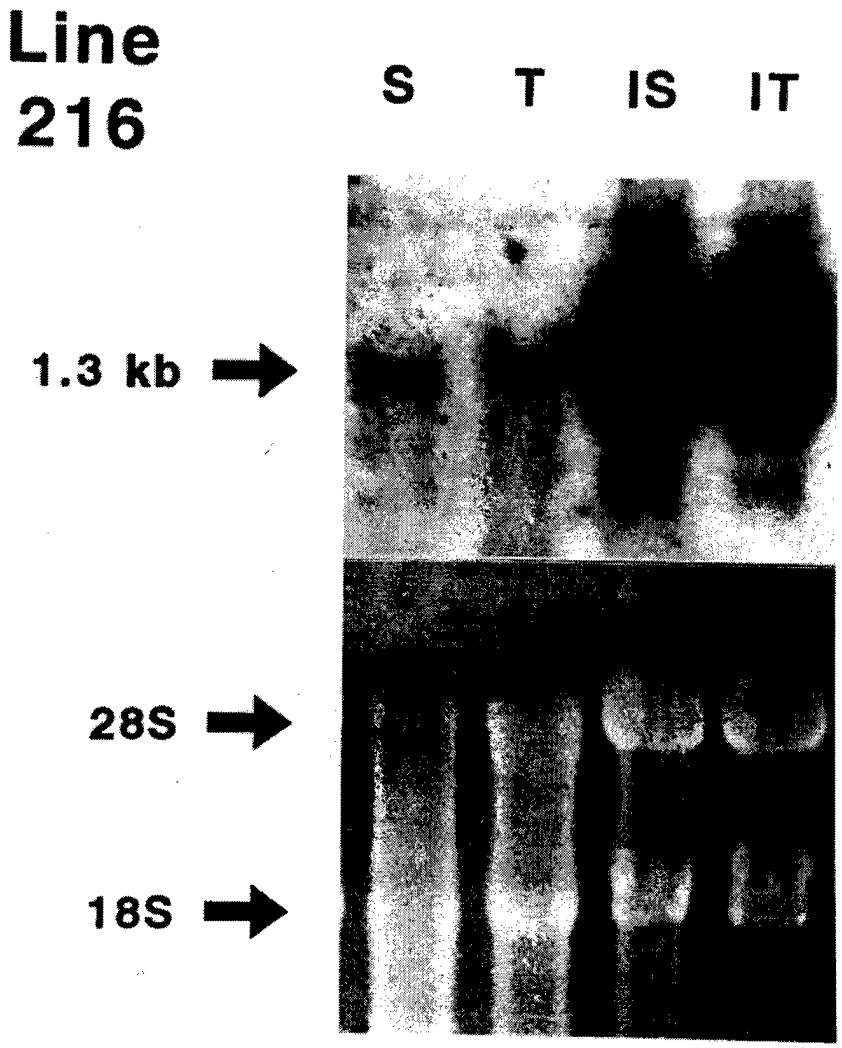

Figure 11 CD7 Transgene Expression *In Utero*. CD7 transgene expression was assayed at varying stages of *in utero* development by direct immunofluorescence assay. In panels A-C, expression of CD7 transgene in day 15 bone marrow was compared with expression of mouse Thy-1. Panel A shows an H & E stain of the bone marrow sectioned for this study. Panel B shows staining of the same region for CD7 transgene expression. Panel C shows staining of a similar region for mouse Thy-1 expression. Arrows point to positive cells. Panels D and E show expression of the CD7 transgene in gestational day 13 yolk sac. The fetus is transgenic as is the mother. Panel D shows an H & E stain of a yolk sac section. Panel E shows staining of the same region for CD7 transgene expression. Arrows point to representative positive cells. In panels F and G, expression of the CD7 transgene in gestational day 15 liver was compared to expression of mouse Thy-1. Panel F shows the results of staining day 15 fetal liver for CD7 transgene expression with arrows pointing out positive cells. Panel G shows the results of staining the same regions for Thy-1 expression, however, only non-specific staining was observed; arrows point to non-specifically stained cells. In panels H and I, CD7 transgene and mouse Thy-1 expression was assessed in day 15 fetal transgenic thymus. Panel H shows the pattern of CD7 transgene expression, while panel I demonstrates the Thy-1 pattern. C=thymic cortex, M=thymic medulla. The dotted line demarcates the thymic cortical/medullary junction. Data are representative of two animals studied.

Figure 11

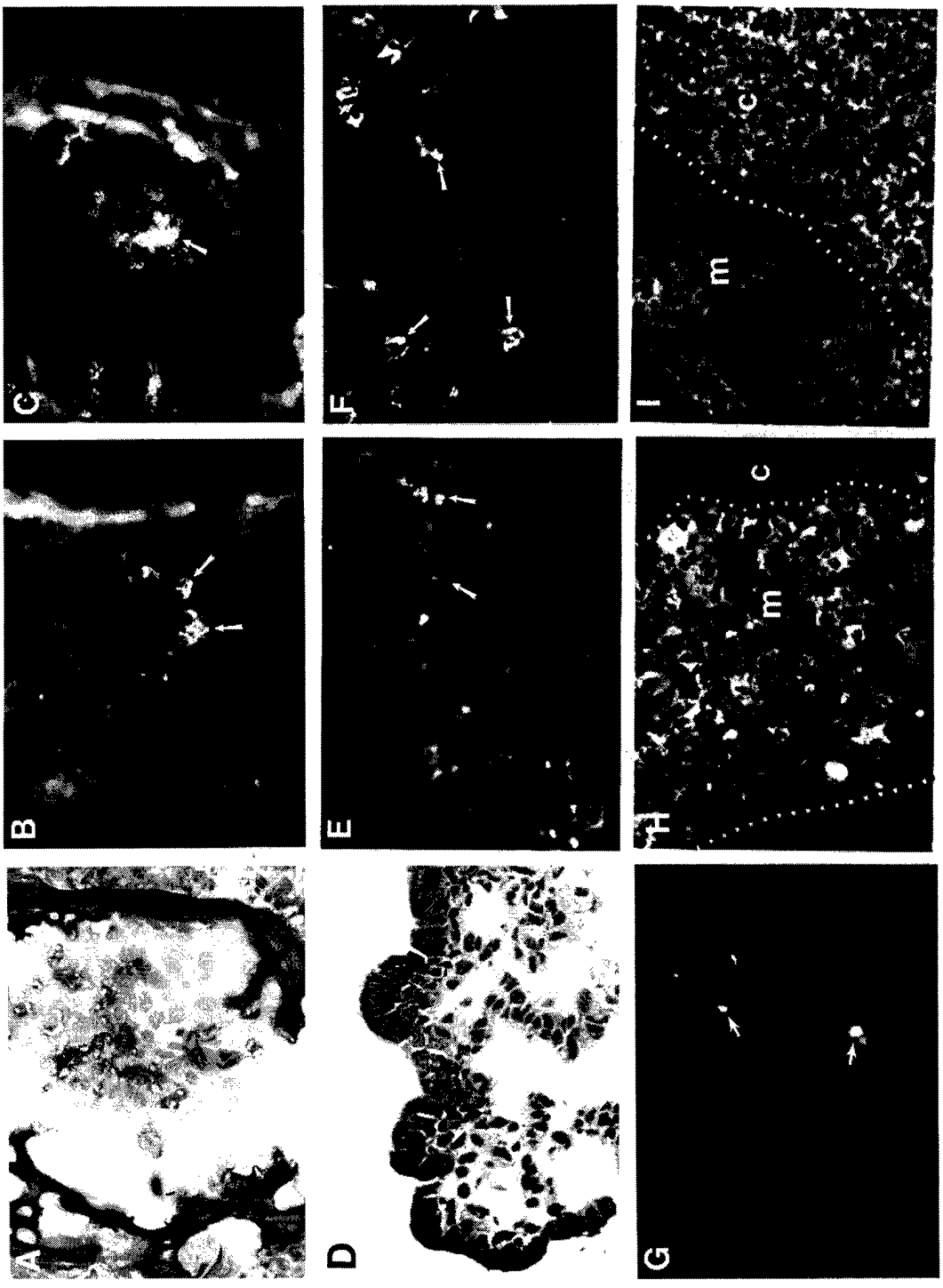

Figure 12 Determination of an Informative Restriction Fragment Length Variant (RFLV) for Chromosomal Mapping. Shown are the results of a Southern blot of DNA from C3H/HeJ-*gld* and (C3H/HeJ-*gld* x *Mus spretus*)F1 parental mice digested with various restriction endonucleases and probed with a mouse CD7 cDNA probe. The informative RFLV, present in the Taq restricted DNA is labeled with arrows and apparent base pair length. Taq, Bam-H1 and Msp-1 restriction endonucleases and the donor DNA genotypes are as labeled.

Figure 12

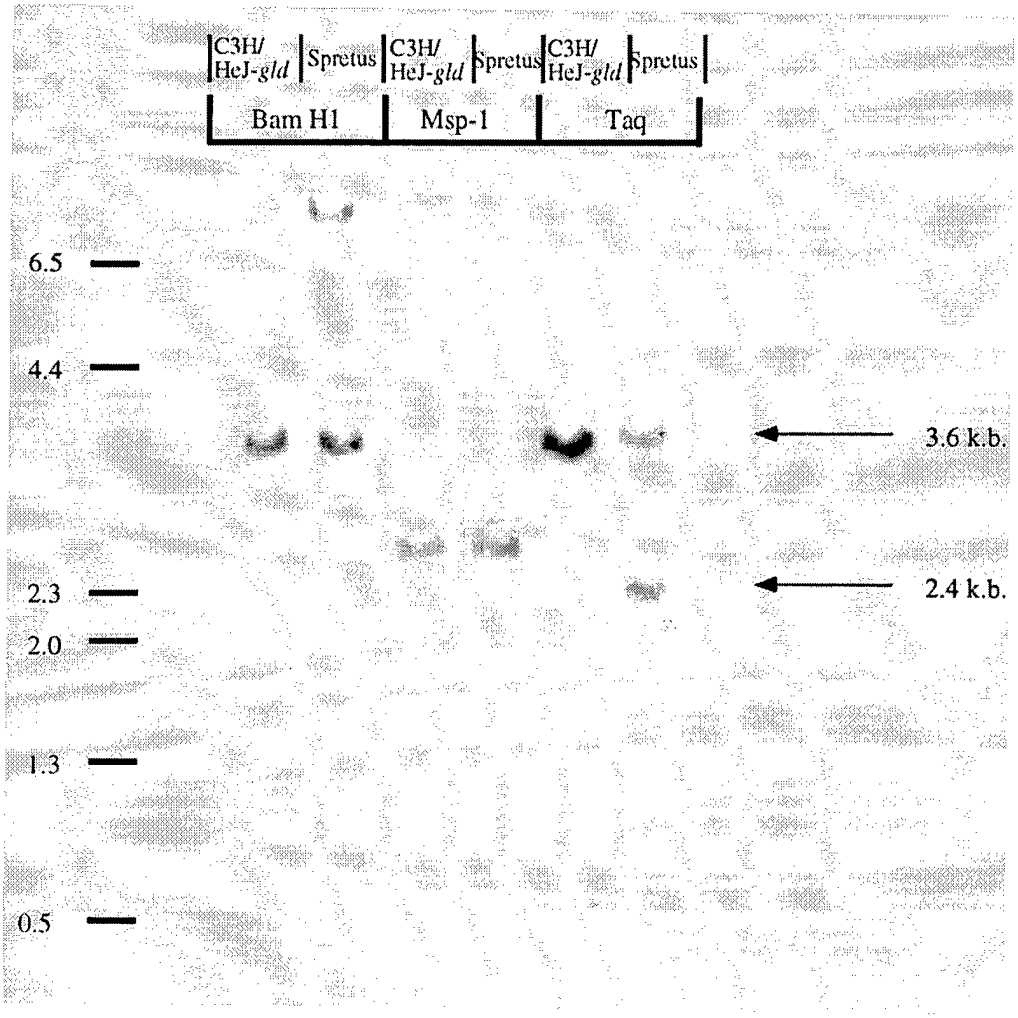
C3H/ HeJ-gld
Spretus
C3H/ HeJ-gld
Spretus
C3H/ HeJ-gld
Spretus
Bam H1
Msp-1
Taq
6.5
4.4
2.3
2.0
1.3
0.5
3.6 k.b.
2.4 k.b.

Figure 13 Chromosomal Map Position of Mouse Cd7. Shown is the segregation pattern of *Pkca*, *Timp*-2 and *Cd7* on mouse chromosome 11 in 114 (C3H/HeJ-*gld* X *M. Spretus*)F_1 X C3H/HeJ-*gld* interspecific backcross mice. Results represent the RFLV patterns obtained by Southern blot of 122 (C3H/HeJ-*gld* X *M. Spretus*)F_1 X C3H/HeJ-*gld* interspecific backcross mice with mouse CD7 cDNA probe. Closed boxes represent the homozygous C3H pattern; open boxes represent the F_1 pattern.

Figure 13

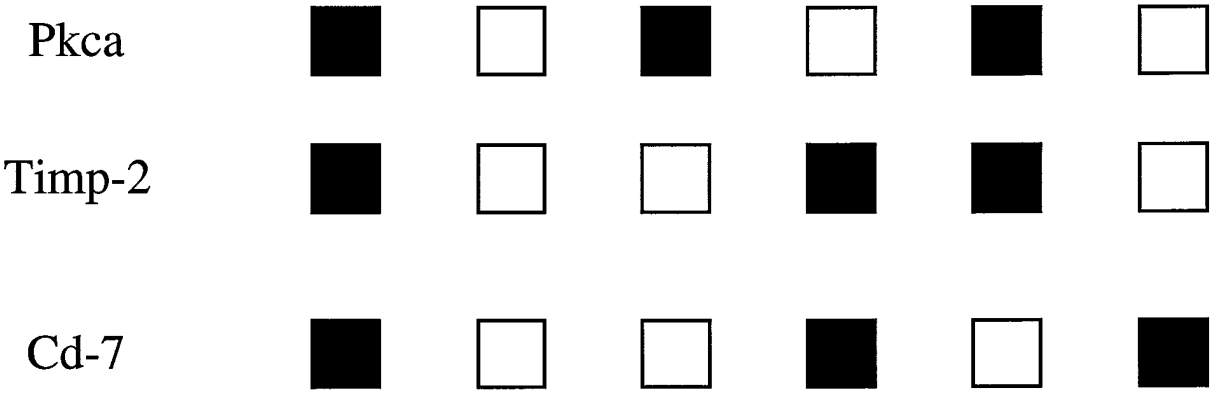

Number of mice	58	49	3	2	1	1

Figure 14 Structure and Restriction Map of Mouse (m) CD7. Shown is a scaled model of the mCD7 gene structure. Panel A shows the two lambda clones of mCD7, 13-2 containing the entire sequence and 21-1 containing partial sequence. Panel B shows the relative sizes of mCD7 introns and exons as well as restriction site locations as labeled. H3=HindIII restriction endonuclease.

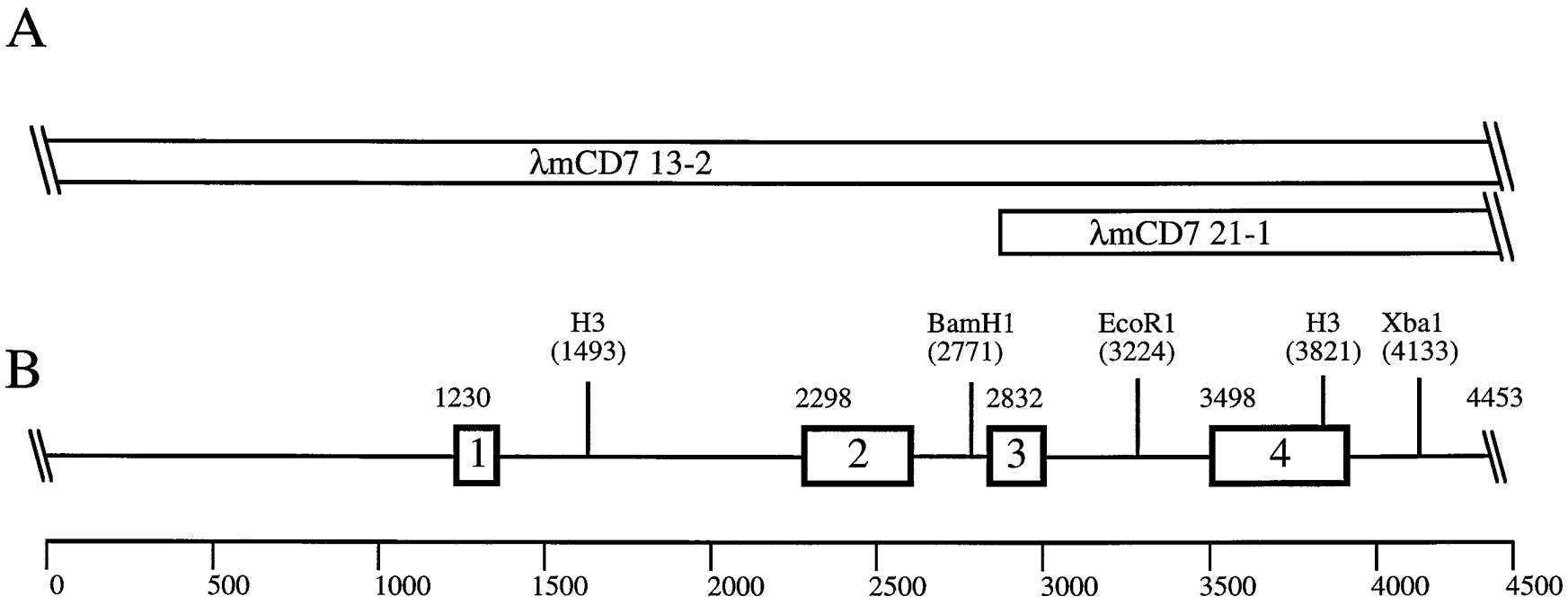
A
λmCD7 13-2
λmCD7 21-1
B
H3
(1493)
BamH1
(2771)
EcoR1
(3224)
H3
(3821)
Xba1
(4133)
1230
2298
2832
3498
4453
1
2
3
4
0
500
1000
1500
2000
2500
3000
3500
4000
4500

Figure 14

Figure 15 Mouse CD7 Sequence. The sequence of the gene and flanking regions of mCD7 are shown. Intronic and flanking sequences are shown in small case while exonic sequence is depicted in bold capitals. Donor splice and acceptor sites for RNA processing are underlined, as is the mRNA polyadenylation signal.

Figure 15

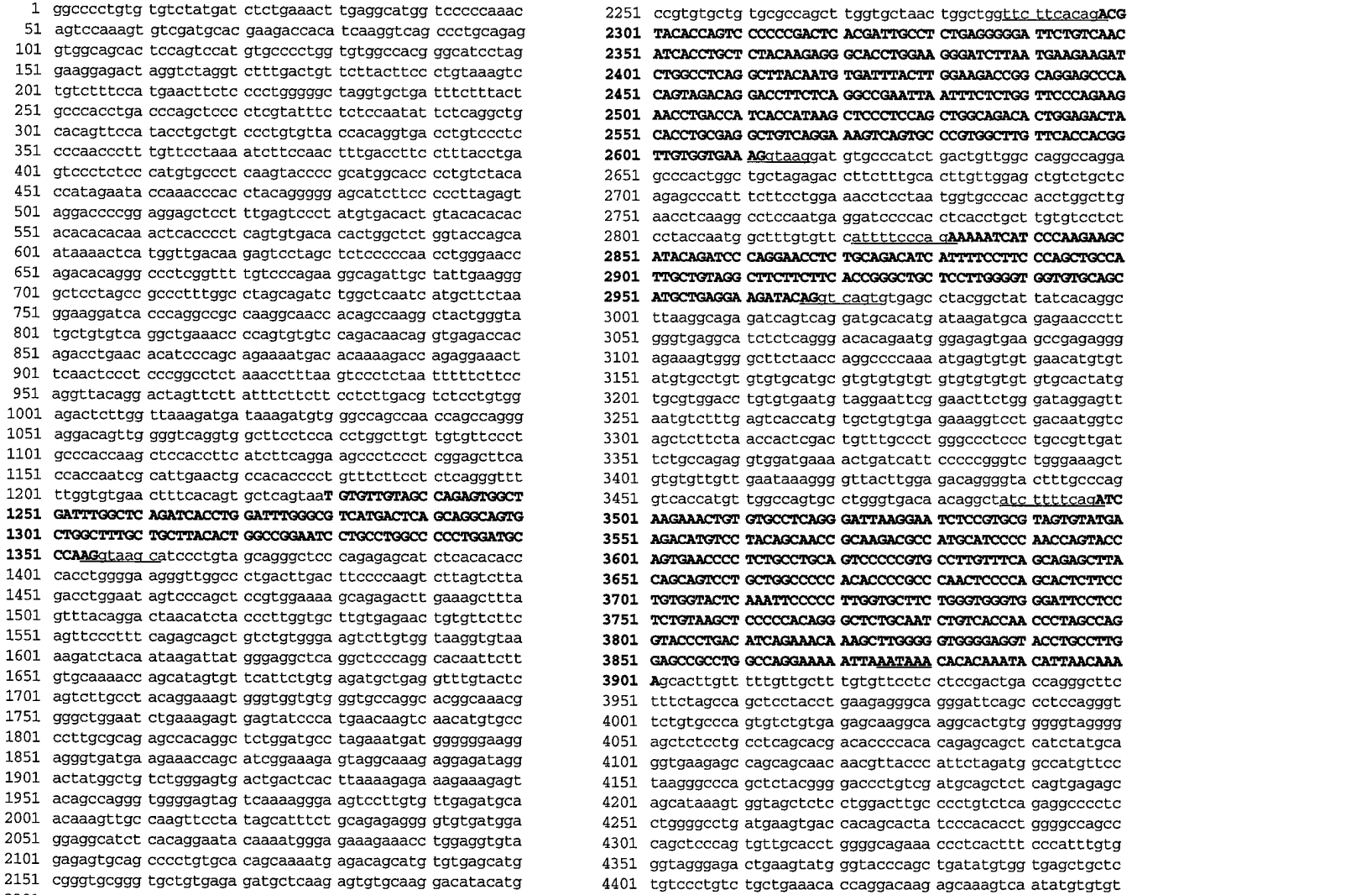
1 ggcccctgtg tgtctatgat ctctgaaact tgaggcatgg tccccaaac
51 agtccaaagt gtcgatgcac gaagaccaca tcaaggtcag ccctgcagag
101 gtggcagcac tccagtccat gtgcccctgg tgtggccacg ggcatcctag
151 gaaggagact aggtctaggt ctttgactgt tcttacttcc ctgtaaagtc
201 tgtctttcca tgaacttctc ccctgggggc taggtgctga tttctttact
251 gcccacctga cccagctccc ctcgtatttc tctccaatat tctcaggctg
301 cacagttcca tacctgctgt ccctgtgtta ccacaggtga cctgtccctc
351 cccaaccctt tgttcctaaa atcttccaac tttgaccttc ctttacctga
401 gtccctctcc catgtgccct caagtacccc gcatggcacc cctgtctaca
451 ccatagaata ccaaacccac ctacaggggg agcatcttcc cccttagagt
501 aggaccccgg aggagctcct ttgagtccct atgtgacact gtacacacac
551 acacacacaa actcacccct cagtgtgaca cactggctct ggtaccagca
601 ataaaactca tggttgacaa gagtcctagc tctcccccaa cctgggaacc
651 agacacaggg ccctcggttt tgtcccagaa ggcagattgc tattgaaggg
701 gctcctagcc gccctttggc ctagcagatc tggctcaatc atgcttctaa
751 ggaaggatca cccaggccgc caaggcaacc acagccaagg ctactgggta
801 tgctgtgtca ggctgaaacc ccagtgtgtc cagacaacag gtgagaccac
851 agacctgaac acatcccagc agaaaatgac acaaaagacc agaggaaact
901 tcaactccct cccggcctct aaacctttaa gtccctctaa tttttcttcc
951 aggttacagg actagttctt atttcttctt cctcttgacg tctcctgtgg
1001 agactcttgg ttaaagatga taaagatgtg ggccagccaa ccagccaggg
1051 aggacagttg gggtcaggtg gcttcctcca cctggcttgt tgtgttccct
1101 gcccaccaag ctccaccttc atcttcagga agccctccct cggagcttca
1151 ccaccaatcg cattgaactg ccacacccct gtttcttcct ctcagggttt
1201 ttggtgtgaa ctttcacagt gctcagtaaT GTGTTGTAGC CAGAGTGGCT
1251 GATTTGGCTC AGATCACCTG GATTTGGGCG TCATGACTCA GCAGGCAGTG
1301 CTGGCTTTGC TGCTTACACT GGCCGGAATC CTGCCTGGCC CCCTGGATGC
1351 CCAAGgtaag catccctgta gcagggctcc cagagagcat ctcacacacc
1401 cacctgggga agggttggcc ctgacttgac ttccccaagt cttagtctta
1451 gacctggaat agtcccagct ccgtggaaaa gcagagactt gaaagcttta
1501 gtttacagga ctaacatcta cccttggtgc ttgtgagaac tgtgttcttc
1551 agttcccttt cagagcagct gtctgtggga agtcttgtgg taaggtgtaa
1601 aagatctaca ataagattat gggaggctca ggctcccagg cacaattctt
1651 gtgcaaaacc agcatagtgt tcattctgtg agatgctgag gtttgtactc
1701 agtcttgcct acaggaaagt gggtggtgtg ggtgccaggc acggcaaacg
1751 gggctggaat ctgaaagagt gagtatccca tgaacaagtc aacatgtgcc
1801 ccttgcgcag agccacaggc tctggatgcc tagaaatgat gggggggaagg
1851 agggtgatga agaaaccagc atcggaaaga gtaggcaaag aggagatagg
1901 actatggctg tctgggagtg actgactcac ttaaaagaga aagaaagagt
1951 acagccaggg tggggagtag tcaaaaggga agtccttgtg ttgagatgca
2001 acaaagttgc caagttccta tagcatttct gcagagaggg gtgtgatgga
2051 ggaggcatct cacaggaata caaaatggga gaaagaaacc tggaggtgta
2101 gagagtgcag cccctgtgca cagcaaaatg agacagcatg tgtgagcatg
2151 cgggtgcggg tgctgtgaga gatgctcaag agtgtgcaag gacatacatg
2201 aatgtaggat ctgtggagcc tctgagatac gtgttagcgt gtttgagtca
2251 ccgtgtgctg tgcgccagct tggtgctaac tggctggttc ttcacagACG
2301 TACACCAGTC CCCCCGACTC ACGATTGCCT CTGAGGGGGA TTCTGTCAAC
2351 ATCACCTGCT CTACAAGAGG GCACCTGGAA GGGATCTTAA TGAAGAAGAT
2401 CTGGCCTCAG GCTTACAATG TGATTTACTT GGAAGACCGG CAGGAGCCCA
2451 CAGTAGACAG GACCTTCTCA GGCCGAATTA ATTTCTCTGG TTCCCAGAAG
2501 AACCTGACCA TCACCATAAG CTCCCTCCAG CTGGCAGACA CTGGAGACTA
2551 CACCTGCGAG GCTGTCAGGA AAGTCAGTGC CCGTGGCTTG TTCACCACGG
2601 TTGTGGTGAA AGgtaaggat gtgcccatct gactgttggc caggccagga
2651 gcccactggc tgctagagac cttctttgca cttgttggag ctgtctgctc
2701 agagcccatt tcttcctgga aacctcctaa tggtgcccac acctggcttg
2751 aacctcaagg cctccaatga ggatccccac ctcacctgct tgtgtcctct
2801 cctaccaatg gctttgtgtt catttttccca gAAAAATCAT CCCAAGAAGC
2851 ATACAGATCC CAGGAACCTC TGCAGACATC ATTTTCCTTC CCAGCTGCCA
2901 TTGCTGTAGG CTTCTTCTTC ACCGGGCTGC TCCTTGGGGT GGTGTGCAGC
2951 ATGCTGAGGA AGATACAGgt cagtgtgagc ctacggctat tatcacaggc
3001 ttaaggcaga gatcagtcag gatgcacatg ataagatgca gagaaccctt
3051 gggtgaggca tctctcaggg acacagaatg ggagagtgaa gccgagaggg
3101 agaaagtggg gcttctaacc aggccccaaa atgagtgtgt gaacatgtgt
3151 atgtgcctgt gtgtgcatgc gtgtgtgtgt gtgtgtgtgt gtgcactatg
3201 tgcgtggacc tgtgtgaatg taggaattcg gaacttctgg gataggagtt
3251 aatgtctttg agtcaccatg tgctgtgtga gaaaggtcct gacaatggtc
3301 agctcttcta accactcgac tgtttgccct gggccctccc tgccgttgat
3351 tctgccagag gtggatgaaa actgatcatt cccccgggtc tgggaaagct
3401 gtgtgttgtt gaataaaggg gttacttgga gacaggggta ctttgcccag
3451 gtcaccatgt tggccagtgc ctgggtgaca acaggctatc ttttcagATC
3501 AAGAAACTGT GTGCCTCAGG GATTAAGGAA TCTCCGTGCG TAGTGTATGA
3551 AGACATGTCC TACAGCAACC GCAAGACGCC ATGCATCCCC AACCAGTACC
3601 AGTGAACCCC TCTGCCTGCA GTCCCCCGTG CCTTGTTTCA GCAGAGCTTA
3651 CAGCAGTCCT GCTGGCCCCC ACACCCCGCC CAACTCCCCA GCACTCTTCC
3701 TGTGGTACTC AAATTCCCCC TTGGTGCTTC TGGGTGGGTG GGATTCCTCC
3751 TCTGTAAGCT CCCCCACAGG GCTCTGCAAT CTGTCACCAA CCCTAGCCAG
3801 GTACCCTGAC ATCAGAAACA AAGCTTGGGG GTGGGGAGGT ACCTGCCTTG
3851 GAGCCGCCTG GCCAGGAAAA ATTAAATAAA CACACAAATA CATTAACAAA
3901 Agcacttgtt tttgttgctt tgtgttcctc ctccgactga ccagggcttc
3951 tttctagcca gctcctacct gaagagggca gggattcagc cctccagggt
4001 tctgtgccca gtgtctgtga gagcaaggca aggcactgtg ggggtagggg
4051 agctctcctg cctcagcacg acaccccaca cagagcagct catctatgca
4101 ggtgaagagc cagcagcaac aacgttaccc attctagatg gccatgttcc
4151 taagggccca gctctacggg gaccctgtcg atgcagctct cagtgagagc
4201 agcataaagt ggtagctctc ctggacttgc ccctgtctca gaggcccctc
4251 ctggggcctg atgaagtgac cacagcacta tcccacacct ggggccagcc
4301 cagctcccag tgttgcacct ggggcagaaa ccctcacttt cccatttgtg
4351 ggtagggaga ctgaagtatg ggtacccagc tgatatgtgg tgagctgctc
4401 tgtccctgtc tgctgaaaca ccaggacaag agcaaagtca atatgtgtgt
4451 gct

Figure 16 Determination of Regions of Similarity Between Mouse CD7 and Human CD7. Regions of similarity between the human and mouse CD7 genes were determined using the COMPARE program from the Wisconsin Package software. Similarities between 30 base pair fragments was analyzed using a minimum stringency of 20 to score on the dot plot shown. Scaled graphic representations of human and mouse CD7 are presented on the dot plot axes for reference.

Figure 16

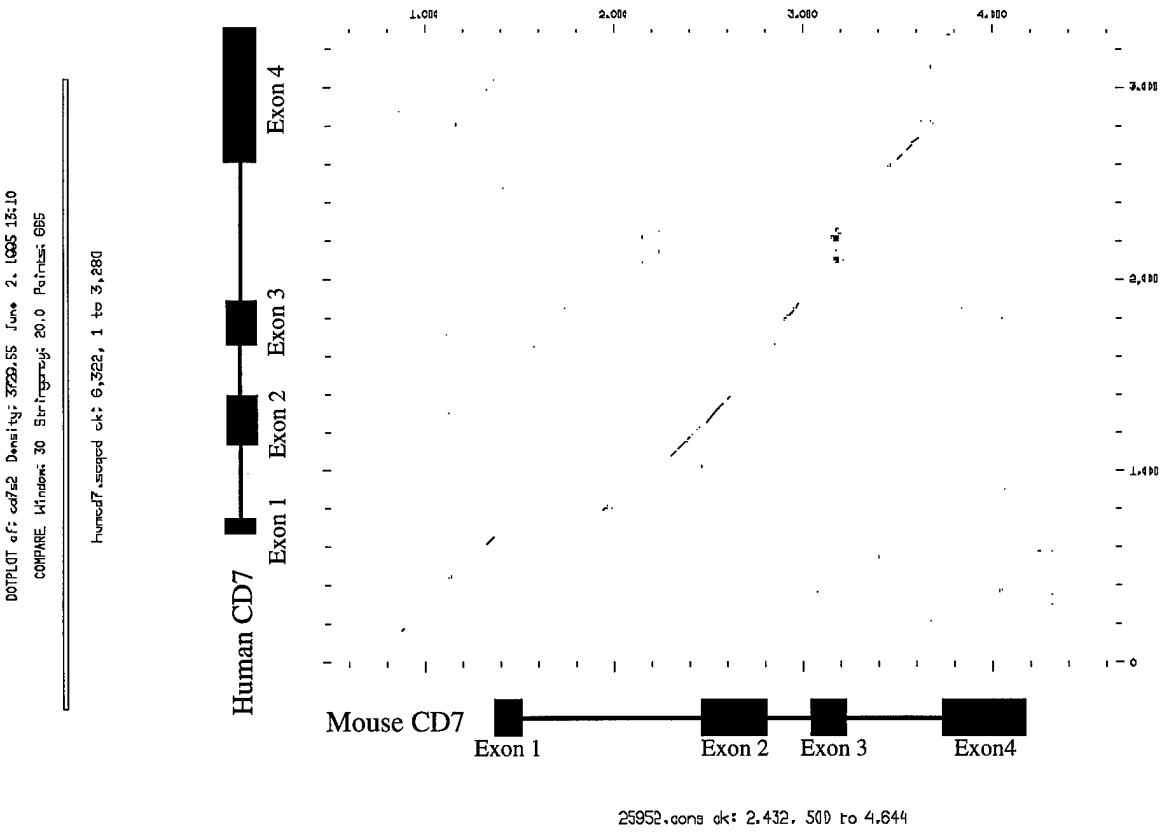
DOTPLOT of: cd7s2 Density: 3729.55 June 2, 1995 15:10
COMPARE Window: 30 Stringency: 20.0 Points: 665
humcd7.seqed ck: 6,322, 1 to 3,280
Human CD7
Exon 4
Exon 3
Exon 2
Exon 1
1,000
2,000
3,000
4,000
3,000
2,000
1,000
0
Mouse CD7
Exon 1
Exon 2
Exon 3
Exon4
25952.cons ck: 2,432, 500 to 4,644

Figure 17 Determination of Regions of Similarity Between Promoter Regions of Mouse CD7 and Human CD7. Regions of similarity between the human and mouse CD7 promoter regions were determined using the COMPARE program from the Wisconsin Package software. Similarities between 21 base pair fragments was analyzed using a minimum stringency of 14 to score on the dot plot shown. Significant regions of homology are denoted with arrows and are aligned in Figure 18. Note, numbers on the axes do not correlate with base pair designations in the reported genes and are only relative positions, with exact positions diagrammed in Figure 18.

Figure 17

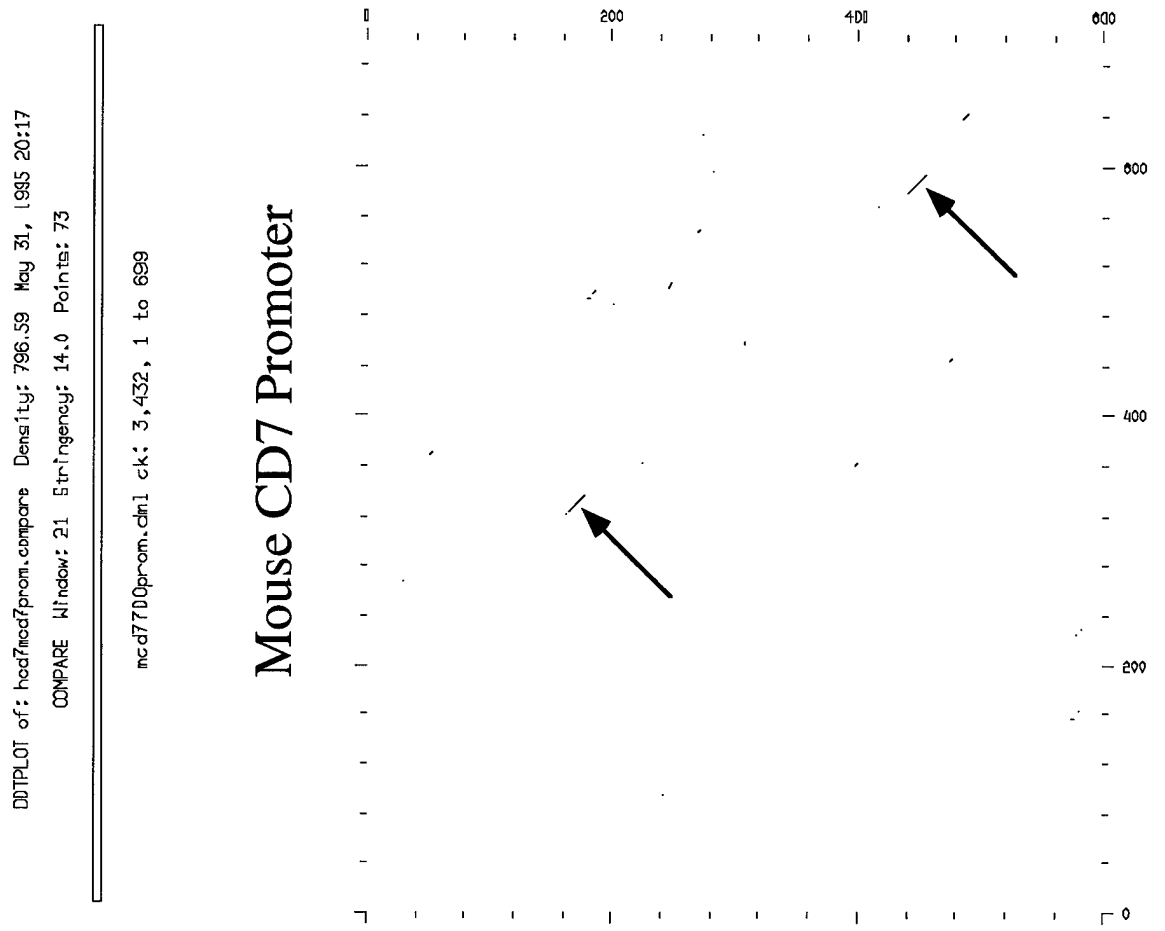
DOTPLOT of: hcd7mcd7prom.compare Density: 796.59 May 31, 1985 20:17
COMPARE Window: 21 Stringency: 14.0 Points: 73
mcd77D0prom.dml ck: 3,432, 1 to 699
Mouse CD7 Promoter
0
200
400
600
800
Human CD7 Promoter
hcd7prom600.dml ck: 450, 1 to 599

Figure 18 Promoter Analysis of Mouse CD7. Panel A shows the 5' flanking sequence of mCD7 labeled with selected transcription factor recognition motifs as identified with the Signal Scan program. This sequence was analyzed for mammalian transcription factors only. Published cDNA sequence begin at b.p. 1230 (bold letters). Panel B shows the downstream most of two identified homology regions present in the promoters of mCD7, hCD7, and mouse Thy-1. Panel C shows the more distal 5' region of homology in the mCD7 and hCD7 gene promoters. Identical sequences are identified with vertical lines. Corresponding base pair sequence locations from the published sequences are identified at the left of the sequences. The regions of similarity in Panels B and C were identified using the COMPARE algorithm shown in Figure 5.6.

Figure 18

A

```
                                                                    TCF-1
   1  GGCCCCTGTG TGTCTATGAT CTCTGAAACT TGAGGCATGG TCCCCCAAAC
                TCF-1
  51  AGTCCAAAGT GTCGATGCAC GAAGACCACA TCAAGGTCAG CCCTGCAGAG

 101  GTGGCAGCAC TCCAGTCCAT GTGCCCCTGG TGTGGCCACG GGCATCCTAG
           PEA-3
 151  GAAGGAGACT AGGTCTAGGT CTTTGACTGT TCTTACTTCC CTGTAAAGTC
                                    AP-2
 201  TGTCTTTCCA TGAACTTCTC CCCTGGGGGC TAGGTGCTGA TTTCTTTACT

 251  GCCCACCTGA CCCAGCTCCC CTCGTATTTC TCTCCAATAT TCTCAGGCTG
          TCF-1                                  TCF-1
 301  CACAGTTCCA TACCTGCTGT CCCTGTGTTA CCACAGGTGA CCTGTCCCTC
            AP-2
 351  CCCAACCCTT TGTTCCTAAA ATCTTCCAAC TTTGACCTTC CTTTACCTGA

 401  GTCCCTCTCC CATGTGCCCT CAAGTACCCC GCATGGCACC CCTGTCTACA

 451  CCATAGAATA CCAAACCCAC CTACAGGGGG AGCATCTTCC CCCTTAGAGT

 501  AGGACCCCGG AGGAGCTCCT TTGAGTCCCT ATGTGACACT GTACACACAC

 551  ACACACACAA ACTCACCCCT CAGTGTGACA CACTGGCTCT GGTACCAGCA

 601  ATAAAACTCA TGGTTGACAA GAGTCCTAGC TCTCCCCCAA CCTGGGAACC
            TCF-1
 651  AGACACAGGG CCCTCGGTTT TGTCCCAGAA GGCAGATTGC TATTGAAGGG
           Sp-1
 701  GCTCCTAGCC GCCCTTTGGC CTAGCAGATC TGGCTCAATC ATGCTTCTAA
          PEA-3          AP-2                  TCF-1
 751  GGAAGGATCA CCCAGGCCGC CAAGGCAACC ACAGCCAAGG CTACTGGGTA
                                                TCF-1
 801  TGCTGTGTCA GGCTGAAACC CCAGTGTGTC CAGACAACAG GTGAGACCAC
                                                TCF-1
 851  AGACCTGAAC ACATCCCAGC AGAAAATGAC ACAAAAGACC AGAGGAAACT

 901  TCAACTCCCT CCCGGCCTCT AAACCTTTAA GTCCCTCTAA TTTTTCTTCC

 951  AGGTTACAGG ACTAGTTCTT ATTTCTTCTT CCTCTTGACG TCTCCTGTGG
                          GATA-1
1001  AGACTCTTGG TTAAAGATGA TAAAGATGTG GGCCAGCCAA CCAGCCAGGG

1051  AGGACAGTTG GGGTCAGGTG GCTTCCTCCA CCTGGCTTGT TGTGTTCCCT
                                        PEA-3
1101  GCCCACCAAG CTCCACCTTC ATCTTCAGGA AGCCCTCCCT CGGAGCTTCA

1151  CCACCAATCG CATTGAACTG CCACACCCCT GTTTCTTCCT CTCAGGGTTT
                TCF-1
1201  TTGGTGTGAA CTTTCACAGT GCTCAGTAAT GTGTTGTAGC CAGAGTGGCT
```

B

```
mthy1prom 450 GAACACC......TCCAGTCAGCCCTCGCCGACCACCCCACCCCCTCCAT 493
                  ||||       | |||  ||||||| |      |  |||| ||
mcd7prom 1111 CTCCACCTTCATCTTCAGGAAGCCCTCCCTCGGAGCTTCACCACCAATCG 1160
                  ||||     || ||||||||||| ||  |||||
hcd7prom 430  AGGCACCGC...CTCCAGGAAGCCCTCTCT..GAGCTCTGAGCGCCTGCG 474
```

C

```
Human CD7  159 TCCCAGCAGAAAGTACCCCAGAGGACCAG 187
               |||||||||||| |  | || | ||||||
Mouse CD7  864 TCCCAGCAGAAAATGACACAAAAGACCAG 892
```

Figure 19 Structural Comparison of Mouse CD7 with Human CD7 and Mouse Thy-1. Scaled models compare the organization of mCD7, hCD7 and mThy-1 gene intron and exon structures. Note that all three genes are composed of four exons separated by short intronic sequences, residing on relatively short spans of DNA. Note the large degree of similarity between mouse and human CD7, with only a small difference in the size of intron 1 apparent.

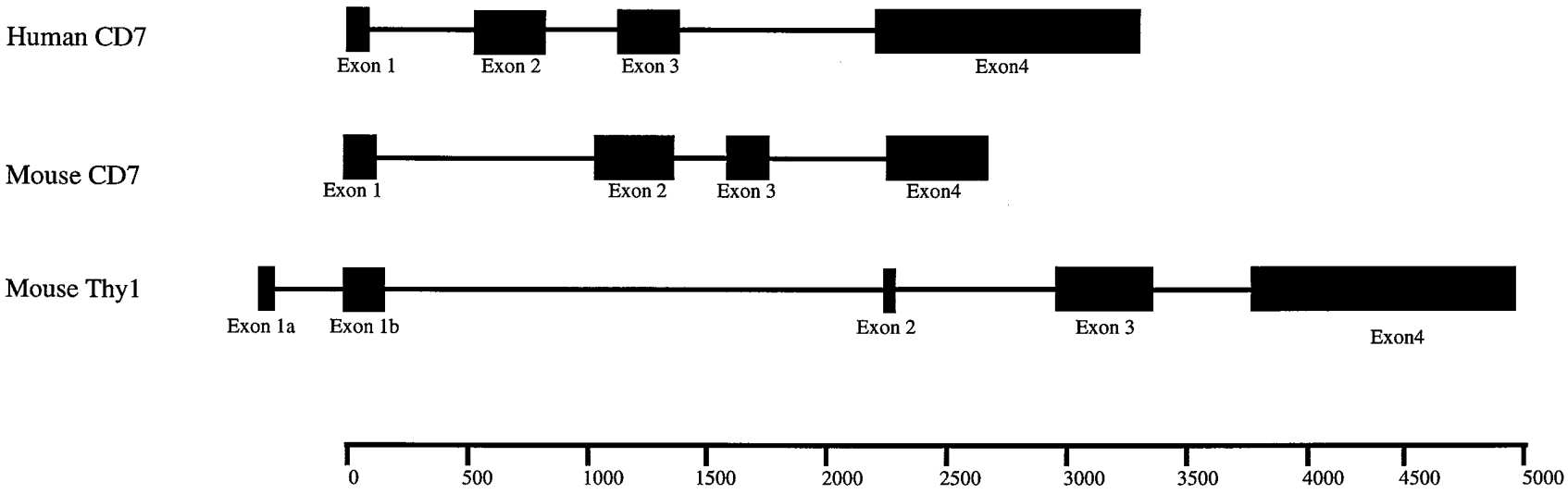
Human CD7
Exon 1
Exon 2
Exon 3
Exon4
Mouse CD7
Exon 1
Exon 2
Exon 3
Exon4
Mouse Thy1
Exon 1a
Exon 1b
Exon 2
Exon 3
Exon4
0
500
1000
1500
2000
2500
3000
3500
4000
4500
5000

Figure 19

Figure 20 Electrophoretic Mobility Shift Assays Electrophoretic mobility shift assays show binding of nuclear proteins from hematopoietic cell extracts to regions of sequence conservation between mouse and human CD7 promoters. The indicated nuclear extracts were assayed for the ability to form specific complexes with oligonucleotide probes using the human and mouse sequences for both homology regions as labeled. Unlabeled competitor oligos used to demonstrate specific binding to labeled probe were as labeled, the presence of the competitor denoted with a (+) sign. Each panel represents a different labeled probe used for EMSA, as labeled. Panel A=human CD7 3' probe, Panel B=mouse CD7 3' probe, Panel C=human CD7 5' probe and Panel D=mouse CD7 5' probe. Arrows demonstrate complexes of interest as referred to in the text. Extracts used were: human cell lines K562-a chronic myelogenous leukemia line, Jurkat-an acute T cell leukemia line and EL-4-a mouse lymphoma line.

Figure 20A

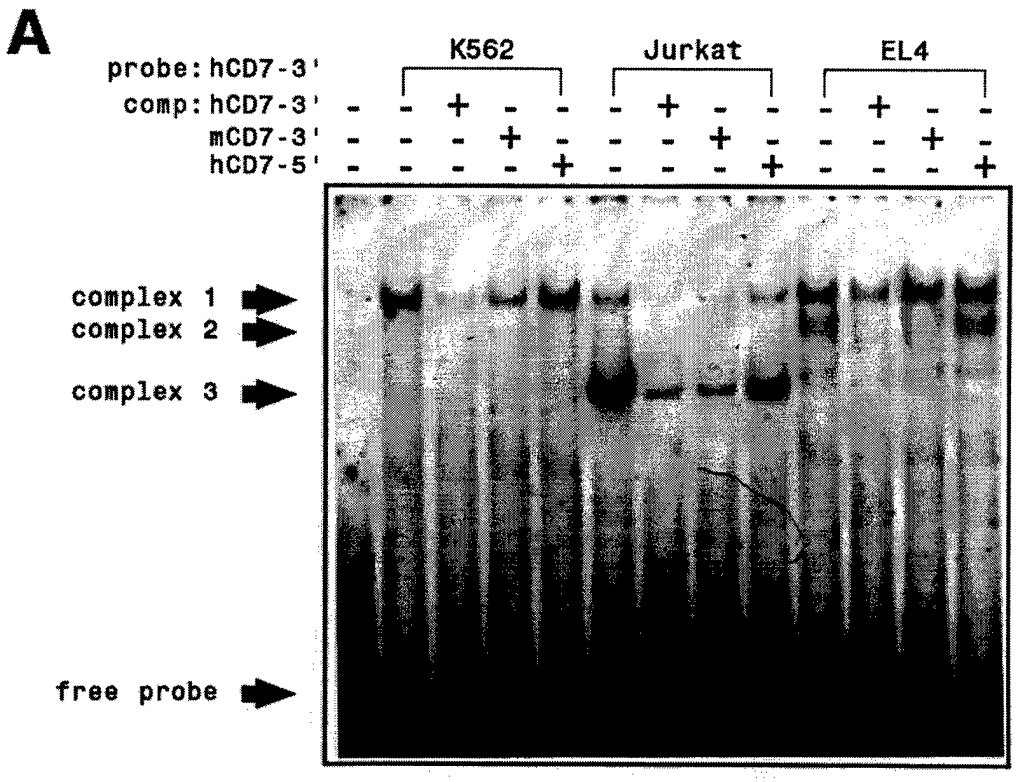
A
K562
Jurkat
EL4
probe: hCD7-3'
comp: hCD7-3'
mCD7-3'
hCD7-5'
complex 1
complex 2
complex 3
free probe

Figure 20B

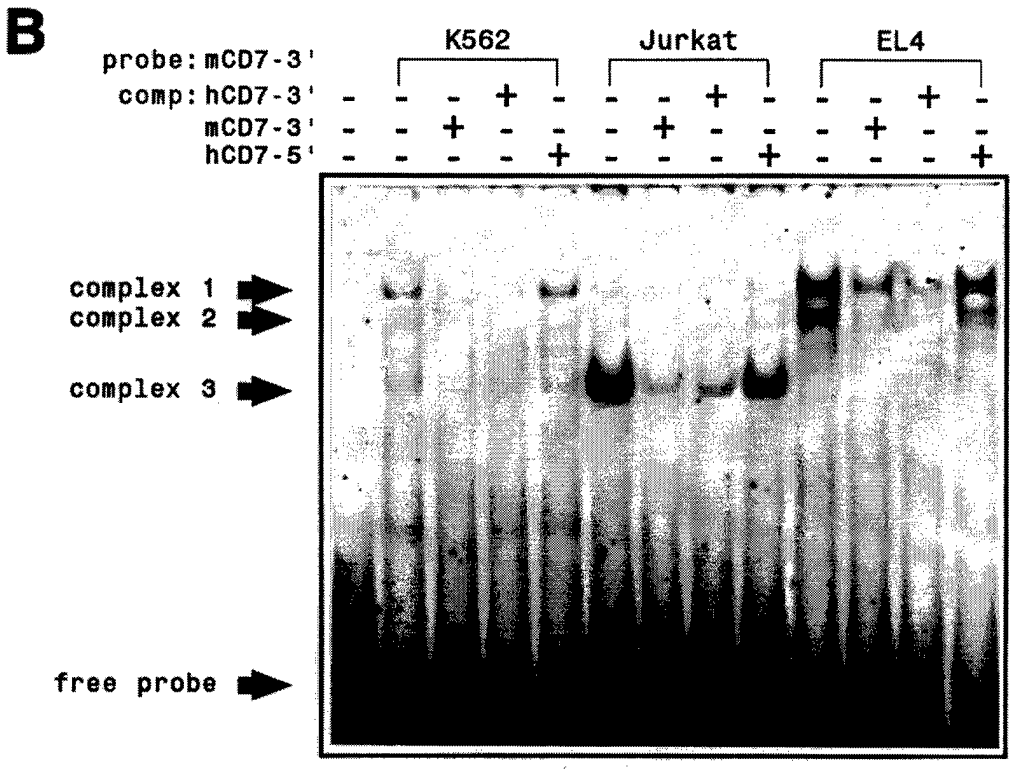
B
K562
Jurkat
EL4
probe: mCD7-3'
comp: hCD7-3'
mCD7-3'
hCD7-5'
complex 1
complex 2
complex 3
free probe

Figure 20 C

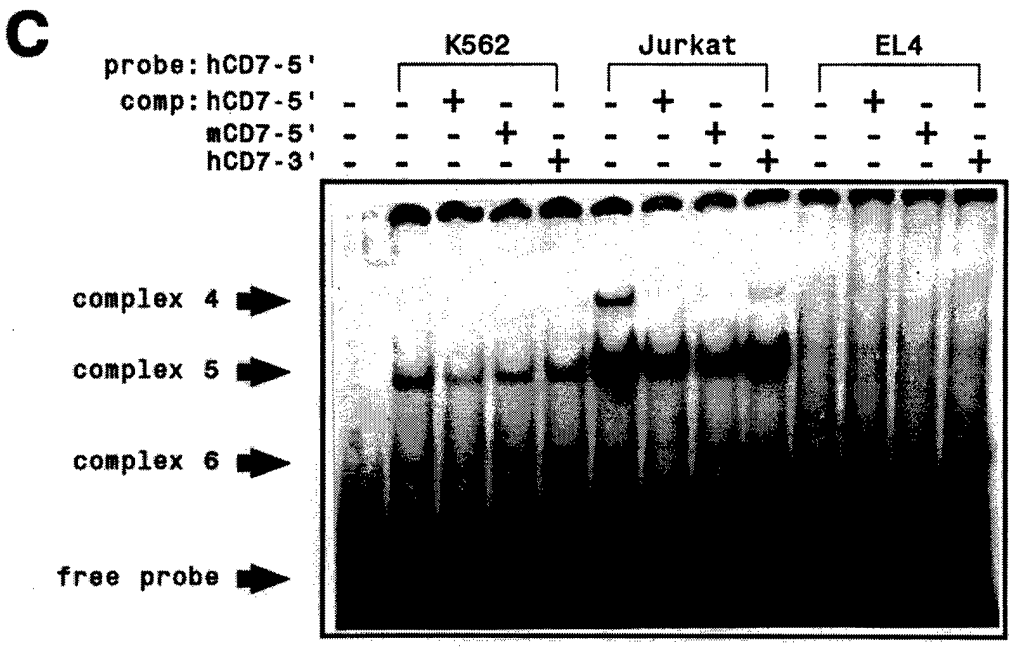
C
K562
Jurkat
EL4
probe: hCD7-5'
comp: hCD7-5'
mCD7-5'
hCD7-3'
complex 4
complex 5
complex 6
free probe

Figure 20D

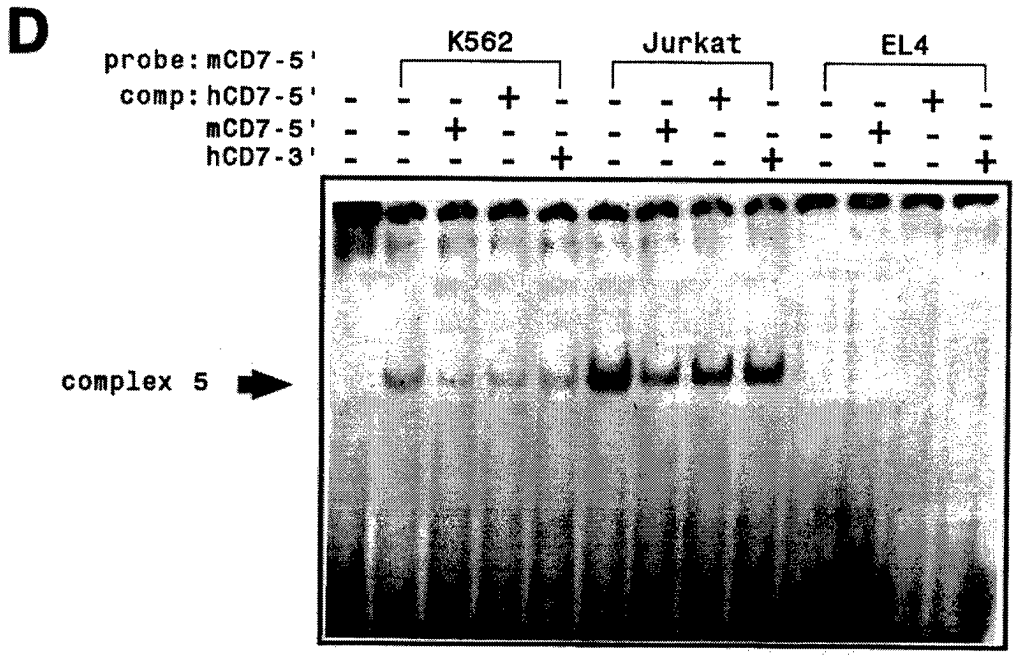
D
probe: mCD7-5'
comp: hCD7-5'
mCD7-5'
hCD7-3'
K562
Jurkat
EL4
complex 5

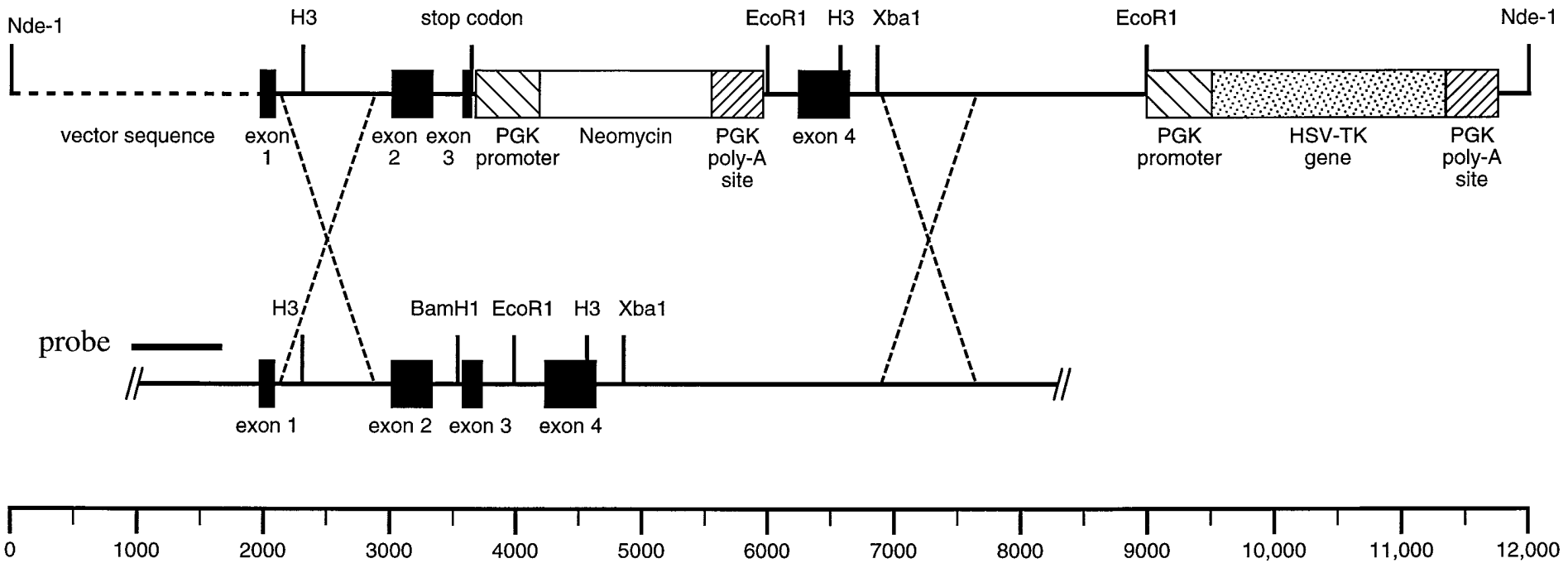

Figure 21: Plamid Design for Homologous Recombination of a Null Allele of Mouse CD7. Panel (A) shows a schematic representation of two regions of mouse CD7 (mCD7) subcloned into the plasmid pPNT. pPNT encodes the neomycin and thymidine kinase genes used for positive and negative selection of transfected 129 strain embryonic stem cells. A null allele of mCD7 is accomplished by interrupting the mCD7 gene sequence in the 5' region of exon 3 (prior to the sequence encoding the transmembrane region) by insertion of stop codons in all three frames and by insertion of the neomycin resistance gene. The 3' region of exon 3 is not included in this plasmid. The solid lines illustrate the region of mCD7 interrupted by the neor gene. Panel B illustrates the structural organization of the mCD7 gene. Hatched lines represent regions where homologous recombination is required. Selected restriction sites are labeled: H3=HinDIII, EcoR1, BamH1, XbaI and Nde-1.

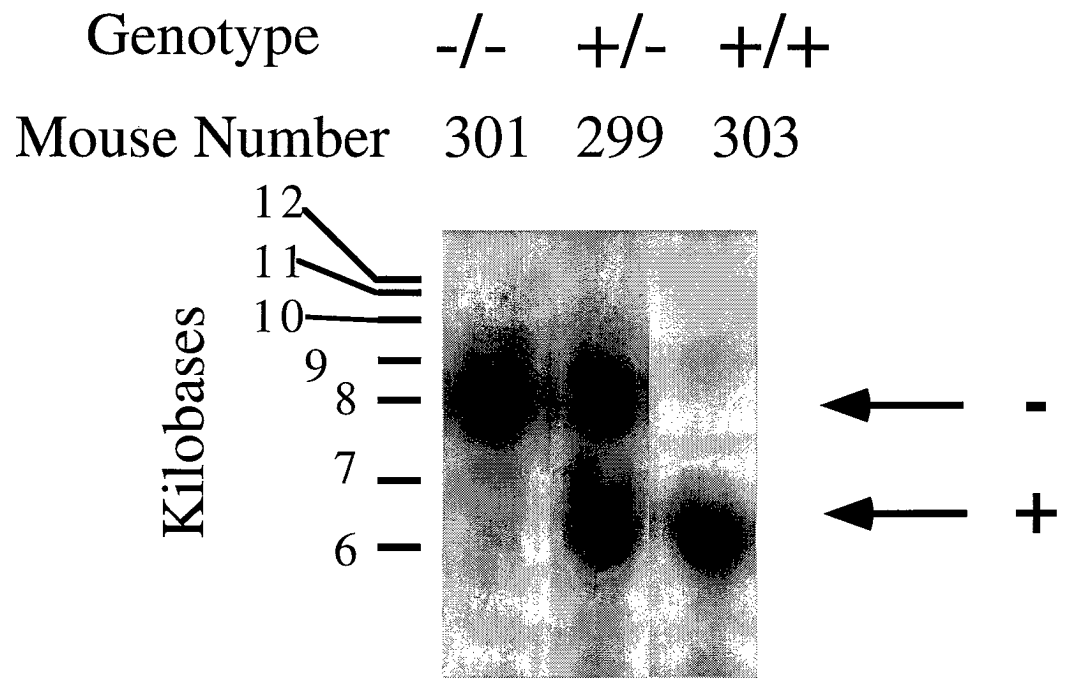

Figure 22: Genomic Southern Blot Demonstrating Disruption of the mouse CD7 Gene. Offspring of heterozygous mice containing a disrupted allele of CD7 were screened for disruption of both copies of CD7. Shown is a genomic southern blot of tail DNA from three offspring digested with the restriction endonuclease EcoR1. Mouse number and genotype are labeled. (+)=wild type CD7, (-)=disrupted CD7.

Figure 23: Western blot of mouse CD7 in splenocyte, thymocyte and recombinant mCD7 extracts. Shown is a western blot of C57BL/6 mouse thymocyte and splenocyte extracts and mouse CD7 recombinant protein probed with mAbs raised against recombinant mouse CD7. Briefly, 5 X 10^6 C57BL/6 mouse thymocytes and splenocytes lysed in 1% NP-40 containing buffer or 1 microgram of recombinant mouse CD7 were loaded in reducing sample buffer and electrophoresed on an 8% Laemelli SDS-PAGE and transferred to nitrocellulose. After pre-hybridization blocking with 10% dried milk containing buffer, these western filters were probed with culture supernatants of either Y3 (control) or 8F8, 9E7 or 35C8 anti-recombinant mouse CD7 rat hybridoma clones, washed and exposed to horseradish-peroxidase containing anti-rat secondary reagent. After exposure to chemiluminescence reagent, filters were exposed to film for 5 minutes. Figure legends: 8F8, 9E7 and 35C8=anti-mouse CD7 rat hybridoma lines, Y3=negative control rat hybridoma line, T=thymocyte extract, S=splenocyte extract, mCD7ec=bacterially expressed recombinant mouse CD7. Apparent molecular weights are as labeled. Arrows point to major reactive bands in splenocytes and thymocytes.

Figure 23

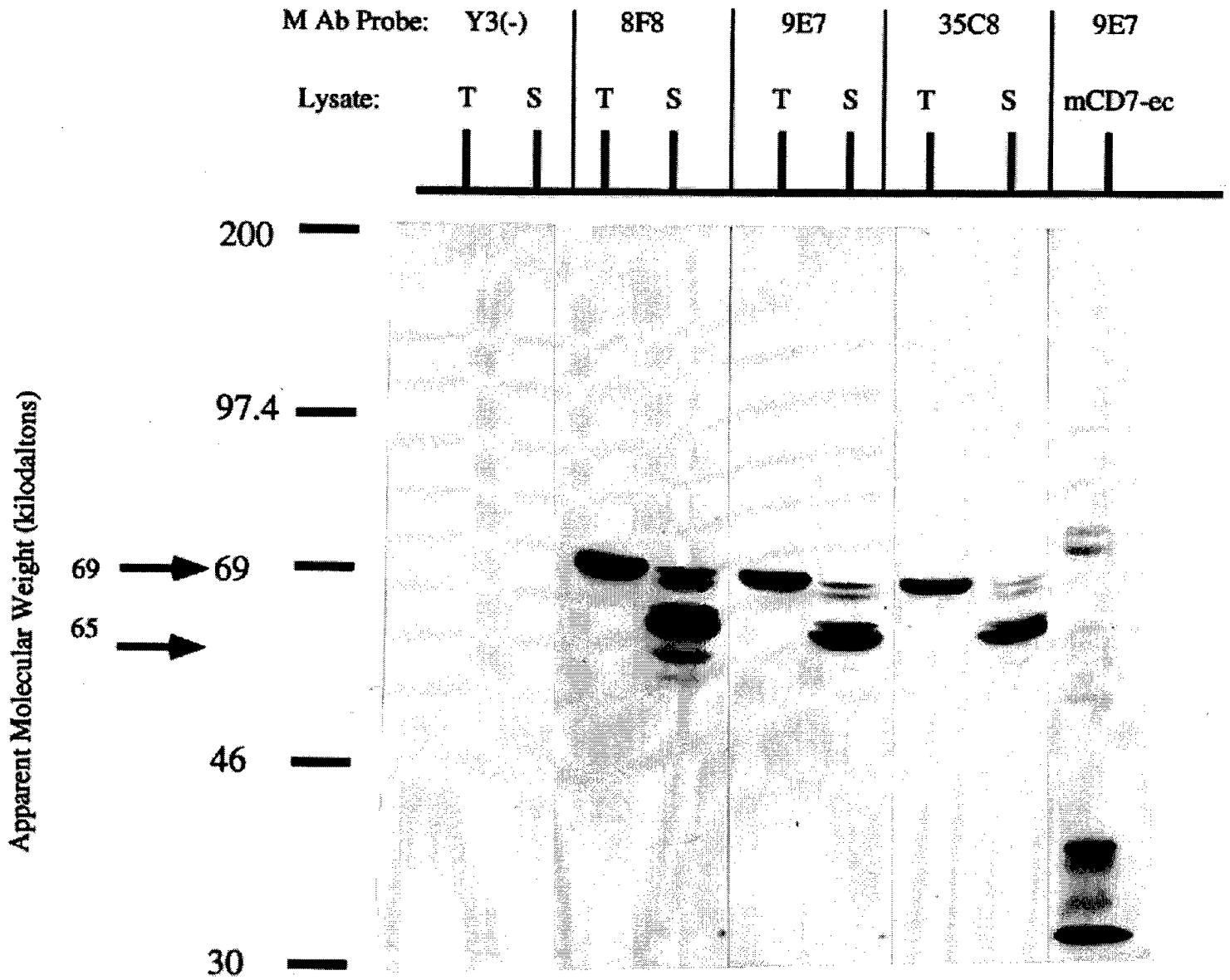
M Ab Probe:
Y3(-)
8F8
9E7
35C8
9E7
Lysate:
T
S
T
S
T
S
T
S
mCD7-ec
200
97.4
69
46
30
69
65
Apparent Molecular Weight (kilodaltons)

Quantitative Lymphoid Mononuclear Populations

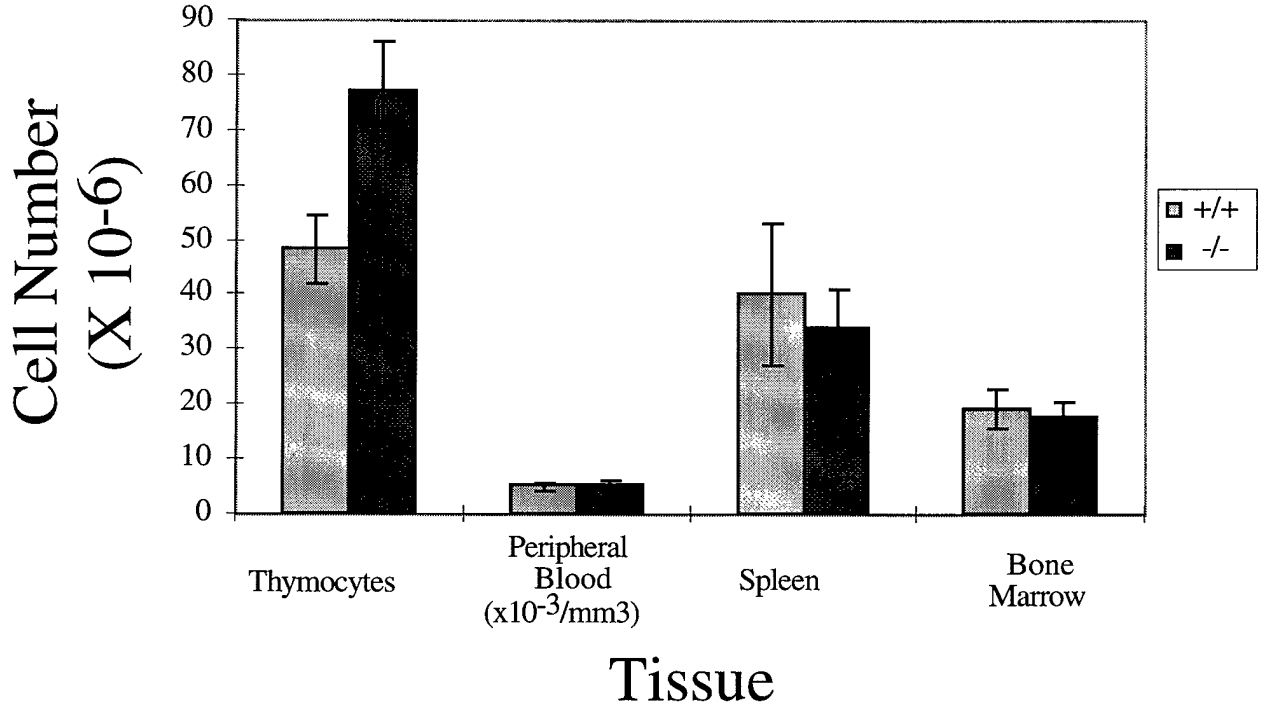

Figure 24: Analysis of lymphoid mononuclear cell populations.

For all experiments, freshly obtained suspensions of cells were used. Peripheral blood was collected from the retroorbital plexus using a heparinized pasteur pipette. Femurs were dissected and flushed with 2ml ice cold RPMI 1640 to obtain bone marrow. Splenocytes and thymocytes were teased into RPMI media using tuberculin syringe plungers and subsequently isolated by Hypaque-Ficoll density centrifugation. Cell suspensions were counted on a Coulter^{tm} counter. Analysis of cell surface phenotype was performed in both direct- and indirect-IF assays. Cell suspensions were subsequently analyzed using a FACStar plus flow cytometer. (n= 6 +/+, 6 -/-)

Quantitative Thymocyte Subpopulations

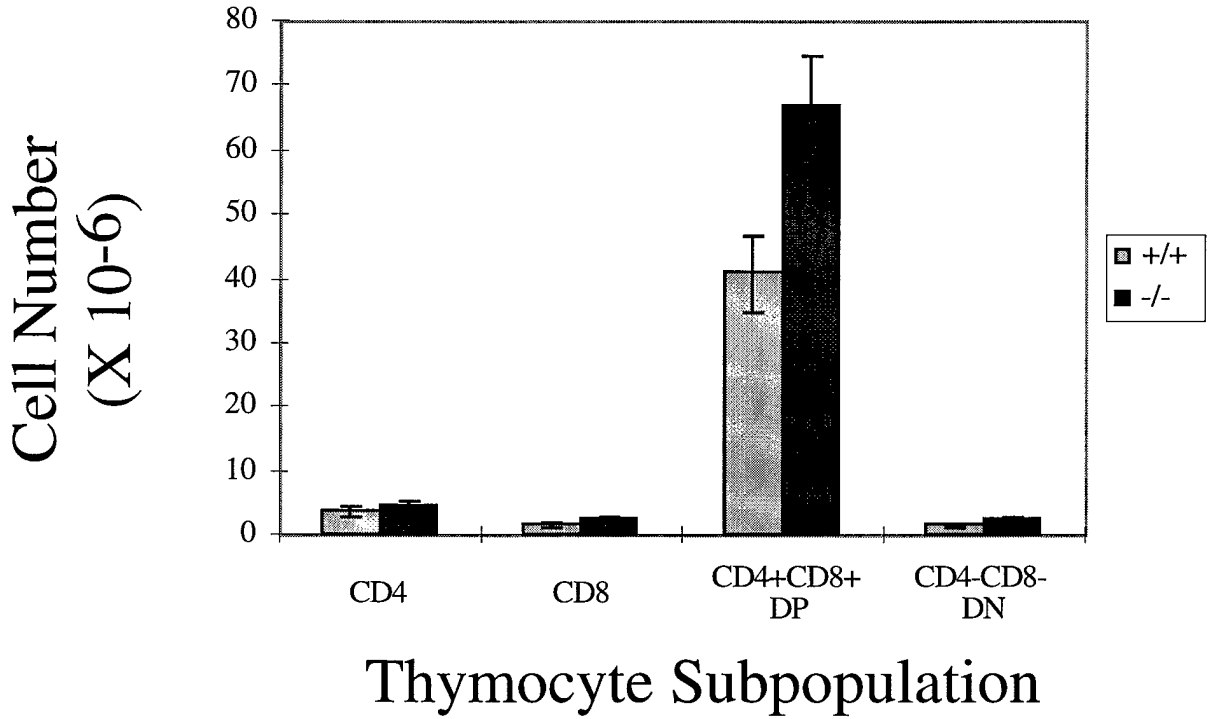

Figure 25: Analysis of lymphoid mononuclear cell populations.

For all flow cytometry experiments, freshly obtained cells were used. Thymocytes were teased into RPMI media using tuberculin syringe plungers and subsequently isolated by Hypaque-Ficoll density centrifugation. Cell suspensions were counted on a Coulter^{tm} counter. Analysis of cell surface phenotype was performed in a direct-IF assay. Cells were double stained with GK1.5-PE (CD4) and Lyt2-FITC (CD8). Cell suspensions were analyzed using a FACStar plus flow cytometer. (n= 6 +/+, 6 -/- p=0.027)

Quantitative Serum Immunoglobulin Levels

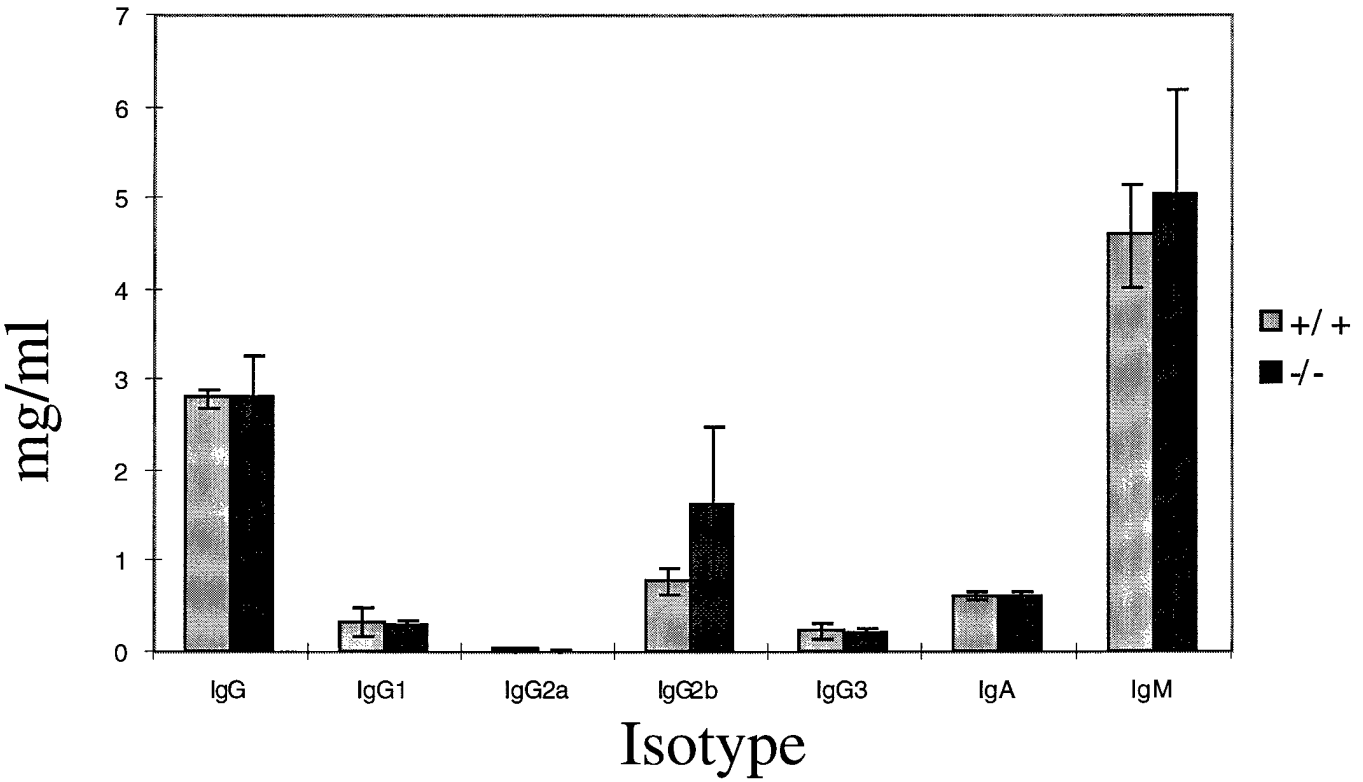

Figure 26: Quantification of serum immunoglobulin isotype levels.
Enzyme-linked immunosorbent assay (ELISA) was used to determine the quantity of antibody isotypes in serum samples. For the determination of serum levels of IgG, IgA, IgM, IgG1, IgG2a, IgG2b, and IgG3 an antigen capture ELISA was used. Plates were coated with goat anti-mouse Ig antibodies (specific for the desired class of Ig) diluted to 5ug/ml in PBS (100µl/well) and incubated overnight at 4° C. The wells were then emptied and washed 3 times with PBS/0.5% Tween 20. Non-specific binding was blocked by incubation with PBS/1% BSA at 100 µl/well for 1 hour. Dilutions of serum and standards were then added to the wells (100µl/well) and incubated overnight at 4° C. Specific Ig classes were detected with class-specific goat anti-mouse Ig-alkaline phosphatase conjugated antibodies. After incubation at room temperature for three hours, plates were washed 4 times with ELISA wash buffer and reacted with the alkaline phosphatase substrate p-nitrophenyl phosphate. After a 10 minute incubation, plates were read at 405 nm wavelength. (n= 4 +/+, 5 -/-)

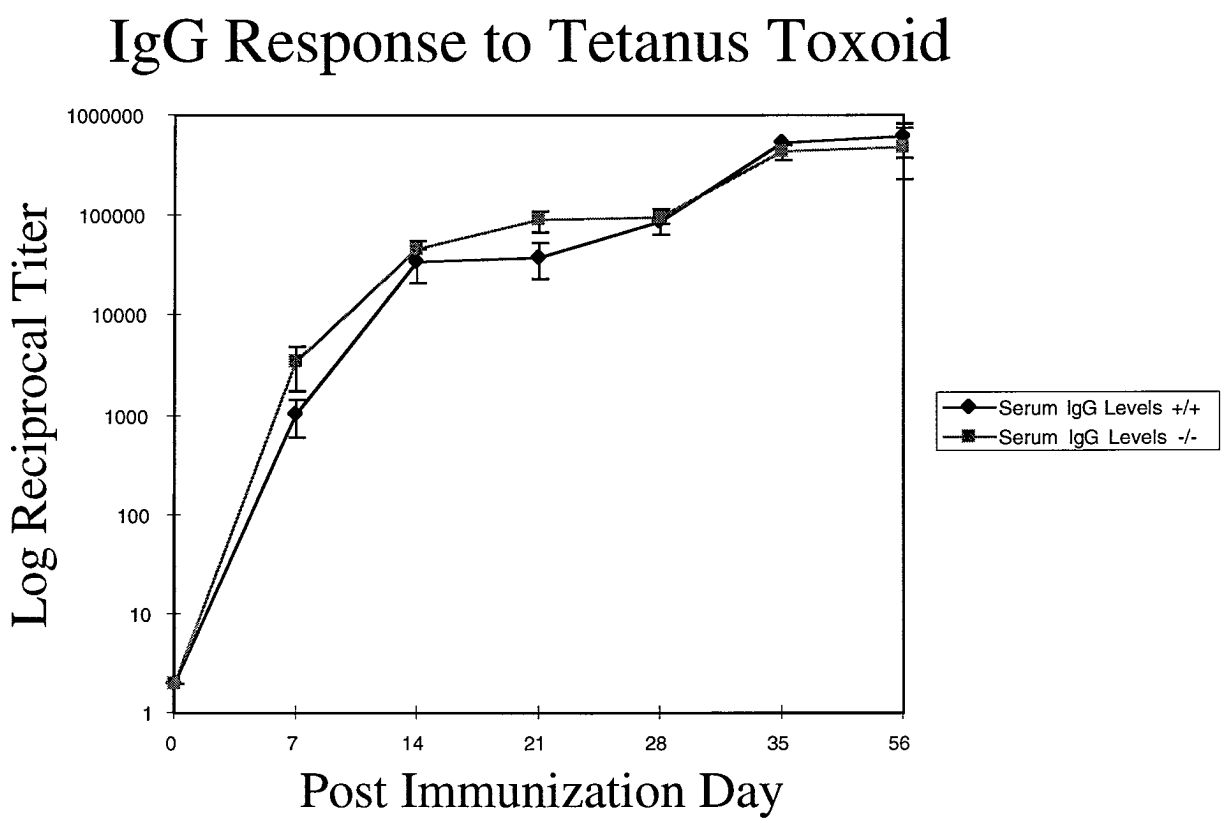

Figure 27: Time course and quantification of IgG response to tetanus toxoid immunization
Enzyme-linked immunosorbent assay (ELISA) was used to determine the presence of anti-tetanus toxoid (TT) antibodies in serum samples. Fot the TT ELISA, TT was diluted to 3µg/ml in PBS and plated to 96 well microtiter plates at 100µl/well. After overnight incubation at 4° C, the contents of the wells were discarded and blocking buffer (3% nonfat dry milk) was added at 200 ul/well. After incubating at room temperature for two hours, plates were stored at -20° C until used. ELISA plates were washed four times with ELISA wash buffer (PBS, 0.05% Tween-20, 0.1% azide) before the addition of serum samples. All samples were diluted in serum diluent (PBS, 2.5% bovine serum albumin, 2.5% non fat dry milk, 5% normal goat serum, 0.1% azide, 0.05% Tween-20) and added to ELISA plates at 100 µl/well. After overnight incubation at 4° C, plates were washed four times with ELISA wash buffer before the detection antibody was added. Alkaline phosphatase conjugated goat anti-mouse was diluted 1:1000 and used as the detection antibody (100 µl/well). After incubation at room temperature for three hours, plates were washed 4 times with ELISA wash buffer and reacted with the alkaline phosphatase substrate p-nitrophenyl phosphate. After a 10 minute incubation, plates were read at 405 nm wavelength. (n= 4 +/+, 5 -/-)

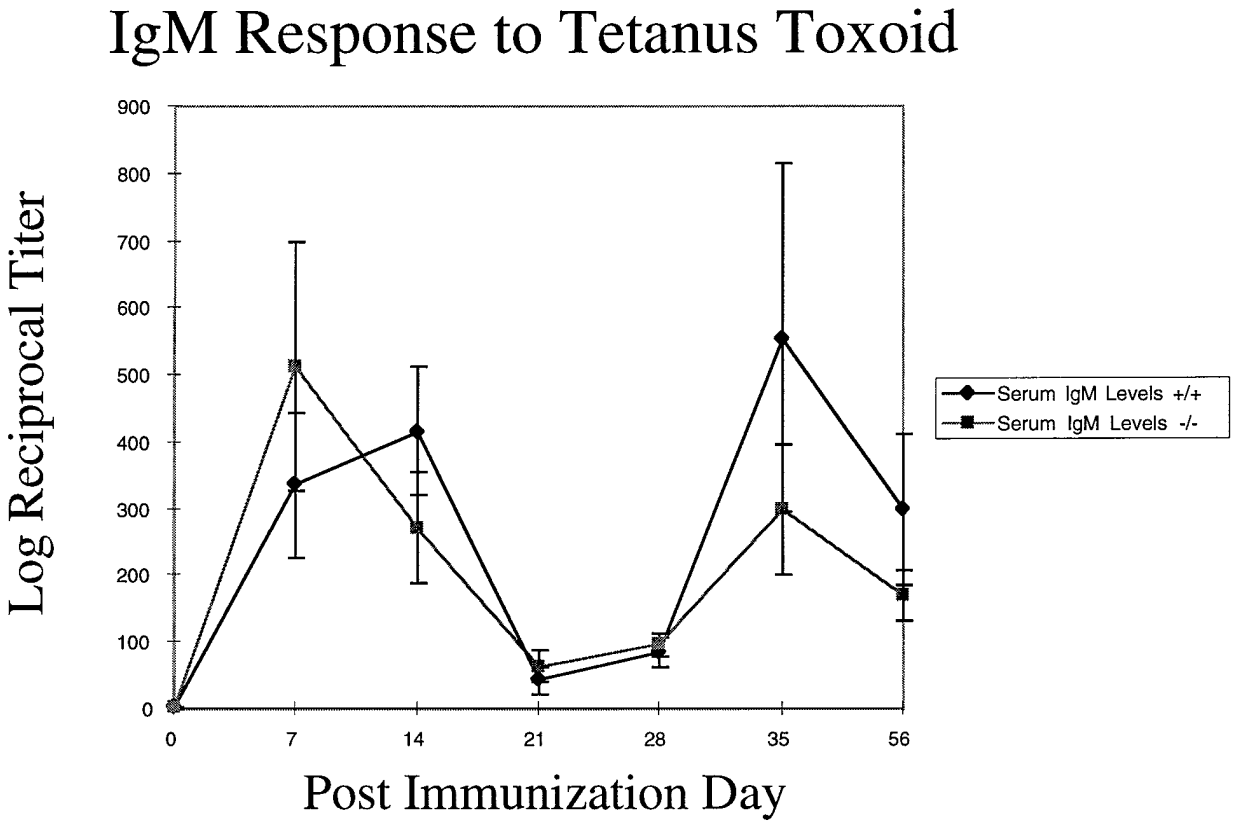

Figure 28: Time course and quantification of IgM response to tetanus toxoid immunization
Enzyme-linked immunosorbent assay (ELISA) was used to determine the presence of anti-tetanus toxoid (TT) antibodies in serum samples. Fot the TT ELISA, TT was diluted to 3 µg/ml in PBS and plated to 96 well microtiter plates at 100µl/well. After overnight incubation at 4° C., the contents of the wells was discarded and blocking buffer (3% nonfat dry milk) was added at 200 µl/well. After incubating at room temperature for two hours, plates were stored at -20° C until used. ELISA plates were washed four times with ELISA wash buffer (PBS, 0.05% Tween-20, 0.1% azide) before the addition of serum samples. All samples were diluted in serum diluent (PBS, 2.5% bovine serum albumin, 2.5% non fat dry milk, 5% normal goat serum, 0.1% azide, 0.05% Tween-20) and added to ELISA plates at 100 µl/well. After overnight incubation at 4° C, plates were washed four times with ELISA wash buffer before the detection antibody was added. Alkaline phosphatase conjugated goat anti-mouse IgM was diluted 1:1000 and used as the detection antibody (100 µl/well). After incubation at room temperature for three hours, plates were washed 4 times with ELISA wash buffer and reacted with the alkaline phosphatase substrate p-nitrophenyl phosphate. After a 10 minute incubation, plates were read at 405 nm wavelength. (n= 4 +/+, 5 -/-)

Quantitative anti-Tetanus Toxoid Immunoglobulin Isotypes

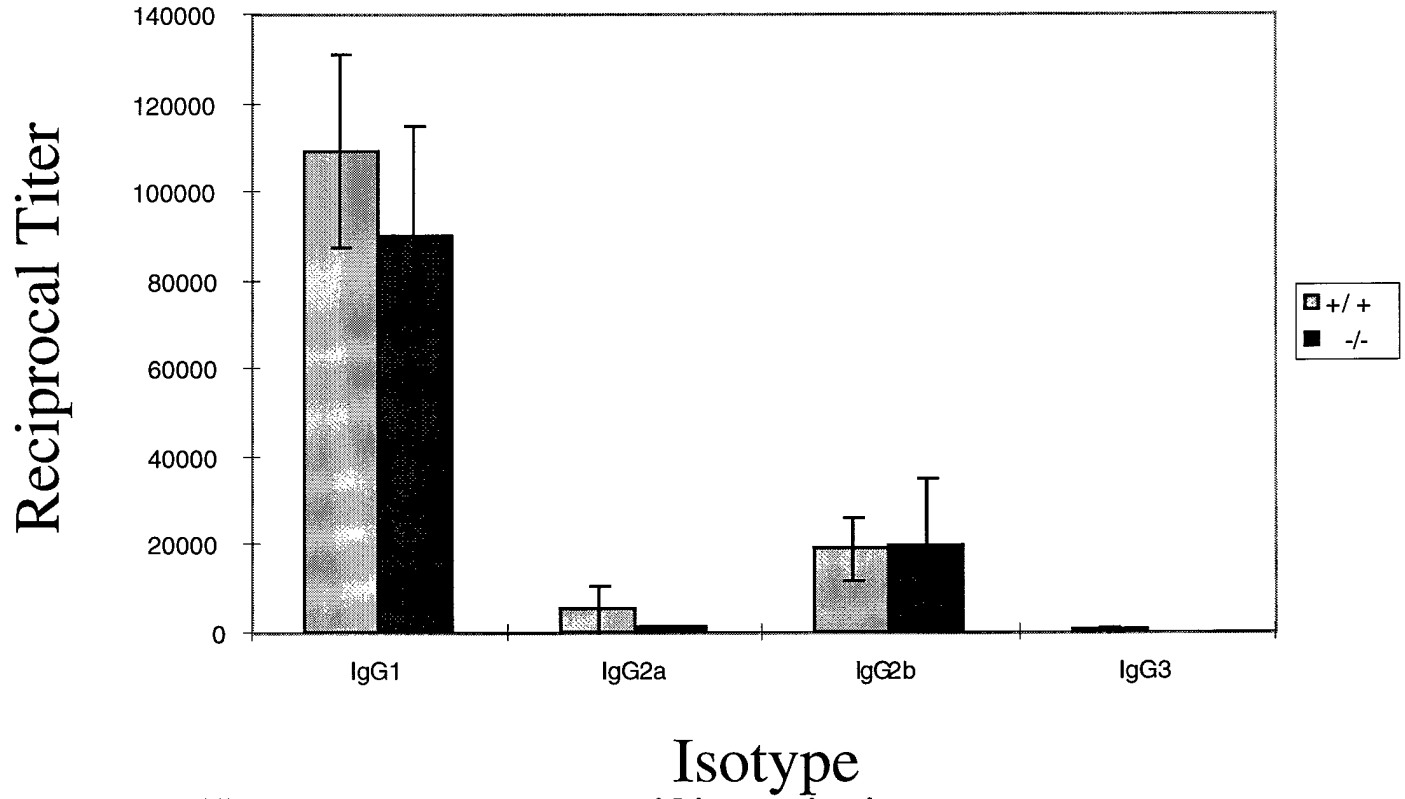

Figure 29: Isotype specific responses to tetanus toxoid immunization

Enzyme-linked immunosorbent assay (ELISA) was used to determine the presence of anti-tetanus toxoid (TT) antibodies in serum samples. Fot the TT ELISA, TT was diluted to 3ug/ml in PBS and plated to 96 well microtiter plates at 100µl/well. After overnight incubation at 4° C., the contents of the wells was discarded and blocking buffer (3% nonfat dry milk) was added at 200 µl/well. After incubating at room temperature for two hours, plates were stored at -20° C until used. ELISA plates were washed four times with ELISA wash buffer (PBS, 0.05% Tween-20, 0.1% azide) before the addition of samples. All samples were diluted in serum diluent (PBS, 2.5% bovine serum albumin, 2.5% non fat dry milk, 5% normal goat serum, 0.1% azide, 0.05% Tween-20) and added to ELISA plates at 100 µl/well. After overnight incubation at 4° C, plates were washed four times with ELISA wash buffer before the detection antibody was added. Alkaline phosphatase conjugated, goat anti-mouse IgG1, IgG2a, IgG2b, IgG3 was dilute 1:1000 and used as the detection antibody (100 µl/well). After incubation at room temperature for three hours, plates were washed 4 times with ELISA wash buffer and reacted with the alkaline phosphatase substrate p-nitrophenyl phosphate. After a 10 minute incubation, plates were read at 405 nm wavelength. (n= 3 +/+, 4 -/-)

Table 3

Thymocyte Subsets in CD7 Transgenic and Non-Transgenic Mice

Mouse Line	Thymus w+ (grams)	Thymocyte No. (x107)	Thy 1.2+ %	Thy 1.2+ no. ($x10^7$)	DN %	DN no. ($x10^7$)	DP %	DP no. ($x10^7$)	CD4+ SP %	CD4+ SP no. ($x10^7$)	CD8+ SP %	CD8+ SP no. ($x10^7$)
216 CD7 Transgene+	.06 ± .01	5.7 ± 1.1	96 ± 4	8.5 ± 5.2	3. ± 1	.2 ± .05	83 ± 3	5.2 ± 2.4	8 ± 2	.4 ± .1	5.4 ± 1	.25 ± .1
555 CD7 Transgene+	.05 ± .01	6.4 ± 1.9	97. ± 0	6.1 ± .8	3 ± 1	.12 ± .04	86 ± 3	3.5 ± 1	7 ± 2	.3 ± .1	3.2 ± .5	.14 ± .04
Transgene-Conticol	.05 ± .003	6.21 ± .9	96 ± 3.	5.8 ± 1.2	3 ± 1	.2 ± .04	86 ± 1	5.4 ± .8	7 ± 1	.4 ± .1	4 ± .3	.26 ± .04

Shown is a comparison of various thymocyte subsets as defined by mouse CD4 and CD8 expression. Data are expressed as average ± standard error of the mean. The average total number of cells in each subset are also shown.

Table 4

Comparison of Lymphocyte Subsets in CD7 Transgenic and Non-Transgenic Mouse Spleen

Mouse Spleen Source	Spleen weight (grams)	Average Total Cell Number (n=) ($x10^7$)	LY-5+ Splenocytes %	LY-5+ Splenocytes no. ($x10^7$)	% Thy 1.2 Splenocytes %	% Thy 1.2 Splenocytes no. ($x10^7$)	CD4+ Splenocytes %	CD4+ Splenocytes no. ($x10^7$)	CD4+ Splenocytes %	CD4+ Splenocytes no. ($x10^7$)	F4/80+ Splenocytes %	F4/80+ Splenocytes no. ($x10^7$)
216 line CD7 Transgenic	.12 ± .02	8.25 ± 1.11	44 ± 2	4.66 ± .21	55 ± 10	5.76 ± .99	20 ± 3	1.52 ± .22	16 ± 2	1.17 ± .17	10 ± 3	1.25 ± 15
555 line CD7 Transgenic	.12 ± .01	6.36 ± 1.50	44 ± 3	3.7 ± ..23	58 ± 8	4.93 ± .72	25 ± 4	1.77 ± .28	24 ± 2	1.71 ± .18	13 ± 3	1.08 ± 24
Non-Transgenic	.09 ± .01	7.20 ± .81	43 ± 6	3.04 ± .39	49 ± 7	4.19 ± .59	22 ± 2	1.55 ± .17	18 ± 2	1.28 ± .15	13 ± 3	1.03 ± 24

Shown is a quantitative analysis of splenic lymphocyte subsets as defined by mouse Thy1 (T-cell), mouse Ly-5 (B-cell), F4/80 (monocyte/macrophage) and mouse CD4 or CD8 (T-cell subsets) expression. Data are expressed as average ± standard error of the mean. The average total number of cells in each subset are also shown.